

7th ESACP Congress in Caen April 1–5, 2001

Abstracts

Edited by

The “Pôle Traitement et Analyse d’Images de Basse-Normandie” and the
“Groupe Régional d’Etudes sur le Cancer”

President's Foreword

As the President of the European Society for Analytical Cellular Pathology, it is a great pleasure to address you in this special issue of Analytical Cellular Pathology on the occasion of the Seventh Conference of the European Society for Analytical Cellular Pathology.

The previous conferences of the Society in Schloss Elmau, Nijmegen, Grenoble, Oslo, and Heidelberg were all great successes. This Seventh Conference is organized at a time of an ever increasing interest in the implementation of techniques and new analytical developments (such as DNA arrays, CGH, new sensitive and specific fluorescent labels, 3D imaging of cell and tissue microscopy, as well as the use of electronic networking e.g. for telepathology), in hematology, oncology, pathology and intracellular investigations of normal and disturbed molecular mechanisms.

Analytical cellular pathology is situated at the crossroads of these approaches and thus involves the close collaboration between basic research oriented scientists and clinical pathologists. This association appears of particular interest as the precise understanding of disease processes, including molecular changes, can be obtained mainly from the exploration of cells and tissues characteristics. In this context, the organizers decided to concentrate on new methods and technologies, focusing on new opportunities offered and applications in human pathology, as well as veterinary pathology and toxicology. The challenging goal of these multidisciplinary approaches could be summarized by the motto of this Conference: "Technologies of the Third Millennium for a better knowledge of cell and tissue functions and disorders."

I very much hope that this Seventh Conference of the European Society for Analytical Cellular pathology will contribute to improve fundamental and practical knowledge of life-threatening diseases and will function as a bridge between fundamental analytical cellular pathology and clinical care, for the benefits of patients.

Jean Dufer
ESACP President

<i>Invited Speakers</i>

Distinguished Ploem Lecture

TOWARDS A NON-INVASIVE, OBJECTIVE SINGLE CELL CANCER DIAGNOSIS

Böcking A.

Institute of Cytopathology, Heinrich-Heine-University, Moorenstr. 5, D-40225 Düsseldorf, Germany

Introduction Lecture

R039

THE UNIVERSALITY OF FRACTAL SHAPES

Sapoval B.

Condensed Matter Laboratory, Ecole polytechnique, 91128 Palaiseau, France.

“Then, the greatest physicists Galileo, Descartes, Newton, were great geometers”

Diderot, Lettre sur les Aveugles (1749)

In classical geometry, a line has a dimension 1, a surface has a dimension 2, and a volume a dimension 3. But is it possible to attribute such a dimension to a mountain or a cauliflower? If nature could show objects with a non-integer dimension, the properties of these objects would depend on this “bizarre” dimension. Such objects do exist, they are called fractal objects. The discovery, in the seventies, of many fractal objects in nature is one of the most important scientific progress of the second part of the 20th century.

The notion of non-integer or fractal dimension applies to objects which possess geometrical details of all sizes with similar shapes. These objects are self-similar in the sense that a part of the object is similar to the whole. They are scale invariant as their shape does not depend on the observation scale.

We will also introduce a new meaning for the word “universality”. This meaning indicates that some systems exhibit properties which are independent of their microscopic nature. This will be shown from various experimental situations where the same fractal geometries appear in electrochemical experiments, in bacterial growth patterns, in fluid propagation in porous media ... What is common (or universal) between these systems is their same fractal

geometry. These geometries are then universal in the same sense that an orange, a soap bubble, or the earth have approximately the same spherical shape. The universality of fractal shapes, or of several classes of fractal shapes, indicates the existence of a common underlying mathematical structure in very different physical situations. These ideas have deeply modified the perception and description of many natural phenomena.

Plenary and Parallel Sessions

B019

QUANTITATIVE AND MOLECULAR PATHOLOGY OF ENDOMETRIAL HYPERPLASIA: TOWARDS NEW CLASSIFICATION AND TREATMENT

Baak J.P.A. 1, 2, 3, Mutter G.L. 3, Orbo A. 4, van Diest P.J. 1

1) Departments of Pathology, Free University Medical Center, Amsterdam and 2) Medical Center Alkmaar, Alkmaar, The Netherlands, 3) The Brigham and Women Hospital, Harvard Medical School, Boston, USA and 4) University of Tromsø, Tromsø, Norway

Goals and Methods: 1. To perform clonal analysis of 93 endometrial tissues and compare the results with pathologist’s diagnosis and the morphometric prognostic D-Score1;

2. To perform a prospective multicenter evaluation of the WHO classification (=WHO) and the morphometric D-Score to predict in 132 endometrial hyperplasias (EH) cancer progression-or-not. The D-Score was assessed blindly by technicians in a routine diagnostic setting. Development of endometrial cancer (in 1-10 year follow-up) was used as end point.

Results: 1. Diagnosis of hyperplasia, especially non-atypical hyperplasias, was not well reproducible between expert gynecological pathologists and did not accurately classify cases as poly- or monoclonal. In contrast, the D-Score resolved these lesions into poly-or monoclonal with a high degree of accuracy and reproducibility 2.

2. Eleven out of 132 patients (8%) developed cancer and of these, 10 had a D-score (0 (“unfavorable” or

Endometrial Intraepithelial Neoplasia = EIN) and one of the 20 (5%) cases with $0 < D(1$ (“uncertain”) developed cancer. None of the 86 cases with a D-Score > 1 (“favorable”) developed cancer. Sensitivity of the D-score was 100%, specificity 82%, the positive and negative predictive values were 38% and 100%. These figures are similar to those in three prior retrospective D-Score studies, but higher than the WHO figures for atypical hyperplasias (which are 91%, 58%, 16% and 99%).

Conclusions: The D-score in endometrial hyperplasias is a more sensitive and specific marker for clonality and cancer progression than the WHO classification, can be assessed in a routine clinical setting on standard H&E sections (15-30' per case), is highly reproducible and cost-effective (US\$50 per case). This has led to a new morphometric classification of endometrial hyperplasias³ and a therapeutic decision algorithm in patients with EH. Nationwide application in The Netherlands of the D-Score in therapeutic decision making will save approximately US 10 million per year by avoiding unnecessary procedures with attendant morbidity.

This work was supported by grant 28-1203 to JPAB from The Health Research and Development Council of the Netherlands (ZON) and by Grant No. EDT-86 to GLM from The American Cancer Society.

References:

J Pathol 1988; 154: 335-341. J Pathol 2000, 190: 462-469. Gyn Oncol 2000; 76: 287-290.

E009

CHROMOSOMES IN CANCER CELLS

Ried T.

National Cancer Institute, NIH

Chromosomal aberrations are key events in the initiation and progression of cancer and can be detected in virtually all tumors. We will discuss novel molecular cytogenetic tools for the visualization of both balanced, reciprocal as well as numerical chromosomal aberrations that induce aneuploidy in cancer cells. Such recent improvements of molecular cytogenetic techniques include comparative genomic hybridization (CGH) and spectral karyotyping (SKY). CGH analyses of large series of carcinomas revealed a pattern of chromosomal aberrations that is (i) highly specific for the different tumors, (ii) specific for discrete stages during progression, and (iii) indicates increased genetic instability during tumor

progression. We will discuss the value of SKY for the identification of patterns of chromosomal aberrations in hematological malignancies and solid tumors and explore the usefulness of cytogenetic techniques for the validation of mouse models of human cancer. Indeed, the comparison of chromosomal gains and losses and chromosomal breakpoints may assist in the identification of genomic alterations that are relevant for tumorigenesis across species boundaries. Because the predominance of numerical chromosomal aberrations in solid tumors of epithelial origin (carcinomas) suggest that aneuploidy and therefore the acquisition of genomic imbalances are the premier cytogenetic abnormality in solid tumors the role of chromosome segregation errors and the involvement of abnormalities of the centrosome as the major organizer of the mitotic spindle apparatus will be discussed.

I008

THE EPIGENOME IN SICKNESS AND IN HEALTH: CHROMATIN STRUCTURE AND GENOME FUNCTION

Wolffe A.P., Urnov F.D.

Sangamo Biosciences, Richmond, CA, USA.

The intricate regulatory pathways that unfold on the metazoan genome during ontogeny are integrated with the chromatin infrastructure of target loci to achieve a wide range of regulation levels and modes, from acute induction and repression, to robust long-term expression state maintenance. Biochemical analysis of the nucleus yielded the surprising observation that it is populated with an extraordinary variety of enzymatic macromolecular assemblies whose action in response to targeting to specific loci by DNA-bound regulators leads to localized remodeling and modification in chromatin structure – which, in turn, has profound consequences for the activity of the underlying regulatory DNA stretches. We will present evidence on several types of recently described complexes that connect both acute – for example, during nuclear hormone receptor signaling, and stable – for example, over methylated DNA segments – gene regulatory pathways to chromatin remodeling. Causative links between genetic lesions on components of such pathways and the etiology of particular human disorders will be highlighted – these illuminate the striking power of chromatin structure alterations on genome activity. Recent

technological advances allow for the targeting of chromatin modifying/remodeling engines to endogenous genomic loci of the experimenter's choosing via the use of designed zinc-finger DNA binding modules fused to regulatory domains of choice (Zhang et al., *JBC* 275: 33850). As we will discuss, the use of such synthetic proteins illuminates the complex rules and restrictions imposed by the native chromatin environment on access and action by transcriptional regulators, and presents a powerful platform to effect endogenous gene control in normal and pathological situations *in vivo*.

N002

MULTI-COLOUR FISH ANALYSIS: METHODOLOGY AND APPLICATIONS

Tanke H.J., Bezrookove V., Szuhai K., Engels H., Wiegant J., De Wind-van de Burg M., Rosenberg C., Raap A.K.

Laboratory for Cytochemistry and Cytometry; Department of Molecular Cell Biology, Leiden University Medical Center; Leiden; The Netherlands.

Present FISH karyotyping is based on the so-called combinatorial use of probes labelled with 5 distinct fluorophores. For such combinatorial labelling, it has been shown that the number of targets (n) recognizable by FISH using (k) different fluorophores results in $n = 2k - 1$ colours.

The principle of COBRA-FISH is based on the simultaneous use of combinatorial labelling and so-called ratiolabelling, which allows for simultaneous staining of many more targets than reported so-far. Three spectrally well-separated fluorophores are used pair wise for ratiolabelling, allowing a total of 12 colours to be distinguished. A second set of 12 probes, recognizing different targets are labelled exactly the same, but in addition are given a fourth label, resulting in a total of 24 colours. The fifth label is subsequently used to repeat this principle once again, to accomplish full staining of p and q arms, using arm specific probes. The fifth label may also be used to label any probe of interest to identify and locate a defined sequence in a FISH karyogram.

Multi-colour COBRA FISH was applied to detect cryptic translocations and abnormalities in patients with abnormal phenotype but normal Giemsa karyotype, to study HPV 16 integration sites in cervical cancer cell lines and to perform 48 colour staining in complex rearrangements karyograms from human solid tumours. Other works relate to the

application of the same methodology for mouse paints to study mouse tumour models, and a full set of sub-telomeric probes for clinical diagnostic use.

N005

SPECTRAL KARYOTYPING (SKY) REVEALS NEW SPECIFIC CHROMOSOMAL ABERRATIONS IN HUMAN TUMORS AND MOUSE MODELS OF HUMAN DISEASE.

Schröck E., Helmrich A., Matthäi A., Güntzschel U., Tänzler S.

Institute for Molecular Biotechnology, Beutenbergstrasse 11, D-07745 Jena, Germany

Recurrent chromosomal aberrations reflect genomic changes that contribute to the transformation of normal cells into tumor cells. SKY-analysis of human and mouse tumors revealed a high number of previously undetected or incompletely identified chromosome aberrations.

SKY permits the simultaneous visualization of all chromosomes in a metaphase spread in different colors. Structural chromosomal aberrations that lead to the formation of new fusion genes or to oncogene activation are readily identified. SKY is based upon combinatorial FISH using chromosome painting probes, optical microscopy, spectral imaging and spectra-based chromosome classification.

Epithelial cancers predominantly show gains and losses of distinct chromosomal regions reflecting copy number changes of oncogenes and tumor suppressor genes. In contrast, recurrent chromosomal translocations are the primary aberrations found in leukemias, lymphomas and sarcomas. The principal biological mechanisms causing either reciprocal translocations or chromosomal gains and losses have not been identified, yet.

Fragile Sites might be hot spots for DNA double-strand breaks at specific sites followed by non-homologous recombination. Using SKY, DAPI and Giemsa staining techniques we screened normal human and mouse lymphocytes and identified several common fragile sites that have not been known before.

O002

CYTOMETRY IN VETERINARY PATHOLOGY

Kerboeuf D.

INRA, PAP, Service Commun de Cytométrie, F-37380 Nouzilly, France

Flow cytometry (FC) is a highly potent methodology for the analysis and sorting of any cells or any biological articles (mitochondria, chromosomes, nuclei) according to their fluorescent or scatter light emissions, after passage of the cells through a laser beam. FC allows rapid (several thousands of cells can be analysed within a few seconds) and very sensitive multiparameter analyses, the only condition being that cells are suspended in a liquid medium. FC is specially adapted to the detection of rare cells. FC was primarily used by immunologists for the identification and quantification of lymphocytes or any other immune cell subpopulations. The applications of FC are proliferating rapidly now, both in the direction of various research fields (immunology, genetic, bacteriology, virology, parasitology, reproduction, cell biology), of clinical diagnosis for domestic and small animals and of food and water control of quality. The analyses are facilitated by the increasing development of a large number of fluorescent antibodies and biochemical probes, which give accurate and highly specific data. All the classes of animal pathogenic agents (bacteria, parasite, virus and fungi), either isolated or included within cells have been studied now using FC. The methodology has been proved to be particularly useful for uncultivable pathogens or those requiring long time cultures. Another field of increasing interest is analysis of germinal or sperm cells for diagnosis of abnormalities, assessment of the quality of sperm or viability. FC is also developing for toxicology and pharmacology studies.

O012

TOWARDS THE PREDICTION OF HUMAN SPORADIC COLORECTAL CANCER (CRC) PROGRESSION WITH THE CONTRIBUTION OF FLOW CYTOMETRY

Giaretti W.

Laboratory of Biophysics and Cytometry, Department of Preventive Oncology National Institute for Cancer Research, Genova, Italy.

Understanding of the mechanisms regulating apoptosis, proliferation and chromosomal instability (CIN) during the colorectal adenoma-carcinoma transition in dependence from the common genotype profile characterised by APC, k-ras and p53

mutations is progressing. Flow cytometry has an important role in assessing quantitative biomarkers in both in vitro models and in human pathological material to contribute to this understanding. The expected results should have clinical impact in both the chemoprevention of CRC progression and in the prediction of long term survival of at risk patients.

Examples of applications will be given. In particular, the presented studies will try to illustrate: the controversial role of DNA aneuploidy (a likely effect of CIN) in predicting CRC patient survival; the possible link between k-ras mutations and DNA aneuploidy and their use to predict CRC patient survival; the possible link between 1p deletions and DNA aneuploidy; the possible links between APC, k-ras and p53 mutations, and aneuploidy with inhibition of apoptosis induced by agents potentially useful in the chemoprevention of CRC progression.

Q003

SAMPLING PROCEDURES IN PATHOLOGY

van Diest P.J.

Department of Pathology, VU Medical Center, Amsterdam, The Netherlands

Sampling is a key issue in pathology, as most material that reaches the pathology lab will be too big for complete scrutiny. Sampling is therefore unavoidable and occurs on several levels: blocks from resection specimens, sections within blocks, and areas within sections. The experience of the pathologist in interpreting the macroscopic aspect of resection specimens is crucial in the selection of material to be processed to paraffin blocks (level 1), but especially tumour specimens often show a morphological (and thereby probably genetic) heterogeneity that is unobvious at macroscopy. Therefore, there are macroscopic sampling rules for many tumours at different sites to ensure sampling of sufficient representative material or proper orientation. These sampling rules may differ from site to site and with the clinical context, e.g. when dissecting a resection specimen of an osteosarcoma after chemotherapy one especially looks for non-necrotic tumour parts, whereas in a uterine leiomyomatous process the necrotic parts only may lead to a diagnosis of sarcoma. Still, characteristic or clinically relevant parts may be missed which may even lead to false diagnosis or suboptimal results of analytical cellular techniques. Also between different levels within blocks (level 2) there may be

heterogeneity, so in some settings (e.g. sentinel lymph nodes) it is advised to cut step sections to arrive at the correct diagnosis or optimal results of analytical cellular techniques. However, as carefully oriented blocks give usually a good section through the (tumour) tissue, heterogeneity within block levels is much less outspoken than between blocks. On the third level of areas within sections, heterogeneity may again be outspoken, so sampling rules to choose relevant areas for analytical techniques (under HE control using microdissection if necessary for non-morphological techniques) are important. These may focus on particularly relevant areas (e.g. the periphery of tumours for proliferation) but will usually comprise some form of systematic sampling as has been well worked out for morphometry, stereology and immunoquantitation. Obviously, the above also holds for frozen material, and should be carefully considered in new approaches which are particularly liable to heterogeneity problems such as tissue arrays.

R038
GENETIC TOXICOLOGY AND IMAGE ANALYSIS

De Méo M., Orsière T.

Laboratoire de Biogénotoxicologie et Mutagenèse Environnementale (EA 1784), Facultés de Pharmacie et de Médecine, Université de la Méditerranée, Marseille, France

Since the 80's, image analysis has been introduced in genetic toxicology to improve speed and accuracy measurements of some assays. The comet assay and the Cytokinesis Blocked Micronucleus assay (CBMA) are two examples of such applications. The comet assays allows the detection and the quantification of induced-DNA damage in individual cells. The DNA lesions include single and double strand breaks, alkali-labile sites and incomplete excision repair sites. This assay is rapid, sensitive, easy to perform and cost-effective. From the first manual quantitative evaluation of DNA damage in 1988, image analysis rapidly improved measurement accuracy and authorized to create new parameters to quantify DNA damage. Several semi-automated softwares became commercially available and finally a fully automated system has been published (1999). CBMA is a mutagenic assay for in vitro studies and human biomonitoring. CBMA assesses both chromosomes loss and chromosome breakage in cells

that complete nuclear division. Loss of chromosomes and chromosome breakage can be distinguished by applying fluorescent in situ hybridization of pancentromeric probes. There is a need for an automated scoring system for rapid and reliable data acquisition that would be based on the scoring of slides prepared for visual scoring. Several image-processing softwares are commercialized. Usually, these softwares are made up of several different components. Developments in automated scoring procedure will be presented.

W004
TISSUE MICROARRAY ("TISSUE CHIP") TECHNOLOGY FOR HIGH-THROUGHPUT MOLECULAR PROFILING OF CANCER

Kallioniemi O.-P.

Cancer Genetics Branch, National Human Genome Research Institute, National Institutes of Health, Bethesda, MD 20892, USA.

Tissue microarray (TMA) technology allows rapid visualization of molecular targets in thousands of tissue specimens at a time, either at the DNA, RNA or protein level. The technique facilitates rapid translation of molecular discoveries to clinical applications. By revealing the cellular localization, prevalence and clinical significance of candidate genes and proteins, TMAs are ideally suitable for large-scale molecular profiling of cancer and other diseases.

TMAs have a number of advantages as compared to conventional molecular pathological techniques. The speed of molecular analyses is increased by more than a hundred fold, precious tissues are not destroyed, and a large number of genes and proteins can be analyzed from consecutive TMA sections. The ability to study archival tissue specimens is an important advantage as such specimens are usually not suitable for other high-throughput microarray technologies, such as cDNA microarrays and protein arrays. Thousands of archival specimens are readily available for TMA construction and often come with associated demographic, clinico-pathological, treatment and follow-up information. Construction and analysis of TMAs can be automated, increasing the throughput even further.

Most of the applications of the TMA technology have come from the field of cancer research. Examples include analysis of the frequency of molecular alterations in large tumor materials, exploration of tumor progression, identification of

predictive or prognostic factors and validation of newly discovered genes as diagnostic and therapeutic targets. TMAs provide a high-throughput methodology for microscopic examination of tissue specimens in the post-genome era.

W005

GLOBAL ANALYSIS OF CELLULAR FUNCTIONS WITH MICRO SYSTEMS

Marguerie G.

CEA Génopole, 2, rue Gaston Crémieux, 91057 Evry, France

security, regulatory issues including multinational physician licensing, hospital credentialing and “impaired physician” supervision, legal issues such as vicarious liability and malpractice exposure, reimbursement issues, and standard-of-care issues. Infrastructure issues include standards, bandwidth requirements, network scalability, and equipment interoperability. Provider and user acceptance of telepathology is variable but improving.

For pathologists and their patients, there are many potential benefits from globalization of telepathology and telelearning.

Y015

GLOBALIZATION OF TELEPATHOLOGY AND TELELEARNING

Weinstein R.S.

Department of Pathology and The Arizona Telemedicine Program, The University of Arizona, Tucson, Arizona, USA.

Globalization of telepathology will enable individual pathologists to render diagnoses for patients in many countries, develop and expand subspecialized clinical practices, and rapidly implement new diagnostic technologies. Globalization of telelearning promises to increase accessibility to high level expertise through direct interactions with experts, including telementoring, participating in “virtual classroom” activities, and increased availability of video-streamed courseware, tutorials, and professional meeting proceedings. Novel activities such as multi-site tumor boards, virtual autopsies, and telepathology-based proficiency testing and case simulations have been validated in test-of-concept demonstrations and could become commonplace.

Globalization of telehealth and teledistance education is being fostered by the rapid build out of broad band Internet, competition among health care service providers to participate in international telemedicine practices, and the endorsement of telemedicine by many governmental agencies including the European Union, the United Nations, NATO, and departments of defense in many countries. Numerous funding agencies sponsor telemedicine/telepathology research.

Some barriers to globalization of telehealth include issues regarding patient privacy and information

Submitted Oral and Poster Contributions
**A001
NUCLEOLAR MORPHOMETRY IN FINE
NEEDLE ASPIRATION BIOPSIES OF THE
PROSTATE**

Buhmeida A., Kujari H., Collan Y.

Department of Pathology and MediCity Research Laboratory, University of Turku, FIN-20520 Turku, Finland

A computerized interactive morphometry program was used to outline nucleoli of prostate cells, to find out efficient morphometric nucleolar features for distinguishing different prostatic atypia groups in FNAB. The samples were classified cytologically into definitely benign (N=10), atypical but benign (N=13), moderately atypical (N=13), highly suspicious (N=13), and definitely malignant samples (N=17). The analysis revealed a difference in the number of nucleoli between definitely benign samples and other atypia groups, but not between the latter. Nucleolar size features were best in distinguishing between atypia groups. The sample-associated mean size features were more powerful than cell group-associated size features. The sample-associated mean area, defined from cells selected by an experienced cytologist, if larger than 2.0 square micrometer, was strongly associated with definitely malignant samples. The same was true for the largest nucleolar area, the mean area of five largest nucleoli, and the mean area of 10 largest nucleoli if larger than 5.0 square micrometer, 4.0 square micrometer, or 3.5 square micrometer respectively. We concluded that morphometric nucleolar size features appeared efficient in distinguishing between definitely malignant samples, and other samples.

**A002
CYTOLOGIC AND DNA-CYTOMETRIC
EARLY DIAGNOSIS OF ORAL CANCER**

Böcking A. 1, Henßge E. 1, Pomjanski N. 1, Knops K. 1, Remmerbach T. 2, Weidenbach H. 3

1) Institute of Cytopathology, Heinrich-Heine-University, Moorenstr. 5, D-40225 Düsseldorf, Germany, 2) Clinic of Oral, Maxillo-facial and Plastic Surgery, University of Leipzig, Nürnberger Str. 57, D-04103 Leipzig, Germany, 3) Institute of

Pathology, University of Leipzig, Nürnberger Str. 57, D-04103 Leipzig, Germany

Aims: To report on diagnostic accuracy of conventional exfoliative brush cytology, taken from white-spotted, ulcerated or other oral lesions suspicious for cancer in combination with DNA-image-cytometry.

Methods: Cytological and DNA-cytometric diagnoses from 250 patients were compared with histological and clinical follow-up's in a blinded prospective-multicenter study.

Results: Sensitivity of conventional cytological diagnosis for the detection of cancer cells was 94.5 %, specificity 99.5 %, positive predictive value 98.1 %, and negative 98.5 %. Sensitivity of cytometry using DNA-aneuploidy as a marker was 96.3 %, specificity 99.5 %, positive predictive value 98.1 %, and negative 99.0 %. The combination of both methods yielded 98.2 % sensitivity, 99.5 % specificity, 98.2 % positive, and 99.5 % negative predictive value. One seemingly false positive case showed reappearing leukoplakia.

Conclusions: Brush cytology is a sensitive and specific sensitive, rapid, nominative and cheap method to early identify oral cancers. Diagnostic accuracy can be improved applying DNA-image-cytometry in dubious cases.

**A003
HUMAN BONE MARROW CULTURES AND
CHROMOSOMAL ABNORMALITY STUDY
OF CML.**

Al Achkar W.

Molecular cytogenetics Lab., Molecular Biology and Biotechnology Dept. Syrian Atomic Energy Commission, Damascus-Syria. P.o Box: 6091.

Human bone marrow cultures to study the chromosomal aberrations associated with some hematological disorders in Syria such as Chronic Myeloid Leukemia (CML) were used.

43 Bone marrow or blood samples of suspected patients were investigated and their karyotypes were obtained, either by direct fixation or after 24 or 48 hours cultures.

By classical cytogenetic study, many abnormal karyotypes reflecting CML cases with Philadelphia chromosome (Ph.C.) were found. 22 Cases of positive Ph.C. or t (9; 22), one case with Trisomy 19/Ph+, a case with t (4;22) classified as CML variant translocation and one case with Trisomy 9 (AML) were observed.

A004

DEVELOPMENT OF A FULLY AUTOMATED DNA IMAGE ANALYSIS ROUTINE FOR EVALUATION OF TESTIS BIOPSIES

Gschwendtner A., Sangha P., Mairinger T.
Department of Pathology, University of Innsbruck, Müllerstr. 44, A - 6020 Innsbruck, Austria

Study objective:

To investigate the possibility of creating an image analysis routine using multiple nuclear texture features to automatically determine a Johnsen Score equivalent of testis biopsies.

Design:

The study population consisted of 144 samples (96 preparations from orchiectomies, 27 specimens of tumour surrounding non-pathological testis-tissue and 21 samples from autopsies). Nuclear texture features were determined using image analysis of single-cell preparations. Discriminant functions were analyzed by multivariate regression analysis in order to build a binary tree for distinguishing cell maturation. A training-set was computed according to multiple regression which facilitated the computing of a Johnsen-score equivalent. The relation was proven by a Pearson's correlation test.

Results:

Due to regression analysis of the training set we could attain a general straight line equation which is based on the partial regression coefficients and the percentages of the single cell types. The analysis of the test-set according to that scheme showed a statistically significant correlation between the common semiquantitative method and the calculated Johnsen-score equivalent (Pearson 0,747 p=0,01). The average difference between both techniques was 0,98 (sd=0,799).

Conclusion:

DNA image analysis using nuclear texture features revealed to be a suitable tool to evaluate the fertility of patients using single cell preparations of testis biopsies. The characteristics of this method ensure a

high degree of accuracy and a maximum potential of automation.

A005

ASSOCIATION BETWEEN EFFECTIVENESS OF ANTI-INFLUENZA VACCINATION AND NK CYTOTOXIC ACTIVITY IN THE HEALTHY ELDERLY

Mysliwski A. 1, Trzonkowski P. 1, Brydak L. 2, Szmit E. 1, Mysliwska J. 1, Machala M. 2, Dobyszek A. 1, Foerster J 3.

1) Department of Histology and Immunology Medical University of Gdańsk, 2) National Institute of Hygiene in Warsaw, 3) Geriatric Outpatient's Department in Gdańsk, Poland

The level of the anti-haemagglutinin and anti-neuraminidase antibodies was compared within a group of 55 healthy elderly (65-92) and 30 young (19-35) people, after an anti-influenza vaccination in the season 1999/2000. Simultaneously the values of NK cell number and NK cytotoxic activity were monitored before, one month and six months after a vaccination. Analysis of the NK cells was done with FITC and PE-conjugated Moab: anti-CD16, CD45RA, CD45RB and CD45RO on flow cytometer (Epics XL) (Coulter). NK activity was measured with the Cytotoxicity Detection Kit (Boehringer Mannheim). About 6 % in both vaccinated age groups contracted influenza. The results of our study revealed that elderly and young had similar levels of all antibodies. The elderly had higher levels of NK cells and NK cytotoxic activity than the young. One month after a vaccination, the healthy elderly had significantly higher levels of anti-H3, HB1 and N2 antibodies together with higher levels of NK cells and NK activity than those elderly who underwent influenza. Their cytotoxic activity raised one month after a vaccination whereas in all the remaining groups it stayed at the same level. Our results suggest that an effective anti-influenza vaccination of the healthy elderly is associated with both high antibody and NK responses.

A006

TWO SUBGROUPS ARE IDENTIFIED IN ATYPICAL CHRONIC LYMPHOPROLIFERATIVE DISORDERS (CLPD) : IMPACT OF CD20 AND P27^{kip1} EXPRESSION

Troussard X., Salaün V., Valensi F., Picard F., Ajchembaum-Cymbalista F.L.
Hematology Department, CHU Caen, Necker, Cochin, Hôtel Dieu Paris. France

The conjunction of clinical and biological features allows to achieve an accurate diagnosis in many cases of CLPD. However some leukemic CLPD do not achieve the criteria for a diagnosis and are referred as atypical CLL. The aim of this multicentric prospective study was to help classifying these cases using independent assessment of blood morphology, immunophenotype, cytogenetics, cyclin D1 and cyclin kinase inhibitor p27^{kip1} expression. Ninety untreated patients with lymphocytosis ($>4 \times 10^9/l$) and an immunologic score ≤ 3 were included since 1999. Scoring was compounded on five markers sIg, CD5, CD22, CD23, FMC7. In seventeen cases, CLPD was classified and in 22 cases an expression of cyclin D1 was detected. The remaining 51 cases with D1- atypical CLPD could be divided in two groups by the intensity of CD20 (17 dim, 34 bright). A strong correlation was also found between intensity of CD20 and p27 expression: Dim CD20 was strongly related to high p27 expression ($p < 0.0001$), which was identical to a control group of 25 typical B-CLL. Conversely, p27 expression in the CD20 bright group was similar to that of the 22 D1 positive cases. These results suggest that D1- atypical CLPD could be distributed into two subgroups: CD20 dim and high p27 expression (close to typical CLL) and CD20 bright and low p27 expression (close to more proliferative lymphomas).

A007
OPTIMIZING STRATEGIES IN BRINGING RESULTS OF CANCER RESEARCH TO CLINICAL PRACTICE

Collan Y., Kuopio T.

Departments of Pathology, University of Turku, FIN-20520 Turku, Finland, and Jyväskylä Central Hospital, Jyväskylä, Finland

Modern cancer research can be viewed as a science which is developing at two levels. New types of results are being gained in the laboratory and they will improve our understanding on the pathogenesis, diagnosis, prognostication, prediction of therapy response, and potential treatment of cancer. The other level is that of association of the results with the clinical setting which finally will result in the

implementation of the valuable methodology in practice. To find the most suitable features, optimization of the features for the planned use is necessary. Only after optimization, different features can be compared reliably.

The features are often quantitated on a continuous scale, and optimization is associated with the selection of the most appropriate cutpoint. Corresponding cutpoints are looked for also when non-continuous or distinct scales are applied. The optimization of the cutpoint can be based e.g. on a search for highest attainable specificity, sensitivity, or efficiency, the best survival association, the best association with recurrence, or metastasis. In many applications, the highest kappa coefficient, or the highest attainable khi square value can be used as the basis for optimization. The last mentioned method can be applied in the comparison between survival curves. The methods can be applied to many situations. We have recently tested the optimization in association with interpretation of the DNA histogram from sections, in finding the DNA cytometric features best suitable for helping to distinguish between stable and progressive prostate cancer, in defining the optimal cutpoints for morphometric grading, and in finding the most optimal immunohistochemistry staining scores for clinical use.

A010
MIB-1 IMMUNOSTAINING IN LUNG CYTOLOGY TO DIFFERENTIATE BETWEEN SMALL CELL LUNG CANCER AND RESERVE CELL HYPERPLASIA

Grefte J., Bulten J., Salet-van de Pol M., Gemmink J., De Wilde P., Hanselaar A.

Department of Pathology, University Hospital Nijmegen, The Netherlands

Background: In degenerated sputa, bronchial brushes, and washings, it may be extremely difficult to differentiate between reserve cell hyperplasia (RCH) and small cell lung cancer (SCLC). The present study investigates whether detection of the proliferation associated

Ki-67 antigen may be of value in this decision.

Materials and methods: Retrospectively, 20 Papanicolaou-stained sputa, bronchial brushes, or bronchial washings from 20 different patients were selected. Ten were diagnosed as RCH (and had no SCLC in follow-up); the other ten as SCLC

(histologically confirmed). All 20 Pap-stains were restained with the monoclonal antibody MIB1, directed against Ki-67 antigen, according to a simple and reliable procedure described recently (J. Pathol. 2000; 190: 545-553). In each specimen 5 coherent cell groups were identified, corresponding with RCH or SCLC, respectively, photographed, and studied for Ki-67 expression. The Ki-67 labeling index (LI) of the specimens was determined as the number of MIB1 positive cells divided by the total number of cells in the photographed cell groups.

Results: All cases of SCLC showed a Ki-67 LI of at least 0.45, whereas in the cases with RCH, the Ki-67 LI was never higher than 0.20. The difference was highly significant ($p < 0.001$). Discriminant analysis resulted in a classifier with which we were able to discriminate correctly between SCLC and RCH in 100% of the described 20 sputa, bronchial brushings and washes.

Conclusion: The results clearly demonstrate that immunocytochemical detection of the proliferation-associated Ki-67-antigen by MIB1 restaining of Papanicolaou-stained sputa, bronchial brushings and washes, helps in accurately differentiating RCH from SCLC.

A011 THE ULTRASTRUCTURAL DIFFERENTIATION OF LYMPHOID TISSUE AND HAEMOTOLOGIC SYSTEM TUMORS

G.Hüseyin G., Kayapinar R.
Trakya Üniv. TIP FAK. Patoloji ABD. 22030-Edirne/Turkey.

10 patients, diagnosed as Hairy Cell Leukemia, Sézary's Syndrome, Giant Cell Lymphoma, non-Hodgkin Lymphoma by light microscopy.

In Hairy Cell Leukemia cases, "B" cell lymphocytes were identified generally. Specific ultrastructural properties of these cells were observed. Thin hairy projections in outer membranes, nuclei with large oval diffuse chromatin and a few organelles in narrow cytoplasm were seen.

In Sézary's Syndrome, leukemia cells consisted of lymphocytes. There was no change of organelles in cytoplasm. Specific changes were identified in nucleus. Nuclei with invaginations and projections, serpentine shape were seen. Tumor cells of Giant Cell Lymphoma, consist in plasmocytes. Nuclei of the plasmocytes were irregular and with diffuse chromatin. In large cytoplasm, large amount

endoplasmic reticulum, free ribosomes, Golgi complex, mitochondria and other organelles was found. The surface of outer membranes were smooth and there were no projections and cell junctions.

In the case of non-Hodgkin Lymphoma a big amount of plasmocytes was seen. Nuclei were generally invaginated, nucleolus were projected and cytoplasm was basophilic. In cytoplasm, phagosomes, lysosomes and azurophilic granules were found.

These tumors are often confused with epithelial tumors, neuroblastoma, rhabdomyosarcoma and other tumors. In our evaluated cases, intercellular junctions, tonofilaments and basal membrane characterizing epithelial cells origin; neurofibrils, neurosecretory granules and synapses characterizing neuroblastomas; myofilaments characterizing rhabdomyosarcomas were present.

With the electronmicroscopic properties, the histogenesis of leukemia and lymphoma were investigated and differential diagnosis were presented in details.

Reference: I.P.C. Cross, *Cell and tissue ultrastructure*. p. 52-103.

A012 ASCUS/AGUS: DETECTION OF PRECANCEROUS LESIONS IN CERVICAL CYTOLOGY

Bertino B., Hammou J.C., Ploem J.S.
Cabinet de pathologie Nice - France

The purpose of this study is to propose a strategy to detect eventual significant lesions in woman with a PAP specimen classified as ASCUS/AGUS:

The use of a liquid based cytology has improved the diagnostic sensitivity over conventional Pap smears. But even with this optimized procedure, rare abnormal cells are not always seen with routine cytology. We estimate that rare abnormal cells below frequency of 0.05% can be visually overlooked by well qualified cytotechnicians in the practice of routine cytology.

Biological tests such as the detection of carcinogenic HPV- DNA show often a higher sensitivity in specimens with very few abnormal cells. High risk HPV has been detected in more than 40% of ASCUS/AGUS cases (Autillo-Touati, 1998, Clavel, 1999). However high grade lesions are found in only about 6% of such cases (Ferris, 1998). Many of the HPV positive cases are known to show clinical regression to negativity with time. There is a need for

a biological method that could detect a sub-class of the HPV-positive cases that already might show high grade lesions. As such, DNA heterogeneity in rarely (<0.01%) occurring abnormal cervical cells could perhaps be used (Van Driel-Kulker, 1985).

In the HPV-positive ASCUS/AGUS specimens were examined for abnormal DNA-heterogeneity in > 50.000 cells. This study confirmed the presence in 24 % of the all HPV-positive cases, of a very small number of cells with high DNA-heterogeneity. These (HPV+DNA positive) cases were subsequently referred for Colposcopy. Biopsies and histological examination showed a lesion in more than 80%, and a high grade lesion in about 50% of the cases (Bertino, 2000).

We conclude that this represents a significant lowering of the false negative rate in cervical cytology by only examining about 3% of all the cervical specimens in our laboratory for HPV and DNA.

**A013
TOWARDS A GENETIC-BASED
CLASSIFICATION OF LUNG CANCER**

Petersen I.

Institute of Pathology, Charité University Hospital, Berlin, Germany

Lung cancer is a highly aggressive neoplasm which is reflected by the multitude of genetic aberrations that are detectable on the chromosomal and molecular level. In order to understand this seemingly genetic chaos, we performed Comparative Genomic Hybridisation (CGH) and gene expression studies on a fairly large number of human lung carcinomas. Despite the considerable chromosomal instability being reflected by the well-known morphological heterogeneity of lung cancer, the comparison of different tumour groups using customized computer software revealed recurrent aberration patterns and highlighted chromosomal imbalances that were significantly associated with morphological histotypes and biological phenotypes such as metastasis formation. Based on the CGH data, we established a new model for the development and progression of lung cancer. It suggests that both small cell (SCLC) and non-small cell lung cancer (NSCLC) evolve from the same stem cell. SCLC representing the most advanced and aggressive subtype is differentiated into primary and secondary tumors. Whereas primary SCLC

corresponding to the classical type evolves directly from the precursor cell, secondary SCLC correlating with the combined SCLC develops via an NSCLC intermediate. In addition, we established libraries of differentially expressed genes and performed expression profiling aiming at the identification of new candidate genes and a refined classification of lung cancer.

**A014
COMBINING THE QUALITATIVE WITH THE
QUANTITATIVE FOR THE
ANALYSIS OF CHEMOPREVENTION DATA**

MacAulay C. 1, Guillaud M. 1, LeRiche J. 1, Gazdar A. 2, Lam S. 1

1) BC Cancer Agency, Vancouver, BC, Canada V5Z 1L3, 2) Univ Texas, Southwestern Medical Centre, Dallas, TX 75235-8593, USA

Over the last 4 to 5 years, the utility of quantitative microscopy on 2D tissue sections in small studies for the grading of preinvasive epithelial lesions in the lung, cervix, prostate and breast have been demonstrated. As part of several NIH funded chemoprevention studies (Retinol, Sialor, Pulmicort and ZSP), we have collected ~3500 bronchial biopsies which have all been analyzed using quantitative microscopy. These analyses have been very informative and show that combining quantitative measurements with histopathological interpretation can improve the robustness and power of the analysis to detect drug efficacy as compared to histopathological interpretation alone. Site by site and subject by subject analysis of these chemoprevention trials will be shown to illustrate the increase in the consistency of the results. The current method of quantitative analysis also strongly suggests that much valuable information is lost in going from the native 3D nature of tissue to the 2D conventional sections currently analyzed. How this information might be retrieved will also be discussed.

**A015
USE OF QUANTITATIVE SPUTUM
CYTOLOGY FOR DETECTION OF EARLY
LUNG CANCER**

Palcic B., Garner D., Beveridge J., Todorovic C.
Cancer Imaging Department, BC Cancer Agency and
Perceptronix Medical Inc., Vancouver, BC Canada

Lung cancer is responsible for nearly 30% of all cancer related deaths. There has been no significant improvement in treatment of lung cancer patients over the last couple of decades. At present, for newly diagnosed lung cancer, 5-year survival probability is less than 15%. The main reason for such poor prognosis is the fact that in the great majority of cases, lung cancer is detected at a late, invasive stage. It has been shown that when lung cancer is detected at an early, non-invasive or micro-invasive stage, that lung cancer can be treated with a success rate of over 95% (stage 0) and 60-85% (stage 1A & 1B), respectively, leaving the surviving patients with a good quality of life.

We have been working on the development of quantitative sputum cytology to improve the detection of early lung cancer in non-symptomatic subjects. This involves special sputum sample preparation, staining of cells with DNA specific and stoichiometric stain and measurements of a large number (several thousand) of cell nuclei of selected sputum cells using a fully automated, high resolution image cytometer. We will report the results of this approach, which yields a several-fold increased sensitivity, compared to conventional cytology, at a specificity of 90%. The discussion will address the role of quantitative sputum cytology in a comprehensive approach to prevention of invasive lung cancer in selected (targeted) sub populations of very high-risk individuals.

A016

RELATIONSHIP BETWEEN THE PRESENCE OF ONCOGENIC HPV DNA ASSESSED BY POLYMERASE CHAIN REACTION AND KI-67 IMMUNOQUANTITATIVE FEATURES IN CERVICAL INTRAEPITHELIAL NEOPLASIA

Kruse A.-J. 1, 2, Baak J. 1,2, De Bruin P. 2, Van de Goot F., Kurten N. 2

1) Departments of Pathology, Free University Hospital, Amsterdam, 2) Medical Centre Alkmaar, Alkmaar, The Netherlands

Aim: To study which Ki-67 immunohistochemical parameters correlate with the presence of oncogenic Human Papillomavirus (HPV) in cervical intraepithelial neoplasia (CIN) lesions.

Materials and methods: HPV polymerase chain reaction (PCR) and Ki-67 immunohistochemical analysis was performed on 90 consecutive biopsies (16 CIN 1, 35 CIN 2 and 39 CIN 3). CIN grade was assessed

routinely by 6 different pathologists. The presence of the lesion was confirmed in a histologic section following the material used for PCR and Ki-67 analysis.

Results: Eight of the nine Ki-67 immunohistochemical features showed a significant difference between the oncogenic HPV positive and negative cases. The best single discriminator was the 90th percentile of the stratification index (SI90). All 61 cases with Ki-67 SI90 > 0.60 were HPV positive (68% of the total group studied). 16 of the 29 cases with SI90 ≤ 0.60 were negative and 13 positive for oncogenic HPV and none of the Ki-67 features (either single or combined) could distinguish these positive and negative cases. Using stepwise multivariate analysis, the best discriminating combination of features was SI90 and the percentage Ki-67 positive nuclei in the deep third layer of the epithelium (PERC DL). The combination of SI90 and the percentage Ki-67 positive nuclei per 100-micrometer basal membrane was nearly as strong as that of the SI90 and the PERC DL. With these two features, 86% of the cases was correctly classified. The subjective estimate of SI90 (> 0.60 or ≤ 0.60) by two independent observers was not accurate and not well reproducible.

Conclusions: In CIN lesions, Ki-67 immunohistochemical features and presence of oncogenic HPV are highly correlated. Subjective impressions of SI90 are not as accurate or reproducible as quantitative image analysis results.

B002

KEY APOPTOSIS AND CELL CYCLE REGULATORY PROTEINS IN COLORECTAL CARCINOMA: RELATIONSHIP TO DUKES' STAGE AND PATIENT SURVIVAL.

Elkablawy M.A., Maxwell P., Williamson K., Anderson N., Hamilton P.W.

Quantitative Biomarker Group, Department of Pathology, Cancer Research Centre, Queen's University of Belfast, UK.

Quantitative assessment of apoptotic index (AI) and mitotic index (MI) using cell counts and the immunoreactivity of p53, bcl-2, p21 and mdm2 were examined in 30 colonic and 22 rectal adenocarcinomas.

Immunohistochemical phenotyping showed eleven different combined immunophenotypes. Individual features and combined profiles were correlated with clinicopathological parameters as well as patient

survival as potential prognostic markers. Increased AI was significantly associated with bcl-2 expression ($p < 0.008$) and the immunoprofiles showing bcl-2, but not with MI, p53, p21 or mdm2. AI was significantly associated with increased Dukes' stage from A, B to C ($P < 0.02$) but not D stage, while MI showed a significant association with all Dukes' stages ($p < 0.05$). No significant association was found between either AI or MI and prognosis. p53, p21, mdm2 and bcl-2 positivity were detected in 65.4%, 53.8%, 65.4% and 34.6% of cases respectively. Mdm2 was significantly associated with p53 ($p < 0.03$) and p21 ($p < 0.04$) expression. p53 immunoreactivity was more prevalent in rectal tumours ($p < 0.008$). In univariate survival analysis, bcl-2 overexpression was associated with more favourable patient survival ($p < 0.03$). Also, positive combined patterns p53+/p21+/bcl2+ and p21+/mdm2+/bcl2+ ($p < 0.005$); p53+/bcl2+, p21+/bcl2+ and mdm2+/bcl2+ ($p < 0.01$) and p53+/p21+ ($p < 0.02$) were associated with favourable clinical outcome. In multivariate Cox survival analysis, bcl-2 ($p < 0.016$) and Dukes' stage ($p < 0.000$) were the only significant independent prognostic indicators. We conclude that bcl-2 immunoreactivity was associated with apoptosis and could be used in combination with Dukes' stage as a means of predicting prognosis in colorectal cancer.

B003

PROGNOSTICATION OF BREAST CANCER BY QUANTITATION OF E-CADHERIN IMMUNOSTAINING: THE METHODOLOGY AND CLINICAL RELEVANCE

Elzagheid A. 1, Collan Y. 1, Kuopio T. 2

1) Department of Pathology, University of Turku, Kiinamyllynkatu 10, FIN-20520 Turku, Finland, 2) Jyväskylä Central Hospital, FIN-40620 Jyväskylä, Finland

In our studies we wanted to develop a method best suited for the evaluation of E-cadherin immunostaining and find patient groups in which aggressive breast cancer could be distinguished from other cancers. We used paraffin embedded tissue sections from 183 patients. The method was based on the intensity and continuity of the membrane staining (graded as 0,1,2,3), and on the fraction of area of cancer tissue which was stained at respective staining grade. The cutpoint giving most significant prognostic information was at 0.35 among all patients ($p = 0.0279$), and node-positive patients

($p = 0.0009$). In multivariate analysis (all patients) E-cadherin immunoscore was inferior to mitotic index (SMI), but still significant. Among postmenopausal patients E-cadherin index was a powerful prognosticator, with a risk ratio of 0.171 for death. Among N+ patients again E-cadherin was a strong prognosticator, and superior to the still significant SMI in this patient group. E-cadherin immunostaining could also be used as a general prognosticator to the degree that the mitotic activity (SMI) and E-cadherin immunoscore alone were enough to predict survival, leaving the lymph node status and tumor size out of the prognostic model.

B005

CYTOKERATIN 19 (CK19), MIB-1, P53 AND INTRATUMORAL HETEROGENEITY IN RENAL CELL CARCINOMA (RCC). A PROSPECTIVE FLOW CYTOMETRIC AND IMMUNOHISTOCHEMICAL STUDY OF 100 CASES

Leonardi E. 1, Luciani L.G. 2, Divan C. 2, Reich A. 2, Scardigli A. 2, Paolo Dalla Palma 1

1) Department of Pathology, Santa Chiara Hospital, Trento, Italy, 2) Department of Urology, Santa Chiara Hospital, Trento, Italy

Introduction: We investigated the relationship between some RCC immunophenotypic features and tumor aggressiveness. To this end, cytoskeleton alterations, studied through CK19 expression, a polypeptide with oncofetal properties in renal tissue, were related to the DNA content and to MIB-1 and p53 expression.

Materials and methods: Up to 7 fresh samples were taken from the primary tumor, in the center and peripherally next to the normal parenchyma. Ethanol fixed pellets were labelled with CK19 (clone A53-BA2, Sigma) by an indirect immunofluorescence technique and stained with 25 gamma propidium iodide. The cells were measured with a PARTEC-PAS flow-cytometer (Partec-Dako). Intratumoral DNA patterns were classified as homogeneously diploid (H-D), homogeneously aneuploid (H-A) and heterogeneously aneuploid (HT-A). Routine histopathological tumor samples were tested for p53 expression (clone DO7) and for MIB-1 by immunohistochemical procedures. Tumors were considered positive when p53 expression was identified in more than 10% neoplastic cells. Expression of MIB-1 in neoplastic cells was divided

in tertiles: low ($\leq 10\%$), medium (11-25%), and high ($> 25\%$).

Results: 41% of cases showed H-D, 26% H-A, 33% HT-A. The expression of CK19 in neoplastic cells was found in 57 tumors (11 diploid and 46 aneuploid) and was strongly related to aneuploidy ($p=0,001$), HT-A pattern ($p=0,001$), MIB-1 values $> 25\%$ ($p=0,001$), p53 expression $> 10\%$ ($p=0,001$), stage ($p=0,05$) and grade ($p=0,001$)

Discussion: The relationships between CK19 phenotype and HT-A pattern, stage, grade and unfavorable prognostic markers, such as p53 positivity and high MIB-1 values, suggest a potential role of CK19 as a predictive factor of RCC clinical behavior.

B006
UNIVERSAL PROGNOSTIC MODEL IN NODE NEGATIVE BREAST CANCER USING DNA FLOWCYTOMETRIC DATA

Bagwell C.B., Baldetorp B., Bendahl P-O., Fernö M., Killander D. and Stål O.

Department of Oncology, University Hospitals, Lund and Linköping, Sweden, Verity Software House Inc, Topsham, Maine, USA.

Flowcytometric (FCM) DNA ploidy and S phase fraction (SPF) have in many studies shown to be important prognostic factors in node negative (N0) breast cancer. However, DNA FCM is still controversial because of lack of detailed guidelines, especially for data interpretation.

Aim: 1. To optimise the evaluation of ploidy and SPF in a model for prognostic considerations (recurrence-free survival), and 2) to test its universal use in a new data set.

Material & methods: Two sets of DNA histograms [American ($n=961$) and Swedish ($n=238$)], obtained from frozen biopsies using "in-house" analytical methods, were included. Cell cycle analysis was performed by using the ModFitLT 3.0 software.

Results: The prognostic value of ploidy status was improved by considering DNA index, size of non-diploid cell population, and number of cell populations ($p=0.00002$ vs. <0.02 , Cox univariate analysis), and that of SPF by considering debris/aggregates, and size of non-diploid population ($p=0.002$ vs. Significant ($p=0.03$) only for diploid cases).

The model including both "optimised" ploidy and "optimised" SPF was highly significant for

recurrence-free survival ($p<0.000005$). This could be confirmed in the second data set ($p<0.0001$).

Conclusion: The prognostic information, obtained from FCM DNA histograms has been improved. The validity of this improvement has been confirmed in a new data set.

B007
INVESTIGATIONS ON CYCLIN EXPRESSION AND DNA PLOIDY FROM INVASIVE DUCTAL BREAST CANCER FOR THE PREDICTION OF THE INDIVIDUAL PROGNOSIS

Theissig F., Hoffmann K., Meyer W., Baretton G., Kunze K.D.

Dresden University of Technology; Institute of Pathology; Fetscherstr. 74; D-01307 Dresden; Germany

Breast cancer is the most common malignancy in women. Therefore it is necessary to find out parameters which were able to predict the individual course of the disease to prevent over – eg undertherapy.

In this study we investigated the expression of Cyclin D1 and B1 as cell cycle regulators and the DNA ploidy in relation to the overall survival time.

116 invasive ductal breast cancer cases from the archival material were selected. The Cyclin expression was evaluated after immunohistological staining with monoclonal antibodies using the immunoreactive score introduced by Remmele.

The DNA ploidy was done on single cell preparations with a cytometry work station consisting on a 486/66 MHz PC, a MFG framegrabber, a CCD camera and an Axioplan microscope. From each case, 250 tumour cells as well as 20 internal reference lymphocytes were measured.

The results of the Kaplan Meyer statistic showed a significant longer survival from patients with euploid cancer cases. Moreover patients with a lower expression from Cyclin D1 and Cyclin B1 had a worse prognosis.

We conclude that the expression of the different Cyclins can play a role for prognosis prediction of the individual case.

Larger studies are needed to reproduce these results.

B008
G2-ARREST - A RESCUE FRACTION FOR RADIORESISTANT TUMOURS?

Erenpreisa J.E. 1, Cragg M. 2, Krampe R. 1, Ivanov A. 1, Illidge T. 2

1) Biomed.Centre Latv.Univ., Riga, LV-1067, 2) TENOVUS Res.Lab, Southampton, UK

Tumours with mt p53 are resistant to genotoxic damage. There are controversial data on the cell cycle checkpoints in them and on the value of these parameters for therapy prognosis. Our studies on four lymphoid human cell lines, wt p53 TK6 and three mt p53 - WI-L2-NS and two strains of Namalwa cell line, N99 and Nold, used DNA flow cytometry, DNA synthesis quantitative radioautography, mitotic counts, and clonogenic assays, after ranged irradiation, from 2 to 10 Gy. They revealed no G1 arrest in TK6 cell line (already known from literature), high early apoptotic response in N99, relatively high apoptotic loss of cells from the S-phase in WI-L2-NS, practically no losses of cells from S-phase in the two Namalwa substrains, however the strongest spindle checkpoint in the latter. The only indicator positively correlating with clonogenicity was the ability of cells to maximally accumulate in G2 arrest fraction, 24 hs post damage, at the increasing irradiation dosage. This value was: Nold - 13.2 Gy; WI-L2-NS- 11.1 Gy; N99 - 8.8 Gy; TK6 - 6 Gy. This research confirmed that individual cell lines in their microevolution can vary in the response of particular checkpoints to genotoxic damage. Preliminary, our data suggest that the G2-arrest fraction volume in the ranged irradiation test may represent an integrative predictive quantitative parameter of the genotoxic resistance of (lymphoid?) tumours.

B010
SIGNIFICANCE OF TH2 PROFILE IN LONG-STANDING DIABETES MELLITUS OF TYPE I

Mysliwska J. 1, Zorena K. 1, Semetkowska-Jurkiewicz E. 2, Rachoń D. 1, Bakowska A. 3

1) Department of Immunology, 2) Academic Clinic of Hypertension and Diabetes, 3) Department of Immunopathology, Medical University of Gdańsk, Poland.

The aim of our study was to look at a cytokine profile in human long-standing diabetes mellitus of type I. Thirty-five (24-67 year old) patients (duration of the

disease =11-35 years) from the Outpatient Department of The Academic Clinic of Hypertension and Diabetes in Gdańsk were enrolled into the study. Except for hypertension, they had no accompanying diseases. All of them had diabetic nephropathy and background retinopathy. The blood levels of the following cytokines: Interleukin 2, 4, 6, 10, 12, Interferon gamma and TNF alpha were measured by ELISA, using commercial kits from The Biosource. Patients were segregated into groups with a humoral response (GAD65-positive) (n=23) and those without the response to GAD65 antigen (n=12). Patients with anti-GAD antibodies were characterised by higher levels of the TH2 cytokines: IL4, IL6, IL10 and lower of IL12 (TH1-cytokine). Patients with predominance of the TH2 cytokines had better controlled levels of HbA1c, glucose and HDL-cholesterol. Moreover, TH2 predominance was associated with a lower rate of albumin excretion and a lower dose of insulin. Our results indicate that the predominance of the TH2 cytokine profile in the long-standing diabetes mellitus type I patients is associated with a better metabolic control of the disease and less progressed diabetic nephropathy.

B011
THE CONCEPT OF STRUCTURAL ENTROPY : BASIC CONSIDERATIONS AND CLINICAL SIGNIFICANCE

Kayser K. 1, Kayser G. 1, Richter N. 1, Zink S. 1, Gabius H.-J. 2

1) Department of Pathology, Thoraxklinik, Heidelberg, Germany, 2) Institute of Physiological Chemistry, University Munich, Germany

Background: Syntactic structure analysis is based upon definition of basic structural elements and an appropriate neighborhood condition. In immune/ligand histochemical images basic elements can be defined by expression of binding sites/presence of molecules detectable by appropriate probes.

Theory: In biology, structure and function form a system with a regularity of defined distances and morphometric features of basic elements which can be used to calculate the additional energies in structural disturbances. The basic formula derived from the definition of entropy in thermodynamics takes into account distance dependent energy forces ($1/\mu\text{m}^2$).

Material and methods: To analyze the clinical significance of the concept of structural entropy, the survival rates of patients with following malignancies were analyzed in relation to the amount of structural entropy and its current: Sixty patients with primary colon/rectum carcinomas and 34 patients with primary breast carcinomas each with their corresponding lung metastases; 80 patients with pulmonary carcinoids; 60 patients with non-small cell lung carcinomas; 66 patients with small cell lung cancer.

Results: In each of the 5 cohorts, the survival of patients and the disease-free interval between surgery of the primary cancer and lung metastases were significantly correlated with the amount of structural entropy. Of specific importance are binding capacities and expression of mammalian lectins.

Conclusions: The concept of structural entropy can be used to estimate the prognosis of patients with various types of lung cancer.

B012
QUANTITATIVE ASSESSMENT OF
PROLIFERATIVE ACTIVITY (PA)
PARAMETERS IN GIANT CELL TUMOURS
OF BONE (GCTB)

Frincu D.L. 1, Chirana A. 2, Frincu L.L. 1, Ardelean C. 3, Ciobanu A. 1

1) Department of Anatomy, University of Medicine "Gr. T. Popa", Iasi, 2) Rehabilitation Hospital, Iasi, 3) "V. Babes" Institute, Bucuresti, Romania

Aims. The cytologic aspect is of limited value in accurately predicting the clinical evolution of a giant cell bone tumour. The present study compare different approaches in the assessment of the proliferative cellular activity in giant cell bone tumours in comparison with their aggressiveness.

Material and methods. We studied fifty-nine patients of both sexes, presenting with bone tumours that were operated and histopathologically diagnosed as giant cell tumours, grouped according to the Jaffe and Lichtenstein's grading system. The quantitative microscopy study on the representative sections, using an interactive video-system with a professional computerized program, estimated systematically the proliferative activity (mitotic activity index, mitotic rate and mitoses/mm²). Immunohistochemical study used cellular proliferative markers as PCNA and P53 correlated with histological grades. We quantified the

number of positive and negative cells after an immunohistochemical technic on fixed paraffin-embedded tissue. *Results.* In the giant cell bone tumours the mitotic figures represent the best indicator of prognosis. Giant cell bone tumours with mitotic rate less 1/mm² were exclusively nonaggressive (Grade I and II). In aggressive tumour group (Grade III and II borderline), the mitotic index is usually in excess of 15 per 10 hpf. The percentage of PCNA-immunoreactive nuclei was low in stromal cells and did not reveal significant differences between aggressive and non-aggressive tumours. *Conclusions.* Quantification of mitotic activity of giant cell bone tumours may aid in diagnosing and predicting the biologic behaviour of these tumours, but the proliferative markers couldn't be used in the discrimination of aggressive and non-aggressive giant cell tumours.

B014
THE PREDICTING SIGNIFICANCE OF
QUANTITATIVE HISTOPATHOLOGICAL
STUDY OF UVEAL MALIGNANT
MELANOMA

Frincu L.L. 1, Frincu D.L. 1, Stolnicu S. 2, Ciobanu A. 1

1) Department of Anatomy, University of Medicine "Gr. T. Popa", Iasi, 2) Department of Pathology, University of Medicine, Targu Mures, Romania

Purpose. The uveal malignant melanoma (UMM) represents the most frequent intraocular malignant tumor. The aim of this study was to appraise the quantitative parameters of UMM in order to establish a correlation with the cell type and clinical evolution.

Material and methods. We examined 56 cases of UMM enucleated from patients of both sexes. The fragments of the tumors were embedded in paraffin, sectioned at 6 µm and H&E stained. For microscopic type we used the Callender's staging modified by AFIP. The quantitative standard and two phases (phase I = nucleus, phase two = nucleolus), nuclear and nucleolar volume measurements and proliferative activity assessment were made on the representative sections, using a professional digitizing interactive program. Statistic evaluation of the parameters and graphic representation were made automatically. We estimate the form and sense of correlations when they exist.

Results. We observed a variability of the size of the

nucleus: the long axis (μm) increase from 11.05 in UMM spindle classic to 11.19 in UMM spindle pleomorphic to 14.07 in UMM mixed classic and to 15.49 in mixed pleomorphic UMM, being able to be useful for predicting fatality. Mitotic rate has the highest values in mixed classic (7%) and mixed pleomorphic (9%) UMM. Mitotic density has the highest values in mixed UMM: classic (49.7/mm²) and mixed pleomorphic (74.8/mm²).

Conclusion. Our results suggest that the assessment of the nucleus and nucleolus dimensions and the proliferative activity have essential prognostic value.

B015
QUANTITATIVE PARAMETERS IN PREDICTING RECURRENCE OF ORAL EPIDERMIOID CARCINOMA

Crisan Dabija R. 1, Frincu L.L. 1, Calin D.L. 1, Radulescu D. 2

1) Department of Anatomy, University of Medicine " Gr. T. Popa ", Iassy, Romania, 2) Department of Pathology, University of Medicine " Gr. T. Popa ", Iassy, Romania

Purpose. In this study we proposed to investigate quantitatively the squamous cell carcinoma of the lips and to discuss the importance of these parameters for diagnosis and prognosis.

Material and methods. It used 18 pieces obtained from 11 patients operated for squamous cell carcinoma of the lip. From 5 patients were obtained tumor's relapses (one with two relapses) which can estimate the evolution and prognosis. The pieces were processed through paraffin-technique and stained with H&E. An interactive digitizing video overlay system with two-phase measurements was used : phase one = cell, phase two = nucleus. In each case, we measured thirty cells and we calculated the area, perimeter, diameter, long axis, short axis, area difference, area ratio, eccentricity, etc. The results were statistically processed and we estimated the form and sense of correlations if they existed.

Results. From among the studied morphometrical parameters, the cellular and nuclear cancerous areas present the smallest stability, and have an accented dispersion of the values. In case of relapses, the quantitative appearance is more evident at fourteen months from the primary tumor ablation. There is an explosive increase of the parameters, similar to the primitive tumor appearance, but at a superior

quantitative level. In the primary tumor that gives relapses, therefore with high-risk, the cellular area is smaller than in case of tumors without relapses, with low-risk. The nucleus has an approximate identical area, but the cancerous cells have a greater variability of the form-factor parameters.

Conclusion. The obtained results indicate that among the studied parameters, the cellular and nuclear areas have an independent prognostic value for the relapse appearance.

B016
OUTCOME PREDICTION IN HIGH-GRADE NON HODGKIN LYMPHOMAS BY DATA PATTERN ANALYSIS OF APOPTOSIS, APO-REGULATING PROTEINS, CELL PROLIFERATION AND CLINICAL PARAMETERS

Valet G. 1, MacNamara B. 2,3, Mazur J. 4, Strömberg M. 5, Liliemark J. 5, Porwit-MacDonald A. 2

1) Max-Planck-Institut for Biochemie, Martinsried, Germany, 2) Depts. Pathology, Karolinska Hospital, Stockholm, Sweden, 3) Biol.Sciences, Dublin Inst.Technology, Ireland, 4) Epidemiology & Health-Care Planning, Inst.Mother & Child, Warsaw, Poland, 5) Oncology, Karolinska Hospital, Stockholm, Sweden

Goal: Disease course prediction by data pattern analysis with the CLASSIF1 triple matrix algorithm (<http://www.biochem.mpg.de/valet/classif1.html>) on cell death/ apoptosis (p53, BCL2, BAX, BAK, WAF, LMP1, %MIB, %APO, %cyclin A, MCL1) related as well as on clinical parameters (age at diagnosis, sex, stage, symptoms at diagnosis, LDH, extranodal involvement, number of risk factors, risk group) in 56 patients with 6-19 years follow up.

Results: Predictive values of 92.8/72.4% for response duration >24m/<24m in the learning set (n=27/17) and of 83.3/55.5% (n=7/5) for the unknown test set with decreased BCL2, risk factor, risk group and disease stage at increased BAK and MCL1 for responders >24m. Lymphoma progression/no progression classified with 81.8/41.0% (n=41/20) at increased LDH, %APO and number of extranodal sites. Survival >120 months/non survival classified with 91.3/42.3% (n=36/13) at increased BCL2, % APO and %cyclin A for non survivors. Classification of molecular and clinical parameters against

morphology provided predictive values between 70.0 to 25.0% for the REAL and Kiel classification.

Conclusion: High predictive values for response >24m, progression and survival >120m as well as robustness for the classification of unknown lymphoma patients show that data pattern analysis has an interesting potential for individually predicting disease outcome.

B017
MEASUREMENT OF MARKERS FOR
BREAST CANCER USING LASER SCANNING
CYTOMETRY

Zabaglo L., Ormerod M.G., Dowsetti M.
 Academic Department of Biochemistry, Royal Marsden Hospital, London, United Kingdom

Because of its sensitivity and precision, laser scanning cytometry (LSC) potentially replace standard immunohistochemical methods for scoring various tumour markers. To date, in solid tumours, LSC has been used to measure estrogen progesterone receptors (ER & PgR), Ki67, cyclins, DNA ploidy and apoptotic cells in exploratory experiments.

We have compared the conventional microscopic scoring of immunoperoxidase-stained cytospin preparations with LSC measurements using both a model system and fine needle aspirates (FNAs) from human breast Ca.

The MCF7 breast carcinoma cell line was used to measure the expression of ER, PgR, Ki67 and apoptosis. Cells were treated with an anti-estrogenic drug in order to obtain different levels of measured markers. Apoptosis was induced by the incubations of cells with camptothecin. Fixed cells attached to microscope slides were stained using either immunofluorescence or immunoperoxidase. The results showed that the pattern of changes in the expression of above markers was similar using both methods.

We also measured Ki67 expression in FNAs from breast carcinomas taken at different times after starting neo-adjuvant therapy of the tumours. Automated scoring using LSC was again compared to the conventional manual scoring of immunoperoxidase stained cytopins. Both methods showed the same changes over time of treatment.

We have also carried preliminary work on counting apoptotic cells in FNAs.

We conclude that LSC could provide faster and more

objective method for scoring ERs, PgRs, Ki67 and apoptosis on cytopins from FNAs than conventional methods. Furthermore, it will be possible to quantify levels of markers in tumour cells and also to obtain an objective assessment of tumour heterogeneity.

Supported by a grant from the US Army no. DAMD 17-97-1-7335.

B018
PROGNOSTIC VALUE OF P53, KI-67,
MITOTIC ACTIVITY INDEX AND MEAN
NUCLEAR AREA (MNA-10) FOR
PROGRESSION IN T_{A,1} URINARY BLADDER
TUMOURS

Bol M., Baak J. 1,2,3, Rep S. 4, Marx W. 4, Bos S. 4, Kisman O. 5

1) Departments of Pathology, Medical Center Alkmaar, Alkmaar1, The Netherlands, 2) Academic Hospital Free University, Amsterdam, The Netherlands, 3) Harvard Medical School, Boston, USA, 4) Departments of Urology, Medical Center Alkmaar, Alkmaar, The Netherlands, 5) Gemini Hospital, Den Helder, The Netherlands

Objective: To analyse the prognostic value for progression of routinely assessed non-revised grade, P53, Ki-67, the mean nuclear area of the ten largest nuclei (MNA-10) and the mitotic activity index (MAI) in T_{A,1} urinary bladder tumours.

Materials and methods: A total of 188 consecutive primary T_{A,1} urinary bladder carcinomas were immunostained for p53 and Ki-67 and the labeling index was determined. Grade, MNA-10 and MAI were assessed in standard histological sections. Single and multivariate analysis was used to assess the progression risk.

Results: In univariate analysis there was a strong association between all the parameters studied and progression. In multivariate analysis the most significant combination for progression was the MAI and p53% positive cells. However, MAI and Ki-67 were nearly as strong prognostically. Moreover Ki-67 was better reproducible than p53.

Conclusions: p53, Ki-67, MNA-10 and MAI are accurate, well reproducible and easy to assess predictors for prognosis in transitional cell carcinoma of the bladder.

C001
NEW NON-STEROIDAL HUMAN
AROMATASE INHIBITORS

Nativelle C. 1, Sourdain P. 1, Moslemi S. 1, Séralini G.-E. 1, Park C.H. 2, Yous S. 2, Depreux P. 2, Lesieur D. 2

1) EA2608, University of Caen, Esplanade de la paix, 14032 Caen cedex, France, 2) UFR Sc. Pharm. University of Lille II, France

Aromatase catalyzes the conversion of androgens to estrogens and it is well-established that estrogens play a role in promoting the growth of breast cancer. Therefore, very selective aromatase inhibitors are still to be developed. Previously, the comparative analysis of the biochemical properties of human and equine aromatases, coupled with their molecular modelisation, allowed us to synthesize new indane and indolizone derivatives(*). Taking into account our previous data, we are presenting our last developed molecules. Aromatase activity is measured in human placental and equine testicular microsomes by $^3\text{H}_2\text{O}$ released from [1 beta- ^3H] androstenedione. The interaction between aromatase and the inhibitor is characterized by spectral studies. Furthermore, the cytotoxicity of compounds is analysed on E293 human cells by the MTT assay. Beyond the 20 new compounds tested, 10 inhibited strongly both enzymes with IC₅₀ range from 12 to 80 nM. These data are confirmed with corresponding K_i between 1-4 and 3-7 nM for human and equine aromatase respectively. These values are similar to those obtained with letrozole (IC₅₀:13 nM), a powerful inhibitor used as a control. Spectral studies with all our compounds showed a type II spectrum characteristic of the interaction between a N atom of the compound with the heme iron of aromatase. None of molecules tested were cytotoxic in E293 cells after 72 h of incubation. These compounds could be good candidates for the treatment of estrogeno-dependant diseases such as breast cancer. They will also be used as probe to understand the structure of mammalian active site of the enzyme. Further in vitro and in vivo studies are needed.

Reference : (*) *Auvray et al., Eur J. Chem. 33 (1998) 451-462.*

C002
CYTOFLUOROMETRIC INVESTIGATION OF
THE HEPATOPROTECTOR BEMITIL
INFLUENCE ON THE GLYCOGEN CONTENT

IN HEPATOCYTES OF PATIENTS WITH
CHRONIC HEPATITIS C AND LIVER
CIRRHOSIS

Kudryavtseva M.V., Bezborodkina N.N., Okovity S.V., Kudryavtsev B.N.

Institut of Cytology RAS, Tikhoretsky av.4, 194064 St.Petersburg, Russia

The content of glycogen and its fractions is a sensitive and demonstrative parameter of the state of the glycogen-forming function in norm and particularly in pathology. By cytofluorometric method, the content of glycogen and its fraction was measured in hepatocytes of normal people (donors) and of patients with chronic hepatitis C as well as with chronic hepatitis C at the stage of liver cirrhosis. The measurements were performed on smear preparation from the material of primary and repeated punctual liver biopsies. The results of these determinations have shown that the content of the total glycogen and its LF fraction in hepatocytes of patients with chronic hepatitis C rises 2.0 and 1.6 times, respectively. The content of the Sf fraction, which has been previously shown to be a sensitive parameter of the liver damage, increases 4.5 times. In studying the repeated biopsy in the patients treated with the application of a hepatoprotector, bemitil, some recovery of the glycogen cell content was revealed. Particularly marked were changes of the SF content, a two-fold decrease, which indicate a positive effect of bemitil. In liver cirrhosis of the viral origin the total glycogen content was higher than norm 2.8 times, while the LF and SF levels increased 2 and 8 times, respectively. Use of bemitil promoted some normalization of the glycogen content in hepatocytes. The most essential changes involved the SF: its content decreased 1.3 times as compared with that in the first biopsy. Thus, cytofluorometric analysis of the glycogen content in hepatocytes of patients with chronic hepatitis and cirrhosis has revealed a significant increase of the content of the total glycogen and its fractions.

C003
COMPARATIVE STUDY OF GFP, B-
GALACTOSIDASE AND LUCIFERASE GENES
AS TOOLS FOR THE DEVELOPMENT OF
NON-VIRAL GENE TRANSFERT VECTORS

Poulain L. 1, Muller C.D. 2, Behr J-P. 1

1) CNRS UMR 7514, Laboratoire de Chimie Génétique, 2) CNRS UMR Laboratoire de

Pharmacologie et Pharmaco-Chimie des Interactions Cellulaires et Moléculaires, Faculté de Pharmacie de Strasbourg, 74 route du Rhin, 67401 Illkirch, France.

Gene therapy has had a fast development in the last few years, and work from numerous teams led to clinical trials in various fields. In particular, the efficiency of such therapies is currently being evaluated for cancer treatment, for which it represents an interesting alternative to chemotherapy, and sometimes even the last chance for the patient. Although the most vectors are of viral origin, non-viral vectors present various advantages, such as an excellent safety profile, a simple production, and they are straightforward to use in a clinical environment. Scientists and clinicians are therefore looking forward towards non-viral vectors presenting also sufficient efficacy in vivo. We have been involved in synthetic gene transfer vectors for over a decade. Initially, our laboratory developed cationic lipids (DOGS - Transfectam®). In 1995, we discovered polyethyleneimine (PEI) derivatives, which are among the most effective non-viral DNA vectors in vitro and in vivo. The goal of the present work was to evaluate the efficacy of PEI derivatives on ovarian tumor cells, as well as to elaborate new therapeutic strategies based on gene transfer using non-viral vectors. Transfection has been characterized using a panel of reporter genes. Indeed, we used complementary approaches for evaluation of gene expression (luciferase, β -galactosidase and GFP), the sensitivity, the qualitative and quantitative information provided by each reporter protein being different. Comparative results obtained with these reporter genes will be discussed and completed with preliminary results using the DsRed gene.

D001

MITOTIC CELLS ARE PREFERENTIALLY LOCATED CLOSE TO BLOOD VESSELS IN INVASIVE BREAST CANCER

Beliën J.A.M. 1, Rottman M. 1,2, Jongbloed G. 2, Van Diest P.J. 1

1) Dept. of Pathology, Academic Hospital Vrije Universiteit, 2) Dept. of Mathematics, Vrije Universiteit, Amsterdam, The Netherlands

We have shown that hot spots of mitotic cells and blood vessels are part of the growing front of a tumour, suggesting a close cell biological relationship between vascularization and

proliferation in invasive breast cancer. In this study, we have investigated whether the distribution of mitotic figures in a tumour can be explained as a random sample drawn from the uniform distribution or not (they are located at preferred locations near blood vessels).

We have studied 9 human invasive breast cancers. The data on the number and location of blood vessels and mitotic cells of one of the 9 cases were used as starting point to set up a mathematical model. We supposed that cells, all of the same type, are to a good approximation spherical with fixed radius $r > 0$. We summarised the cell configuration by their point of gravitation. The points were observed in a compact region, a breast tumour. In a mathematical model we supposed that a cell i is in mitosis with probability $p_d(i)$ and not in mitosis with probability $1 - p_d(i)$. This probability p_d depends on the distance to the closest blood vessel.

We considered a null model, in which the probability $p_d(i)$ is constant. Furthermore, we supposed that the cell density in a tumour is constant. The null hypothesis we tested was that the distribution F of an arbitrary coordinate X_j ($j = 1, \dots, n$, with n the number of mitotic cells) of the 'shortest distance' vector X equals a hypothesised distribution F_0 . The test statistic we used was a modified Kolmogorov-Smirnov test statistic. We used a bootstrap sampling scheme to approximate the p -value.

In only two out of nine cases we could not reject the null hypothesis. The other p -values gave very strong evidence against H_0 . In those seven cases we could decisively reject the possibility that H_0 is true, supporting the concept that mitotic cells are preferentially located close to blood vessels.

D002

MICROVASCULATURE QUANTIFICATION IN A GLIOMA MODEL TREATED BY ANGIOSTATIN GENE TRANSFER AND RADIOTHERAPY

Griscelli F. 1,2, Opolon D. 1, Connault E. 1, Li H. 1, Soria J. 3, Soria C. 4, Perricaudet M. 1, Yeh P. 1, Opolon P. 1

1) UMR 1582 CNRS/Aventis/Institut Gustave-Roussy, 94805 Villejuif, 2) Laboratoire d'Hématologie Biologique, Institut Gustave-Roussy, 94805 Villejuif, 3) Laboratoire de Biochimie, Hôtel Dieu, 75004 Paris, 4) DIFEMA, Faculté de Médecine, 76000 Rouen, France

Objective : to evaluate the benefit of image analysis in histological microvasculature quantification and its correlation to tumor size in a glioma model treated by a recombinant adenovirus coding for angiostatin (AdK3) or AdCO1 (without transgene) associated with radiotherapy (RXT).

Methods : Pre-established C6 rat gliomas were grafted in nude mice which were sacrificed at day 26. Paraffin sections of the tumor were immunostained for smooth muscle actin with a red substrate (AEC). Tumor vasculature was quantified by expressing the surface ratio within 18-42 fields (0,78 mm²) that stained positive. Image processing algorithms were specifically developed for quantification using Matrox Inspector 2.2 software.

Results : Quantification showed a marked reduction ($p < 0.001$) in the vasculature of the sections in the treated group AdK3 + RXT (1.0+0.6%) as compared with the tumor sections from the other groups AdCO1+RXT (5,1 + 2%) or AdCO1 (4,4 + 1,6%) which was correlated with the reduction in tumor size observed in the treated group vs control groups ($p < 0,005$).

Conclusion : Image analysis demonstrated the inhibition of intratumoral vascularisation was tightly correlated with the anti-tumoral effect of AdK3 + RXT.

D003

IN VITRO STUDY OF OVARIAN TUMOR ANGIOGENESIS: IMMUNOFLOUORESCENCE LOCALIZATION OF ADHESION RECEPTORS AND THEIR LIGANDS IN HUVECs AND IGROV1 TUMORAL CELLS CO-CULTURE

Leroy-Dudal J. 1, Thiébot B. 2, Breton M.F. 2, Darbeida H. 2, Gauduchon P. 1, Carreiras F. 2

1) Laboratoire de Cancérologie exp., Centre régional de Lutte Contre le Cancer François Baclesse, route de Lion/Mer BP 5026,14076 CAEN Cedex 05, 2) ERRMECe, Laboratoire de Biologie Cellulaire, Université de Cergy-Pontoise, Av. Adolphe Chauvin, 95302 Cergy-Pontoise, France

Tumoral angiogenesis process is under cells tumor influence and conversely the tumoral expansion is critically dependent on vascular networks. Neovascularisation has been studied in several carcinomas as for example the breast, lung or colon carcinomas but there is only a few report regarding angiogenesis in patients with advanced ovarian carcinoma. For a few years, the importance and the

characterisation of cell adhesion properties, during tumor neovascularisation, as been of interest and the potential role of adhesion receptor and their extracellular matrix (ECM) ligands are being investigated. Several data revealed in one hand the importance of adhesion receptor in endothelial behaviour and, in the other hand, in the ovarian cancer behaviour. In this context, using in vitro coculture models, IGROV1 human ovarian adenocarcinoma cell line and HUVECs primary culture of endothelial cells, we explored the interactions between both cells. Immunofluorescence (IF) experiments revealed the expression and the organization of adhesion molecules such as $\alpha 2$ -, $\alpha 3\beta 1$ and $\alpha v\beta 3$ integrins, of VE-cadherin and of CD44 during IGROV1 cells adhesion cinetic on endothelial cells. Moreover, we demonstrated the remodelling of HUVECs fibronectin when IGROV1 cells attached on a HUVECs monolayer as well as on HUVECs-ECM. The functionality of these receptors was investigated in adhesion and migration assay.

E001

CYP1A1 AND CYP1A2 GENE EXPRESSION DURING INDUCTION WITH DIFFERENT XENOBIOTICS IN LIVER OF C57BL MICE

Mikhailova O. 1,2, Filipenko M. 2, Timofeeva O. 2, Kaledin V. 3, Gulyaeva L. 1, Lyakhovich V. 1

1) Institute of Molecular Biology and Biophysics, Siberian Branch of the Russian Academy of Medical Sciences, Timakov St., 2, Novosibirsk, 630117, 2) Novosibirsk Institute of Bioorganic Chemistry, Siberian Branch of the Russian Academy of Sciences, Lavrentiev Ave., 8, Novosibirsk, 630090, 3) Institute of Cytology and Genetics, Siberian Branch of the Russian Academy of Sciences, Lavrentiev Ave., 10, Novosibirsk, 630090, Russia

Among the numerous cytochrome P450s, the CYP1A subfamily (CYP1A1 and CYP1A2) is of major interest due to the abilities to activate many procarcinogens, including polycyclic aromatic hydrocarbons (PAH) and heterocyclic amines. Their metabolism by CYP1A enzymes leads to highly reactive intermediates. These metabolites cause the mutagenic events responsible for tumor initiation. We investigated the expressions of hepatic microsomal cytochrome P4501a isozymes in C57BL male mice during induction with o-aminoazotoluene (OAT), benzo[a]pyrene (BP) and 1,4-dihydroxyanthraquinone (AQ).

The CYP1A1 mRNA level determined by a very sensitive quantitative RT-competitive PCR increased more than three orders of magnitude during induction with OAT and BP in comparison with untreated animals and did not change during induction with AQ. The CYP1A2 mRNA level was only 8,5, 18,7 and 1,9 times higher during induction with OAT, BP and AQ, respectively, than in untreated mice. At the same time, EROD and MROD activities of CYP1A in liver were investigated. The increase of CYP1A1 mRNA level correlated with the increase of EROD activity; this can testify to the transcriptional mechanism of the inducibility of this enzyme. For CYP1A2, despite the insignificant increase of the mRNA level in liver in response to treatment by inducers, MR metabolism was enhanced sufficiently, implying the posttranscriptional mechanism of CYP1A2 induction. During induction with AQ, the CYP1A1 mRNA level did not change, but the EROD activity increased almost 20 times, that testifies to insufficient specificity of this substrate for CYP1A1. Thus, on the strength of the data obtained, the mRNA level can be considered to be a more accurate estimation of CYP1A1 and CYP1A2 inducibility, than the determination of the enzyme activity.

E002
RADIATION-INDUCED NEOPLASIC PULMONARY TRANSFORMATION IN THE RAT

Poncy J.-L. 1, Tourdes F. 1, De Grandmaison G.L. 1, Dumas P. 2, Gault N. 1, Lefaix J.-L. 1
 1) CEA-DSV-LRT, BP 12, 91680 Bruyères le Châtel, France, 2) Lure, Bat. 209D, BP34, 91898 Orsay, France.

Purpose: to characterise the different stages of pulmonary epithelial cells transformation in radiation-induced lung cancer.

Material & Methods: normal primary cell cultures and immortalised cell line (RTIV3) from tracheal epithelial cells and rat tumour cell line (RT97) were assessed using doubling time measurement, plating and cloning efficiencies, cytogenetic characterisation, clonogenic growth in soft agar, FT-IR microscopy, radiation sensitivity and tumour induction in nude mice. RT97 tumours were studied using usual pathological stainings, FT-IR and immunohistochemical characterisation.

Results:

Cell type	Chromosomes	Doubling time (h)	Plating (%)		γ sensitivity D_0 (Gy)
			Normal	Agar	
normal	42	34 ± 1.45	0.5	0	3.16
RTiv3	74	13 ± 1	15.5	0.7	6
RT97	64	17 ± 0.5	37.5	22	2.87

Primary cells, stained for cytokeratins, were diploid. Aneuploidy was early detected during establishment of the immortalised cell line. RT97 cells induced tumours after injection in nude mice in contrast with normal and Rtiv3 cells. Deconvolved FT-IR spectra of the different cell types were analysed in the two major absorption bands 2800-3000 and 1750-900 cm^{-1} . Structural alterations in transformed cells lead to spectral changes referring to functional groups of nucleic acids and proteins. Tumours induced by RT97 cells were described as undifferentiated carcinoma with spreading of metastasis in pulmonary tissue exclusively.

Conclusion: This model of neoplastic transformation and tumour induction may be interesting to develop experimental studies in radio and/or chemotherapy.

E004
DETECTION OF ANTIRADICAL ACTIVITY IN BIOLOGICAL FLUIDS: COMPARATIVE STUDY OF TWO METHODS

Bochkareva N., Kondakova I., Kolomijets L.
 Institute of Oncology, 5 Kooperativny str., Tomsk, 634009, Russia

Two chemiluminescent methods have been used for the detection of antiradical activity (ARA) in 12 samples of blood serum and saliva. Both methods are based on inhibition of luminol-dependent chemiluminescence by non-enzymatic antioxidants (AO). One of these methods allowed to investigate the total activity of lypophyl and hydrophyl AO in the reaction of radical production from 2,2'-azo-bis-isobutyronitrile (AIBN), dissolved in dimethylsulfoxide. This method was compared with standard technique where 2,2'-azo-bis-(2-amidinopropane) was used as the free radical source. Only hydrophyl AO were tested by this method. A good quantitative coincidence of both methods with $r=0,744$ was obtained. Method with AIBN was more preferable for determination of blood serum ARA. Both methods can be used for evaluation of saliva ARA. Blood serum ARA, saliva ARA and gastric juice were tested in 86 patients with gastric dysplasia and gastric cancer. ARA was significantly decreased

in all tested biological fluids both in patients with gastric dysplasia and gastric cancer patients compared with healthy subjects. The decrease in the level of ARA in biological fluids may be considered as an additional risk factor for cancer development due to a reduction of free radical trapping by AO, a depressed protection of DNA against free radical damage and an inhibition of nitrozocompound formation in the oral cavity and the stomach.

E005

EXPRESSION OF ALPHAVBETA5 AND ALPHAVBETA6 INTEGRINS AND THEIR RELATED LIGANDS IN NORMAL OVARIAN EPITHELIUM AND OVARIAN CARCINOMA

Maubant S. 1, Cruet-Hennequart S. 1, Dutoit S. 1, Denoux Y. 2, Gauduchon P. 1, Staedel C. 1

1) Laboratoire de Cancérologie Expérimentale, Groupe Régional d'Etudes sur le Cancer (EA 1772), C/JF INSERM 96-03, Centre François Baclesse, route de Lion-sur-mer, 14076 Caen Cedex 05, France, 2) Laboratoire d'anatomie-pathologique, Centre François Baclesse, route de Lion-sur-mer, 14076 Caen Cedex 05, France.

Ovarian cancer arises, in 90% of cases, from the malignant transformation of ovarian surface epithelium (OSE). Tumour cells proliferate locally, spread out and disseminate into the intraperitoneal cavity. Both countless tumour foci adherent on the peritoneal wall and tumour cell clusters floating in an ascitic fluid characterise advanced stages of this cancer. This suggests that alterations of adhesion processes could be involved in ovarian tumour development. Integrins are alpha/beta heterodimeric transmembrane receptors, which mediate cell-to-cell interactions and represent the main extracellular matrix receptors.

The presence of alphav, beta5 and beta6 integrin subunits and their preferential ligands vitronectin, fibronectin and tenascin was investigated by immunohistochemistry in normal ovary (n=5), in primary ovarian carcinoma (n = 33) and paired peritoneal grafts (n = 16). Alphav was expressed in normal OSE as well as in primary ovarian carcinoma and graft. Alphavbeta5 was present at high level in normal OSE, grade I and borderline carcinoma. The proportion of positive cells noticeably decreased in grade II and in the majority of grade III tumours, suggesting that alphavbeta5 expression was associated with tissue organisation. In contrast,

alphavbeta6 was absent in normal OSE but expressed in the majority of grade I, borderline and grade II carcinoma. Alphavbeta6 expression was less frequent in grade III primary carcinoma but increased in the majority of the peritoneal grafts. This reveals the double function of alphavbeta6 as mediator of adhesion and tissue remodelling. The appearance of tenascin in tumour stroma reveals the importance of this alphav integrins ligand in ovarian carcinogenesis.

E006

DISTRIBUTION OF NUMERICAL ABERRATIONS FOR CHROMOSOME 1 AND INFECTION WITH HUMAN PAPILOMAVIRUS TYPES 16 AND 18 IN

CERVICAL INTRAEPITHELIAL NEOPLASIA

Bulten J. 1, Kooy-Smits M. 1, Robben J. 1, Bakker J. 2, Melchers W. 2, Massuger L. 3, Poddighe P. 1,4, Macville M. 1, De Wilde P. 1, Hanselaar A. 1

1) Department of Pathology, University Medical Center St Radboud, Nijmegen, 2) Department of Medical Microbiology, University Medical Center St Radboud, Nijmegen, 3) Departments of Obstetrics and Gynecology, University Medical Center St Radboud, Nijmegen, 4) Department of Medical Genetics, University Medical Center, Leiden, The Netherlands

Abrogation of the p53 protection mechanism for signalling genetic defects by HPV oncoprotein E6 is a biological mechanism that underlies cervical carcinogenesis. HPV-induced genomic instability is manifested by aneusomy for chromosome loci as revealed by interphase ISH and CGH. However, there are no data on how HPV infection and chromosome aneusomy are spatially distributed in cervical intraepithelial neoplasia (CIN) and invasive cervical carcinomas (ICC). In this study, we assessed the relation between numerical aberrations for chromosome 1 and the presence of high-risk HPV by in situ hybridization on serial tissue sections of 5 normal cervix tissues, 11 CIN1, 15 CIN2, 20 CIN3, and 9 ICC. A PCR technique was used to detect any HPV type. The mean number of chromosome 1 per nucleus (chromosome index, CI) was calculated, and the fractional areas of dysplastic epithelium with HPV16/18 infection, and chromosome 1 aneusomy were estimated. Tetrasomy was observed in 64%, 27% and 15 % of CIN1, -2, and -3, respectively. Hypertetrasomy was found in 67%, 85% and 100% of CIN2, -3 and ICC, respectively. Infection with

high-risk HPV was detected in 78% of the tetrasomic lesions and 89% of the hypertetrasomic lesions. In 77% of the HPV16/18 positive CIN lesions, the fractional area of HPV infected epithelium was equal to or larger than the fractional area with aneusomy (i.e. tetrasomy or hyper-tetrasomy). Aneusomy was always found inside areas infected with high-risk HPV. These data comply with the theory that HPV infection precedes and causes genomic instability.

E007

USE OF ALKALINE COMET ASSAY TO DETECT DNA DAMAGES IN LYMPHOCYTES AND CD19 POSITIVE LYMPHOCYTES OF FARMERS OCCUPATIONALLY EXPOSED TO PESTICIDES

Briand M., Lebailly P., Lebrethon E., Gauduchon P. CJF-INSERM 96-03 & GRECAN EA1772, Centre Régional François Baclesse, route de Lion-sur-Mer, 14076 Caen Cedex 05, France

The alkaline comet assay was used to quantify the level of DNA damage in whole lymphocytes as well as in B-lymphocytes of farmers occupationally exposed to pesticides. Blood samples were collected at the beginning of the spraying season (S0=January-February), after the first use of pesticides (S1) and at the peak season of spraying activity (S4).

Thirty one farmers were included in that study including 19 with 3 samples (S0,S1 and S4) and 8 with 2 samples (S0 and S4). Lymphocytes were isolated using Ficoll and cryopreserved. After thawing, comet assay was done on whole lymphocytes and on B-lymphocytes isolated using immunomagnetic microbeads.

Preliminary results showed that DNA damage level 1) was different according to lymphocyte subsets and 2) was not significantly different in S4 compared to S0 in whole lymphocytes in contrast with B-lymphocytes.

E008

ASSESSMENT OF DNA DAMAGE INDUCED IN VITRO BY HYDROQUINONE AND 1-4 BENZOQUINONE IN HUMAN LYMPHOCYTES USING THE ALKALINE COMET ASSAY

Lebailly P. 1, Wild C.P. 2

1)CJF-INSERM 96-03 & GRECAN EA1772, Centre Régional François Baclesse, route de Lion-sur-Mer,

14076 Caen Cedex 05 France, 2)Molecular Epidemiology Unit, University of Leeds, United Kingdom.

The effects of two metabolites of benzene (hydroquinone and 1-4 benzoquinone) on the induction of DNA damage in human lymphocytes were investigated using the alkaline comet assay. Results indicate that both compounds were able to induce DNA damage in a dose-dependent manner. At the highest doses tested, a significant change was observed on fluorescent intensity suggesting change of DNA structure. Co-incubation with MethylMethanSulfonate, an alkylating compound, seemed to demonstrate that these 2 metabolites were able to induce DNA strand breaks, but also DNA crosslinks. Some results will also be presented on the effect of these compounds on isolated B lymphocytes.

F001

FUNCTIONAL DIFFERENTIATION OF BOVINE MYELOID BONE MARROW CELLS

Van Merris V., Meyer E., Dosogne H., Burvenich C. Ghent University - Faculty of Veterinary Medicine; Department of Physiology & Biochemistry, Salisburylaan 133, 9820 Merelbeke, Belgium

Bovine myeloid maturation proceeds within the bone marrow and results in morphological and biochemical mature poly-morphonuclear leukocytes (PMN) that are released into circulation. Depletion of the marginal pool triggers the release of PMN from the marrow's storage pool resulting in a left-shift. We hypothesize that this left-shift jeopardizes the animal's resistance by supplying functionally less immature cells. The aim of this study was to detect the sequence of development of the functional properties of PMN during granulopoiesis. Myeloid cells are obtained from bovine bone marrow of normal adult cows. Cells are separated into different stages of maturation by their physical properties using density gradient separation. Three cell fractions are enriched for either early immature, late immature or mature myeloid cells. The myeloid cell population is identified flow cytometrically based on forward and side scatter properties. Following myeloid functions are studied: relevant adhesion receptors, phagocytosis of *E. coli*, oxidative burst activity and chemotaxis. In humans, it is known that these functional properties of PMN appear in a distinct

order upon maturation. Our data indicate that CD11b receptor expression in bovine is strongly increased with maturational stage. Differences were also observed in pilot experiments with other functional tests.

This study is supported by the Flemish Institute for the Encouragement of Research in the Industry (IWT-gra).

F002

IMMUNOLocalIZATION OF MUSCLE-SPECIFIC PROTEINS IN VESSEL-LIGATED SALIVARY GLANDS

Groma V. 1, Zalcmane V. 1, Salms G. 2, Skagers A. 2

1) Institute of Anatomy and Anthropology, Medical Academy of Latvia, Riga, Latvia, 2) Department of Oral and Maxillofacial Surgery, Medical Academy of Latvia, Riga, Latvia

Normal salivary gland myoepithelium bears dual epithelial/myogenic cytological characteristics. Muscular phenotype of myoepithelial cells has been shown to undergo significant changes under exposure to pathological stimuli. Vessel-ligated (facial and/or carotid) submandibular and parotid glands of rabbits were evaluated immunohistochemically for changes in muscle-specific proteins: alpha-smooth muscle actin, calponin and intermediate filament desmin by ABC-immunoperoxidase method using formalin-fixed, paraffin embedded and glutaraldehyde-fixed, Epon embedded tissues. Salivary glands revealed atrophic changes occurring in acinar and ductal cells, more prominent in acinar portion. In a control, periacinar and periductal myoepithelial cells demonstrated diffuse immunostaining by monoclonal antibodies to alpha-smooth muscle actin and calponin (acinar and ductal epithelial cells were entirely negative), whereas immunostaining with an antibody to intermediate cytoskeletal protein desmin was negative. Ligated myoepithelial cells revealed occasional desmin expression. All myoepithelial cells expressed alpha-smooth muscle actin of a different intensity, more marked in cases with nonsevere atrophy. Spectra of calponin expression changes differed from actin. In ligated glands calponin expression was restricted to some myoepithelial cells, enclosing nonatrophic acini and ducts.

F003

SPATIAL INTERPHASE CENTROMER DISTRIBUTION DURING DIFFERENTIATION OF PROMYELOCYTIC LEUKEMIA CELLS

Duerschmied D. 1, Paschke S. 2, Bruel A. 3, Nolte U. 1, Beil M. 1, Irinopoulou T. 4

1) University of Ulm, Germany, 2) Imagenium, Paris, 3) Hôpital St. Louis, Paris, 4) INSERM U430, Paris, France

Background:

The transcriptional activity of genes during differentiation is regulated by epigenetic processes, e.g. the remodeling of chromatin. Promyelocytic leukemia cells can be differentiated along the neutrophil pathway in-vitro and in-vivo by all-trans retinoic acid (ATRA). We used these cells as a model system for investigating the remodeling of higher order chromatin structures during differentiation.

Methods:

Differentiation of the promyelocytic leukemia cell line NB4 was induced by ATRA for 4 days. Preparation of cells was optimized to preserve the three-dimensional (3D) architecture of interphase nuclei. DNA was stained with YoPro-1. Centromeres were visualized by immunofluorescence (IF) or FISH. High-resolution 3D imaging was performed with a confocal microscope. Image resolution was enhanced by deconvolution with a maximum likelihood estimator. 3D distribution patterns of centromeres were analysed by the minimum spanning tree method (MST) and the K and L functions.

Results:

ATRA induces alterations of the 3D DNA distribution in NB4 cells. Although IF and FISH demonstrated a similar quality of centromer visualization, IF preserved the DNA structure more accurately. The 3D distribution of the centromeres were statistically different in differentiated NB4 cells.

Conclusions:

Differentiation of NB4 cells is associated with marked changes of higher order chromatin structures in interphase nuclei as reflected by the spatial rearrangement of centromeres. The developed methods provide the opportunity to investigate epigenetic processes with a high spatial resolution.

F004

MORPHO-HISTOCHEMICAL ANALYSIS OF HAIR GROWTH IN HUMAN SCALP TISSUES:

EFFECTS OF A NEW PROPOSED THERAPY ON HAIR LOSS

Linares-Cruz G.1, Lequeux N.2, Homsy C.3, Soussaline F.3

1) Lab. Pharmacologie Exp.IGM St. Louis, Paris, 2) CRLC Val D'Aurelle Montpellier, 3) IMSTAR SA, Paris, France.

The present work is being promoted by BX3 General Labs, Switzerland, and realized by IMSTAR SA, France. The aim is to analyze the effects of the proposed new therapeutic approach on human scalp biopsies after 3 and 6 months of treatment.

The hair follicle is one of a few human tissues containing stem cells. The stem cells are interspersed within the basal layer of the outer root sheath and in an area called the bulge. From this reservoir, stem cells migrate to hair matrix and start to divide and differentiate. Their behavior is controlled by numerous cytokines produced by cells of the dermal papilla and also by different epithelial cell layers forming the hair follicle under participation of mesenchymal and nerve factors. This study characterizes hair follicles dynamics before and after treatment for hair loss. It is focused on both: - the morphological analysis of dermal appendages at the light microscopic level assisted by a fully automated tissue cartography (IMSTAR proprietary technology) and - the analysis of functional markers associated with proliferation and apoptosis in the same structures. Proliferation marker Ki67 and apoptosis marker Apoptatin (F-7 26) and TUNEL are analyzed by immunohistochemical methods. They are quantitatively expressed as a labeling index and measured in histograms showing heterodispersion of immunostaining (IMSTAR software). Immunostained cells are located to specific hair follicle structures by tissue cartography. Methodological approach is described and preliminary results presented.

G001 CORRELATION BETWEEN THE PROCESS OF CELL PROLIFERATION AND APOPTOSIS IN ADENOMYOSIS

Tugusova V.

Polotckaya str., 23/17, 29 121351 Moscow, Russia

Objective : To determine the relationship between processes of cell proliferation and apoptosis in eutopic endometrial and lesion of adenomyosis.

Patients: 37 women with adenomyosis and 10 women without adenomyosis (control group).

Methods : The expression of bcl-2 (DAKO), bax (DAKO), c-myc (NOVOCASTRO), Ki-67 (DANOVA) in ectopic and eutopic endometrial was evaluated. Immunohistochemical staining was carried out on the paraffin section using streptavidin-biotin method. To analyse cells undergoing apoptosis, we used the TUNEL-method (Enzo ApopDETEC Cell Death Assay System). Negative controls were prepared by replacing the primary antibody with bovine serum. A specimen of small cell carcinoma was used as a positive control. The immunostaining intensity was assessed in semi-quantitative manner.

Results : In light of Immunohistochemical results was examined the stronger intensity for the oncomarkers bcl-2, bax, c-myc in the eutopic endometrium, myometrium, epithelial cells of the endometrial glands in the lesions of adenomyosis and stronger Immunohistochemical staining for Ki-67 that in tissue of the control group. The expression of bcl-2, c-myc, Ki-67 is rather stronger in the lesions of adenomyosis than in the eutopic endometrium. The expression of bax and the highest level of apoptosis were observed in endometrium of the control group.

Conclusions : The endometrial cells with high proliferation and low level of apoptosis can invade in myometrium. The disruption of regulation between apoptosis and cell proliferation may involve in the pathogenesis of adenomyosis.

G002 OPTIMIZATION OF FLOWCYTOMETRIC DETERMINATION OF TUMOUR POTENTIAL DOUBLING TIME (TPOT)

Johansson M.C. 1, Baldetorp B. 1, Oredsson S.M. 2

1) The Jubileum Institute, Dept of Oncology, Lund University Hospital, S-221 85 Lund, Sweden, 2) Dept of Animal Physiology, Lund University, S-223 62 Lund, Sweden

TPOT of bromodeoxyuridine (BrdUrd)-labelled cells estimated by FCM, may be of importance in the planning of tumour treatment protocols. Formulas for calculation of TPOT are based on the DNA synthesis time (TS) of BrdUrd-labelled cells and on labelling index (LI). Some TPOT expressions show however dependence of the time between BrdUrd labelling and cell sampling, i.e. the post-labelling time (plt). We have earlier presented a TS and a LI formula, both theoretically independent of plt, thus giving

time consistent TPOT values. To compare our TPOT formula with two others, regarding plt dependency, we pulse-labelled three different cell lines with BrdUrd. Cells fixed at increasing plts, were prepared for simultaneous FCM-mediated analysis of DNA content and incorporated BrdUrd, using propidium iodide and a monoclonal antibody against BrdUrd, respectively. A TPOT value was calculated for each plt as well as the mean TPOT for all plts. The mean TPOT values were approximately the same using any of the three formulas. However, the time dependence differed. In two moderately proliferating cell lines, our TPOT formula alone gave values independent of plt. In the third, very fast proliferating cell line, all formulas yielded time dependent TPOT values. In conclusion, we present a method to estimate TPOT which is independent of plt. This is of great importance in applications where only one sample, regardless of plt, can be taken.

G004
EFFECTS OF PHENOLIC COMPOUNDS ON THE CELL CYCLE KINETICS AND CELL PROLIFERATION OF SYRIAN HAMSTER EMBRYO (SHE) CELLS

Goutet M., Elias Z., Danière M.C., Terzetti F., Poirot O.

INRS, Avenue de Bourgogne, BP27, 54501 Vandoeuvre Cedex, France

The phenolic chemical class includes chemicals for which it is difficult to predict the carcinogenic potential by short-term bioassays. In previous works, we have found that SHE cell transformation assay accurately predicts their carcinogenicity; in addition, some of the phenols stimulated cell survival and proliferation. The purpose of this study was to evaluate the effects of nontoxic concentrations of phenol (P), catechol (C), hydroquinone (HQ) 2-methoxyphenol [guaiacol (G)] and 4-methoxyphenol (4MP) on SHE cell cycle progression by flow cytometry. SHE cells in exponential growth were treated with C (0.6-2.5 μ M), HQ (2.5-10 μ M), 4MP (5-20 μ M), G (25-100 μ M) and P (125-500 μ M) for 3d. The distribution of cells among various phases of cell cycle was determined after 1, 3, 5, 7, 24, 48 and 72 h of exposure. All the compounds enhanced the G1-S transition on different degrees, precipitating cells towards early S phase as soon as 3 h and up to 48 h. The cell increase in S phase was not due to a delayed progression through the cycle as the

proliferation was higher in treated cells than in controls. Rather, the results indicated a reduction in the duration of the G1 phase and/or the recruitment of a population of the G0 phase into the cell cycle, as observed by the enhanced colony forming efficiency after 7d (C,HQ,P). Taking into account the lowest active concentrations and the potency to increase S phase and cell proliferation, it appears that (i) the hydroxylation of phenol leads to an enhancement of its activity: C,HQ>>P; (ii) the methylation of the hydroxyl group leads to a decrease of this activity: C>G; HQ>4MP. In conclusion, the ability of some phenols, in relation to their chemical structure, to act at non cytotoxic concentrations as mitogenic agents could explain in part their carcinogenic or tumor promoting effects.

G005
GENOMIC CHANGES IN BREAST CANCERS WITH DIFFERENT FEATURES OF PROLIFERATION

Friedrich K. 1, Scheithauer J. 1, Dimmer V. 1, Meyer W. 1, Theissig F. 1, Kotzsch M. 1, Haroske G. 2, Baretton G. 1, Kunze K.D. 1

1) Dresden University of Technology, Institute of Pathology; Germany; Fetscherstr. 74; D-01307 Dresden, 2) Dresden-Friedrichstadt General Hospital; Germany; Friedrichstr. 41; D-01067 Dresden

The proliferation is regulated by promoting and inhibiting gene products. Disturbance of this regulation is a characteristic sign of malignancy. The aim of the study was the detection of chromosomal imbalances in breast cancers with different proliferation features. Ninety-two breast cancers were examined by CGH, by immunohistochemistry for the Ki-67 antigen by the MIB-1 antibody, by flow cytometry for S-phase fraction and by counting of mitosis in ten high power fields on H&E sections. A high proliferation activity was associated with a high number of chromosomal imbalances for all proliferation features. Breast cancers with more than 20% of MIB-1 positive cells differ from tumours with 10% positive cells at the most in gains at 17q and in losses at 15q. A S-phase fraction higher than 5% was associated with gains at 8q, 17q and with losses at 4q. Losses at 5q, 9p, 8p and Xp and gains at 17q and 8q are characteristic imbalances of tumours with a high number of mitosis. The search for combinations of two chromosomal imbalances reveals further differences

between low and high proliferating tumours for all features analysed.

In conclusion, a high proliferation in breast cancer is associated with a high number of chromosomal imbalances and with gains at 17q and 8q. Additional imbalances were detected in association with each proliferation feature, reflecting influences of different proliferating factors.

G006

NITRIC OXIDE ABATES FREE-RADICAL INHIBITION OF TUMOR CELL PROLIFERATION

Malahova E.V., Zagrebelnaja G.V., Kondakova I.V.
Institute of Oncology, Russian Academy of Medical Sciences, 634009, Tomsk, Russia

Previous studies have demonstrated that nitric oxide (NO) has a wide range of actions on tissues and cells including toxic and physiological functions. Elimination of tumor cells in host organism is associated with production of oxygen metabolites by immunocompetent cells. However, the possible interaction between NO and free radicals in cytotoxic activity against tumor cells was not estimated. The present study demonstrates that a combination of toxic concentrations of chemically generated NO and peroxy radicals did not lead to inhibition of tumor cell proliferation.

Mouse Ehrlich's carcinoma cells were used for experiments. Peroxy radicals were generated from 2,2'-azo-bis(2-amidinopropane) and tert-butyl-hydroperoxide and NO - from sodium nitroprusside, sodium nitrite and L-arginine. The [3H]-thymidine incorporation in DNA was determined for estimation of cellular proliferative activity. Exposure of tumor cells to peroxy radicals or NO-generators separately allowed to reveal the toxic and subtoxic concentrations of these compounds. Combining NO donors with peroxy radical generating substances did not decrease tumor cell proliferation. The addition of non-toxic concentrations of NO failed or impaired the toxic effects of free radical agents. This protective action of NO may be associated with antioxidant properties of nitric oxide and play a negative role in anticancer immunity.

G007

INVOLVEMENT OF ANTIOXIDANT ENZYMES IN REGULATION OF TUMOR CELL PROLIFERATION

Smirnova L.P., Kondakova I.V.

Institute of Oncology, Russian Academy of Medical Sciences, Tomsk, Russia

Antioxidant enzymes play an important role in the control of free radical level in cells and may be significant in the modulation of various functions. Low concentrations of superoxide radicals are able to stimulate cellular proliferation. The aim of this study was to investigate the activities of antioxidant enzymes in tumor cells depending on the pattern of structural organization and different phases of cellular growth.

Ehrlich's carcinoma cells were maintained in CBA mice by passages into the abdominal cavity or by subcutaneous injection. The determination of enzyme activities were carried out by spectrophotometric methods. The activities of superoxide dismutase (SOD) and catalase in liquid form of Ehrlich's carcinoma were lower than those in the solid tumors. Logarithmic phase of cell growth was characterized by decreased activities of SOD, glutathion peroxidase and glutathione transferase compared to confluent phase in both ascitic and solid tumor cells. These data suggest the involvement of antioxidant enzymes in regulation of tumor cell proliferation.

G009

EXPRESSION OF CYCLIN-D1 AND P21 IN APOCRINE METAPLASIA OF THE BREAST: RELATIONSHIP TO THE CELL CYCLE PROLIFERATION ANTIGEN, KI-67

El-Ayat G., Selim A.A., Jordan S., Wells C.A.

Department of Histopathology, St. Bartholomew's Hospital, London EC1A 7BE, UK.

Cyclins, cyclin dependant kinases and cdk inhibitors are frequently deregulated in cancer. Apocrine metaplasia (APM), a common finding in fibrocystic change, was previously regarded as having little or no significance in relation to malignant breast disease. Although some studies have suggested a premalignant potential of these cells, the subject remains controversial. We have examined the expression of the cell cycle-associated markers cyclin-D1 and p21 in APM and have correlated the results with the proliferation marker Ki-67 in an

attempt to clarify the biologic significance of these markers in this type of metaplasia. 63 cases of APM were examined immunohistochemically for the expression of cyclin-D1, p21 and Ki-67 proteins using the standard ABC technique. 35 (55.6%) cases showed overexpression of cyclin-D1 and 36 (57.1%) cases showed overexpression of p21. The mean percentage positivity for Ki-67 was (4.3%), but in the 35 cases showing cyclin-D1 overexpression, the mean was higher (5.5%). In addition, in the 36 cases showing p21 overexpression, the mean percentage positivity for Ki-67 was 6.3% which is significantly higher than the one noted (1.7%) in the 27 cases showing no overexpression of p21. The results suggest that a subset APM of the breast shows higher levels of expression of cyclin- D1 and p21 than the normal breast epithelium & that these two markers are associated with elevated Ki-67 proliferation rate. This may reflect a significant level of epithelial unrest associated with some cases of apocrine metaplasia which may contribute to the oncogenic potential of these cells.

H001

HYDROGEN PEROXIDE-INDUCED APOPTOSIS ASSOCIATED WITH NUCLEAR BCL-2 AND CELL CYCLE DNA CONTENT IN COLORECTAL CANCER CELLS

Elkablawy M.A., Arthur K., Maxwell P., Williamson K., Hamilton P.W.

Quantitative Biomarker Group, Department of Pathology, Cancer Research Centre, Queen's University of Belfast, UK.

Our group have reported previously that in colorectal carcinoma, apoptotic cells and bodies showed dense nuclear bcl-2 immunostaining and that this was associated with positive bcl-2 immunoreactivity. In this study, we followed the nuclear distribution of bcl-2 through the induction of apoptosis using hydrogen peroxide (H₂O₂) on 5 human colorectal cancer cell lines (HT115, LS174T, SW480, WIDR and CACO₂). The relationships between H₂O₂-induced apoptosis, bcl-2 immunoreactivity and alterations in the cell cycle DNA content were assessed. Apoptosis, as assessed by morphology, was significantly associated with H₂O₂ in a time- and concentration-dependent manner. HT115 and LS174T cells were the most sensitive to H₂O₂ treatment. Four cell lines showed marked bcl-2 immunoreactivity while CACO₂ was bcl-2 negative.

Bcl-2 intensity of staining increased within each cell line in tandem with H₂O₂-induced apoptosis. Nuclear bcl-2 immunoreactivity increased with increased sensitivity to H₂O₂, which was confirmed by confocal laser microscopy in most apoptotic cells and bodies 24 hours after exposure. The DNA content of cells measured by flow cytometry demonstrated a time- and dose dependent increase in the number of events falling in the sub-G1 peak region of the DNA histogram. This was associated with H₂O₂-induced apoptosis. These results confirm the association between colorectal apoptosis and bcl-2 expression and distribution. The significance of the occurrence of nuclear bcl-2 in morphologically identifiable apoptotic cells remains to be explained and further studies investigating the functional role of bcl-2 in colorectal carcinoma are required.

H002

INTERFERON-INDUCED APOPTOSIS CORRELATES WITH THE PRESENCE OF ENDOGENOUS DOUBLE-STRANDED RNA

Pjanova D. 1, Bruvere R. 1, Volrate A. 2, Feldmane G. 2, Loza V. 1

1) Biomedical Research and Study Centre, University of Latvia, Ratsupites 1, Riga, LV-1067, Latvia, 2) Institute of Virology and Microbiology, Ratsupites 1, Riga LV-1067, Latvia

The interferon-induced double-stranded RNA (dsRNA) activable protein kinase (PKR) is of central importance in the antiviral defence by interferon (IFN). PKR plays also an important role in cell growth and differentiation and is an essential span in the signaling pathway linking cellular stress stimuli to the apoptotic protease cascade. Nevertheless, the origin and conditions of the induction and localization of cell-derived dsRNA are still far from being clear. The formation of dsRNA was studied in cells incubated with homologous IFN for 5 min - 24 h and the relation of IFN-induced apoptosis to the intracellular presence of dsRNA was evaluated. The dsRNA structures were demonstrated by monoclonal antibodies against the A-helix structure of natural dsRNA. It was shown that IFN induces protein-non-linked dsRNA structures in the cell nuclei and nucleoli whereas in the cytoplasm dsRNA appeared as a ribonucleoprotein complex as it could be visualized only after pretreatment of cells with proteinase K. It was shown that IFN-induced apoptosis is preceded by the appearance of dsRNA

as a ribonucleoprotein complex in the cytoplasm and by conditions when the nuclear and nucleolar dsRNA is suppressed by actinomycine D. The used anti-dsRNA antibodies react also with full length Alu RNA. The relationship of IFN-induced cell-derived dsRNA to full length Alu RNA will be discussed.

H003

THE IMPORTANCE OF APOPTOSIS IN CHRONIC LYMPHOCYTIC LEUKEMIA

Borba G., Pereira F.G., Lorand-Metze I.

Department of Internal Medicine, Faculty of Medicine, State University of Campinas SP Brasil

Spontaneous apoptosis in culture has been observed in neoplastic lymphocytes in chronic lymphocytic leukemia (B-CLL). We studied this apoptosis after a 48-hour culture and analysed its relationship with peripheral blood cell counts, staging (Rai) and total tumour mass (TTM). Apoptosis was measured by flow cytometry using annexin V. Among the 27 patients enrolled, median age was 73 (55-86). Stage: 0 - 7 cases; I - 6 cases; II - 4 cases; III - 4 cases; IV - 6 cases. The percentage of annexin V positive cells had an inverse correlation with TTM ($r = -0.67$), peripheral lymphocytes ($r = -0.42$) and Rai stage ($r = -0.36$). A positive correlation was found for platelet count ($r=0.44$). We conclude that a more aggressive disease is related to the inability of CLL cells to undergo apoptosis.

H004

DEPENDENCE OF CELLULAR CONTENT UPON THE LEVEL OF PERSISTENCE EPSTEIN-BARR VIRUS IN CELLS WITH CYTOGENETIC AND OF ACTIVITY OF APOPTOSIS OF PERIPHERAL BLOOD LEUKOCYTES DISORDERS

Ivanchuk I.

634050, Tomsk, Moskovsky trakt 2, Siberian Medical University, Central Research Laboratory (CNIL), Russia

Epstein-Barr virus (EBV) belongs to potentially oncogenic viruses, which can have effects on apoptosis response mechanisms of infected cells. Besides that, it is known, that Epstein-Barr virus induces specific lesions of certain chromosome loci in areas of oncogenic location, resulting in structural disorders of chromosomes. We

investigated apoptosis response of lymphocytes in dependence on average-geometric titer of antibodies to Epstein-Barr virus in short-term cultural test-system. We examined 187 persons from 15 up to 65 years old. The chromosome preparations of lymphocytes culture of peripheral blood were prepared with conventional macromethod with little modifications. The estimation of content of binuclear lymphocytes with micro-nuclears (cytocholasine-B test) was done with the help of standard mode. Titer of virus-specific antibodies to EBV antigens was determined with an indirect immunofluorescence method in Henle modification. Apoptosis of lymphocytes was induced by removing of serum in short-term cultural test-system. Percentage estimation of apoptosis cells was done just after separation of lymphocytes and then within 3, 6, 9 and 12 hours after the cultivation began. To define qualitative and quantitative parameters of apoptosis, the method of definition of DNA-fragmentation, DNA electrophoresis in agar gel with ethidium bromide and percentage of pyknotic nuclei by the acridine orange were used. The increase of resistance of cells to apoptosis stimulant at high antibody titers to EBV was found. Besides that, significant increase of number of cells with cytogenetic disorders was revealed, that is probably caused by the effect of accumulation of aberrant cells in culture.

H005

INDUCTION OF LYMPHOCYTE APOPTOSIS IN PERIPHERAL BLOOD OF THE PATIENTS WITH MAMMARY AND LUNG CANCER IN VITRO AND OF ACTIVITY OF APOPTOSIS OF PERIPHERAL BLOOD LEUKOCYTES DISORDERS

Ivanchuk I.

634050, Tomsk, Moskovsky trakt 2, Siberian Medical University, Central Research Laboratory (CNIL), Russia

Nowadays pathogenesis of many diseases is related to the loss of normal control of cell death. The role of the mechanisms of apoptosis in carcinogenesis course attracts particular interest among scientists. We studied the dynamics of lymphocytes apoptosis of peripheral blood of the patients with mammary gland and pulmonary cancer. 65 patients with malignant tumor of mammary gland and lungs were examined. Apoptosis of lymphocytes was induced by removing of serum in short-term cultural test-system.

Percentage estimation of apoptosis cells was done just after separation of lymphocytes and then within 3, 6, 9 and 12 hours after the cultivation began. To define qualitative and quantitative parameters of apoptosis, the methods of definition of DNA-fragmentation, DNA electrophoresis in agar gel with ethidium bromide and percentage of pyknotic nuclei by the acridine orange were used. It was stated, that cultivation of lymphocytes in free-serum medium stimulates lymphocytic apoptosis in both experimental and control groups. However, heterogeneity in dynamics of lymphocytes apoptosis course is revealed in patients with cancer in comparison with the control group data. It was stated, that for patients up to 37 years old cancer was more often accompanied with significant decrease of lymphocytes apoptosis reaction to stimulus and on the contrary, in the patients over 37 years old, the significant increase of lymphocytes apoptosis percentage was more often observed at serum removing in comparison with control group data.

H006
FRACTAL MORPHOMETRY REVEALS
ULTRASTRUCTURAL MODIFICATIONS OF
CELL COMPONENTS AT THE EARLY
PHASES OF APOPTOSIS IN BREAST
CANCER CELLS

Losa G. A. 1,2, Castelli C. 1

1) Laboratory of Cellular Pathology, Institute of Pathology, 6600 Locarno, 2) Faculty of Sciences, University of Lausanne, 1015 Lausanne, Switzerland

Fractal morphometry was used to investigate the ultrastructural features of the plasma membrane, perinuclear membrane and nuclear chromatin in SK-Br-3 human breast cancer cells undergoing apoptosis. Cells incubated with 10⁻⁶ M calcimycin (A23187) for 24 h were in the early stage of apoptosis and had fractal dimension (FD) values indicating that their plasma and perinuclear membranes were less rough and less differentiated (lower FD) than those of control cells. Ultrastructural changes of the chromatin texture (due to chromatin condensation and marginalization) within the entire nucleus and in selected nuclear domains were more pronounced in treated cells. This confirms that the morphological reorganization imputable to a loss of structural complexity (reduced FD) occurs in the early stage of apoptosis and precedes the onset of

functional/cellular markers and enzymatic events, characteristics of the active apoptotic process.

H008
MAPPING TEMPORAL SEQUENCE AND
CAUSE-EFFECT RELATIONSHIP OF EARLY
APOPTOTIC EVENTS WITH LASER
SCANNING CYTOMETRY (LSC)

Darzynkiewicz Z. 1, Bedner E. 1, 2, Smolewski P. 1
 1) Brander Cancer Research Institute, NYMC, Hawthorne, NY. 10532, USA (ZD, PS), 2) Pathology Dept., School of Medicine, Szczecin, Poland (EB)

New approach utilizing LSC was developed to directly correlate, *within the same cells*, the apoptosis-associated events revealed supravivally with the events that can be unveiled only after cell permeabilization. With this approach, we were able to directly correlate the supravivally detected changes, namely: (a) collapse of the mitochondrial potential ($\Delta\Psi_m$); (b) exposure of phosphatidylserine on cell surface; (c) oxidative stress; and (d) activation of caspases-3, -6, -8, or -9, with: (a) translocation of Bax to mitochondria; (b) leakage of cytochrome c to cytosol; (c) activation of NF- κ B; (d) PARP cleavage, and (e) DNA fragmentation. All these events were correlated with the cell cycle position. A new method, based on binding of fluorochrome labeled inhibitors of caspases (FLICA) to caspase enzymatic centers was developed. The FLICA was also helpful to reveal localization of caspases: most were present in mitochondria and co-localized with MitoTracker Red. Apoptosis triggered by DNA damage and by the cell surface death ligands was studied. In some cell types, PARP cleavage and DNA fragmentation were observed with no evidence of $\Delta\Psi_m$ collapse or oxidative stress. This suggests that the latter events are not essential for initiation of the execution stages of apoptosis. Our approach opens a possibility to study causal and temporal relationships between other events related to cell (or organelle) function detected in live cells *vis-à-vis* the changes that cannot be analyzed supravivally. It allows one to map the sequence of critical events not only during apoptosis but also during mitogenic stimulation, differentiation or carcinogenesis.

H009
ACTIVE CASPASE-3 AND CLEAVED
CYTOKERATIN-18 EXPRESSION IN

GASTRIC CANCER AND ADJACENT NON-MALIGNANT TISSUE

Grieken N.C.T. van 1, Meijer G.A. 2, Bloemena E. 2, Meuwissen S.G.M. 1, Baak J.P.A. 2, Kuipers E.J. 1

1) Dept of Gastroenterology, Free University Hospital, Amsterdam, The Netherlands, 2) Dept of Pathology, Free University Hospital, Amsterdam, The Netherlands.

Introduction: Apoptosis is the endpoint of the normal lifecycle of the gastric epithelial cell, while inhibition of apoptosis frequently occurs in cancer. Caspase-3 activation and subsequent cleavage of cytokeratin-18 (CK18) are key steps in epithelial apoptosis. The aim of the present study was to evaluate the expression of these proteins in different conditions of the gastric mucosa.

Methods: Twenty-nine samples were included in the study. Material from 6 gastric carcinomas and adjacent non-malignant tissue were studied. In these non-malignant samples, intestinal metaplasia was present in 3 cases. The remaining 30 (15 from the antrum and 15 from the corpus) samples consisted of biopsies collected from the archives of the pathology department. These contained dysplasia in one case, intestinal metaplasia in 4 cases, and chronic gastritis in 12 cases. Four mm sections were cut and immunohistochemical staining for active caspase-3 and cleaved CK18 was performed using the monoclonal antibodies anti-active caspase-3 antibody (BD PharMingen) and M30 CytoDeath (Boeringer Mannheim), respectively.

Results: Two out of 6 carcinomas showed positive staining for both active caspase-3 and CK18. In addition, in 3 cases the non-malignant tissue samples next to a tumor were positive for both antibodies. No positivity for active caspase-3 and CK18 were detected in the 30 biopsy specimens. As expected, lymphfollicles did not show positive cells for cleaved CK18, whereas a small percentage of positive cells for active caspase-3 was detected.

Conclusion: A proportion of gastric cancer showed expression of active caspase-3 and CK18. Positive epithelial cells for active caspase-3 and CK18 were found in the adjacent non-malignant tissue of part of the stomachs with a cancer. In contrast, none of the biopsy specimens, containing chronic gastritis, intestinal metaplasia and dysplasia, showed positive epithelial cells.

H011

EX VIVO DETECTION OF SEPSIS INDUCED CARDIOMYOCYTE APOPTOSIS WITH 123 I-ANNEXIN V

Pétilot P. 1,4, Lahorte C. 2, Nevière R. 3, Marchetti Ph. 1, Slegers G. 2

1) INSERM U 459, Faculty of Medicine, Lille Cedex, 59045 France, 2) Department of Radiopharmacy, Faculty of Pharmacy, Gent, Belgium, 3) Physiology Department, Faculty of Medicine, Lille Cedex, 59045 France, 4) Anesthesiology Department II, CHRU, Lille Cedex 59037, France

Introduction : Radiolabelled Annexin V is a programmed cell death marker investigated by Blankenberg which can be used to detect apoptosis in vivo or ex vivo. Recently, cardiomyocyte apoptosis has been reported during septic shock. To evaluate the presence of sepsis-induced apoptosis, we measured, ex vivo, the myocardial uptake of 123I-Annexin V in normal and septic rats.

Methods : Sprague-Dawley rats were given intravenously either 10 mg/kg of endotoxin (septic group, n = 9) , or saline (control group, n = 5) and were injected 24H later into the carotid artery +/- 30 µCi of 123I-Annexin V (1.5 +/- 0.1 µg protein). 30 min after tracer injection, rats were sacrificed , organs perfused with Ringer and hearts divided into apex, septum, left and right ventricle (LV and RV) for counting. Organ radioactivity was determined with a LKB gamma-counter, and 123I-Annexin V uptake was expressed as a percentage of injected dose per g of tissue (%ID/g). Statistical analysis was performed by Mann-Whitney U test, determination of confidence intervals (CI95%) and a p value < 0,05 was considered as significant.

Results : only mean RV uptake of 123I-Annexin V in the septic group, 0.69 +/- 0.12 %ID/g, with CI95% ranging from 0.41 to 0.96, was significantly increased (p = 0.007), compared to control group, 0.23 +/- 0.03 % ID/g with CI95 ranging from 0.16 to 0.30 .

Conclusion : RV cardiomyocyte apoptosis has been detected 24H after endotoxin injection. Histological and cytological studies of both ventricles are required to establish the sensitivity and specificity of apoptosis isotopic detection with 123I-Annexin V. Further studies might search for LV delayed apoptosis and in vivo imaging possibilities by Single Photon Emission Computed Tomography (SPECT).

H012 CYTOCHEMICAL FEATURES OF THE TUMOUR SPOROTIC MICROCELLS

Buikis I., Freivalds T., Harju L.

Institute of Experimental and Clinical Medicine,
University of Latvia, Ojara Vaciesa 4, LV 1004, Riga,
Latvia

By the term "sporosis", we called the path of microcell formation from nuclear bodies of an interphase macronucleus (Anal Cell Pathol 1999; 18: 73-85). The aim of this study was to investigate the cytochemical features of sporotic microcells, with the purpose to identify simple markers of sporosis. For induction of sporotic microcells the monolayer of human sarcoma cell line HT-1080 was exposed to thiophosphamidum (10-20 µg/ml) or to vincristinum 2-3 ng/ml at 37 °C for 24 h. At 24-96 h intervals, after resupply with a fresh medium, the cells were incubated in a medium with acridine orange (AO) or rhodamine 123 (Rh 123), both in concentration of 5 µg/ml at 37 °C for 30 min. Another sample was incubated in 0,001% of Indian ink suspension in maintenance medium at 37 °C for 2h. Cells fixed in acetone (4 °C), were used for immunocytochemical assay of vimentin and macrophage CD-68 protein. Routine methods were used for oxidoreductases and acid hydrolases cytochemical assay. The developing microcells via sporosis were distinguished from intact, necrotic or apoptotic tumour macrocells by outstanding uptake of AO by cytoplasmic acidic organelles expressing bright red AO fluorescence. The body of microcells also showed a prominent uptake of Rh 123. Microcells rapidly enclosed particles of Indian ink.

Sporotic microcells expressed very strong vimentin and moderate macrophage CD-68 protein. After aldehyde fixation, the microcells can be distinguished by strong NADPH diaphorase activity. The microcells arising via sporosis are viable, undifferentiated, metabolically very active, macrophage like cambial cells with great potential of xenobiotic and drug sequestration and biotransformation.

H013 NECROSIS / APOPTOSIS DISCRIMINATION DIRECTLY ON LIVE ADHERENT CELLS IN MICROPLATE USING DNA PROBE (HOECHST 33342) AND CYTOPLASMIC

MEMBRANE PROBES (YOPRO-1, ANNEXIN V)

Pouzaud F. 1, Rat P. 1,2, Warnet J.-M. 1,2

1) Unité de Pharmacotoxicologie Cellulaire -CHNO
des XV-XX-75012 Paris France, 2) Laboratoire de
Toxicologie- Faculté Pharmacie Université Paris V-
75006-Paris, FRANCE

Apoptosis is distinguished from necrosis, or accidental cell death, by characteristic morphological, biochemical changes, including compaction and chromatin condensation, cytoplasmic membrane permeability and loss of membrane asymmetry. The aim of this study was to evaluate the apoptosis phenomenon with different fluorescent probes directly on live adherent cells after apoptosis induction using Microplate Fluorometry Assay on Live Cells (MiFALC test (1)) using Cold Light Cytofluorometry (2). Fluorescence signal was directly scanned in live adherent cells on 96-well microplate (1). After Apoptosis induction with Camptothecin and Etoposide, different probes such as Hoechst 33342 / Propidium iodide, Neutral Red, Yopro-1 and Annexin V are added on live cells to evaluate chromatin condensation, membrane integrity, membrane permeability (P2X7 receptor) and phosphatidylserine asymmetry respectively. In conclusion, Annexin V probe is not adapted to discriminate apoptosis in our adherent cells, but Hoechst 33342 / Neutral Red assay (MiFALC test) was adapted to adherent human hepatic (Hep G2), fibroblast (L929), tendons and conjunctival cells) and suspension cells (U937) for early screening of apoptosis / necrosis discrimination directly in microplate. Good results were observed on U937 cells, but some interpretation problems were observed with live adherent cells.

References :

1. Rat P. et al (1997) In: *Animal Alternatives, Welfare and Ethics* (LFM van Zutphen & M. Balls Eds.) Elsevier, Amsterdam, 27, 813-823.
2. Rat P. et al (1995) *Methods Enzymol.*, 252, 331-340.

H014 SIMULTANEOUS VIDEOMICROSCOPICAL ANALYSIS OF MITOCHONDRIAL AND NUCLEAR CHANGES OCCURING DURING APOPTOSIS

Zahm J.M., Lizard G., Gambert Ph., Puchelle E.,
Bonnet N.

Inserm U514, Reims and U498, Dijon, France.

Apoptosis is a particular mode of cell death characterized by a typical disruption of the mitochondrial transmembrane potential which is one of the earliest intracellular events occurring under the action of numerous apoptotic signals. We analyzed by videomicroscopy the dynamic of mitochondrial transmembrane potential variations associated with nuclear changes (fragmentation and/or condensation of the nuclei). To this end, ECV-304 cells were incubated with the mitochondrial potential probe DiOC6(3) at 40 nM and with Hoechst 33242 at 50 μ M to simultaneously analyze transmembrane mitochondrial potential and nuclear morphology, respectively. The cells were thereafter treated with etoposide (50 μ M). Images of the DiOC6(3) and Hoechst fluorescence were successively recorded every 30 mn for 15 h. The association of DiOC6(3) and Hoechst images and the construction of a movie from these images allowed to visualize, within a cell population, the cells entering in an apoptotic process. Within 30 mn, we observed an aggregation of mitochondria and a loss of transmembrane mitochondrial potential in 40% of the cells. In parallel, condensation or fragmentation of nuclei corresponding to the morphological hallmark of apoptosis was detected; this event preceded the loss of cellular adhesion. Taken together, the present results support that videomicroscopic techniques are well adapted to follow simultaneously different events in apoptotically dying adherent cells.

H015

A MICROSPECTROFLUORIMETRIC DETERMINATION TO MEASURE APOPTOSIS UNDER OXIDATIVE STRESS

Pichon J. 1, Plantin-Carrenard J. 1, Derappe C. 1, Gendron M.C. 2, Bringuier A. 3, Guillot R. 3, Feldman G. 3, Aubery M. 1, Braut-Bouche F. 1

1) Laboratoire de Glycobiologie et Reconnaissance Cellulaire, UFR Biomédicale des Saints-Pères-Université Paris 5, France, 2) UMR 7592 CNRS, Institut J. Monod, 3) INSERM U-327, Université Paris 7, France

We report a new one step staining procedure that permits rapid determination of cell death in adherent endothelial cell line ECV 304 and non adherent leukemic cell line HL 60.

The use of two fluorescent probes: the membrane permeant Yopro-1 and the nuclear probe Propidium iodide combined to the fluorimetric microtitration allow us to determine the ratio apoptosis/necrosis. Both cell lines are exposed to tert-butylhydroperoxide t-BHP to induce oxidative stress and to study associated apoptosis. Etoposide (ETO) and staurosporine (STAURO) are used as reference apoptosis inducers. Under these conditions, in HL60 treated cells, the percentage of apoptosis measured by microspectro-fluorimetry (MSF), compared to untreated cells are 70%, 55% and 40% after exposition to t-BHP, ETO and STAURO respectively. Comparison of these data with those registered in FACS analysis using the same probes revealed that MSF measurement is reliable to the FACS analysis. In the case of ECV 304, the results are very similar to those obtained with HL60 cells, but MSF appeared the most powerful method taking in account the fact that cells could be analysed directly in situ on cell monolayers avoiding the membrane-damage after trypsination. Moreover, the apoptotic state of both cell lines is checked by well-known appropriate methods that reveal apoptosis at different levels: morphological using DAPI nuclear staining, nuclear event by visualizing PARP cleavage and mitochondrial level by the activation of the caspase family (caspases 3 and 8).

In conclusion, we demonstrated the interest of MSF, using probes to measure apoptosis with high sensitivity and good compatibility with vital metabolic functions specially well.

I001

TUMOUR CELL LINES WITH NUCLEAR MULTIDRUG RESISTANCE

Levina V.V., Drobchenko E.A., Filatov M. V., Shabalina E.V., Sukhareva E.B.

Petersburg Nuclear Physics Institute Russian Academy of Science, 188350, Gatchina, St. Petersburg, Russia.

Multidrug resistance (MDR) of tumour cells is regarded as one of the major causes of the failures of the human malignancies therapy. Several mechanisms have been suggested to contribute to MDR. The best-characterised one is associated with the overexpression of transport proteins.

In this study, we show another possibility of MDR, based directly on the mechanisms of drug interaction

with genetic material of the tumour cells- NUCLEAR DRUG RESISTANCE.

The process of active dissociation of noncovalently bound agents from DNA or "DNA clearing" in the living cells was described earlier. "DNA clearing" is energy-dependent and could be suppressed by topoisomerase-2 inhibitors, protein kinase inhibitors and DNA breaks. We made a step by step selection with increasing concentration of the Hoechst 33342, which resulted in the series of Hoechst -- resistant rodent and human cell lines. Some of them (MCF7 HoeR-7) were characterised by an enhanced dissociation of the bisbenzimidazole dye -- DNA complex.

Human breast carcinoma MCF7 HoeR-7 cells differ from parent MCF7 and MF7/Adr - "typical" MDR-1 mediated multidrug resistant cells in the "DNA clearing" efficiency: they have a drastic magnification of the process. MCF7 and MCF7HoeR-7 cells are similar in rhodamine 123 staining and only the resistance phenotype of MCF7/Adr is modulated by verapamil. Therefore, it was concluded that Hoechst resistance of MCF7HoeR-7 cells is not caused by overexpression of transport proteins, but by the enhancement of "DNA clearing". Selected for effective "DNA clearing" Hoechst -- resistant cells have obtained the cross -- resistance to other drugs differing in chemical structure and in the mechanism of action on the DNA: mitomycin C, etoposide, camptothecin and ethidium bromide.

I002

HIGHER-ORDER CHROMATIN STRUCTURE OF TISSUE AND BLOOD CELL NUCLEI AND ITS RELATIONSHIP TO GENE EXPRESSION

Koutná I. 1, Kozubek S. 2, Kozubek M. 1, Hložek P. 1, Lukášová E. 2, Matula Pa. 1, Bártová E. 2, Skalníková M. 1, Ganová A. 2, Jirsová P. 2

1) Faculty of Informatics, Masaryk University, Botanická 68a, 602 00 Brno, Czech Republic, 2) Institute of Biophysics, Academy of Sciences, Královopolská 135, 61265 Brno, Czech Republic

Using single and dual colour fluorescence in situ hybridisation (FISH) combined with image analysis techniques, topographic characteristics of chromosomes, genes and centromeres were studied. The distributions of the centre-of-nucleus to signal and signal to signal distances for different genetic loci such as chromosomes, genes and centromeres

were studied in normal colon tissue cells, in cell line HT-29 and HL-60 cell line for comparison. Our results show that the topography of genetic loci determined in 3D-fixed cell tissue corresponds to the one obtained for 2D-fixed cells separated from the tissue. The above mentioned distributions and their average values are different for various genetic loci, but similar for normal colon tissue cells, HT-29 cell line and HL-60 cell line. The relation between chromatin structure and gene expression was studied using chromosomes with different proportion of euchromatin (which is actively transcribed) as compared to heterochromatin (which is inactive). The centre-of-nucleus to domain weight centre distances were determined and averaged for each chromosome. It was found that the higher proportion of heterochromatin in a chromosome is correlated to the more peripheral location of its domain. The investigations of trisomic loci in HT-29 cells revealed that the location of the third genetic element is not different from the location of two homologs in diploid cells. On the other hand, we found differences in the topography of the APC gene in human blood and tissue samples. In the human blood cells, where the expression of APC is naturally down-regulated, the APC gene is located near to the nuclear periphery as compared to cells of tissue origin. These differences in topographic parameters support the hypothesis that the higher-order chromatin structure and the level of gene expression are correlated.

I003

CHROMATIN TEXTURE, HISTONE H4 ACETYLTATION, AND MULTIDRUG-RESISTANCE GENE EXPRESSION IN HUMAN OVARIAN CARCINOMA CELLS

Dufer J. 1, Yatouji S. 1, Trentesaux C. 1, Liautaud-Roger F. 2

1) Unité MÉDIAN, CNRS FRE2141, IFR53, Faculté de Pharmacie, Reims, 2) Institut Jean-Godinot, Reims, France

We showed previously that multidrug-resistant cancer cells, selected in increasing concentrations of anticancer drugs and overexpressing P-gp, displayed nuclear texture changes as assessed by image cytometry. In this work, two tumoral cell lines were studied: the human ovarian carcinoma cell line IGROV1 and its multidrug-resistant variant OV1-VCR, selected with vincristin. Cell smears were

stained with Feulgen method and analyzed by image cytometry. As compared to sensitive cells, OV1-VCR displayed a global decondensation of the chromatin as assessed by textural features analysis. In order to correlate this decondensation with alterations in chromatin structure, DNase I was used as a probe to preferentially digest potentially active genes in chromatin. OV1-VCR displayed an increased (about 5 fold) DNase I sensitivity, suggesting an increased chromatin accessibility. It has been shown that high levels of chromatin acetylation across complete chromatin domains induced chromatin changes detected as "general DNase I sensitivity". By western blotting, the level of acetylated histone H4 appears increased in OV1-VCR cells. Furthermore, treatment of IGROV1 sensitive cells with the histone deacetylase inhibitor trichostatin A induces an increase in histone H4 acetylation level, followed by a significant expression of *mdr1* mRNA and leads to nuclear chromatin supraorganisation changes similar to those observed in OV1-VCR resistant cells.

This work was supported by the "Comités Départementaux de la Haute-Marne et de l'Aube de la Ligue Française contre le Cancer".

I005
CHANGES OF CHROMATIN
CONFORMATION IN HUMAN
LYMPHOCYTES IN AGING AND
CYTOGENETIC DISEASES

Ekhtiar A., Al-Achkar W.

Flow Cytometry Lab., Molecular Biology & Biotechnology Dept. Syrian Atomic Energy Commission, Damascus-Syria. P.O.Box: 6091.

It has been shown that DNA in nucleus is less sensitive to external and internal DNA damaged agents than DNA in scavenger-free aqueous solution. This protection is thought to be due to the scavenging of OH radicals by soluble intracellular compounds as well as chromatin structure. It has been found: that mutation frequencies, DNA damage, chromosomal aberrations and free radicals are increased with aging. While the DNA repair capability undergoes a decrease.

The aim of the present work was to detect the changes of chromatin conformation during the aging process and the changes associated with some cytogenetic diseases. To this end, human lymphocytes were separated from various aging

patients using Phycols columns, and the lymphocytes were further fixed in graded 40, 60, 80, 95% ethanol series. After staining the samples with Propidium Iodide (PI) (106 cells per ml of PI at 10⁻⁶ M final concentration), the cells were analyzed on a FACS Vantage flow cytometer (Becton Dickinson, USA). Our results showed increases in chromatin decondensation with aging, and some changes with chromatin conformation associated with cytogenetic diseases.

I006
FLUORESCENT EXAMINATION AND
COMPUTER ANALYSIS OF INTERMEDIATES
OF CHROMOSOMAL CONDENSATION
WITHIN THE NUCLEI OF SYNCHRONIZED
CHINESE HAMSTER OVARY (CHO-K1)
CELLS

Szepessy E., Nagy G., Banfalvi G.

University of Debrecen, Faculty of Natural Sciences, Department of Animal Anatomy and Physiology, H-4010, Debrecen, Egyetem ter 1., Hungary

The eukaryotic DNA is a molecule organised in a complex manner. The structural details of the DNA from the primary level, i.e. the base pair sequence, to the nucleosomal level, have been well established by biochemical and radiological studies. The structural aspects of the chromatin condensation beyond the supranucleosomal level are still poorly defined.

In the background of the lack of knowledge in this field stands the fact that the chromatin folding process is taking place inside the nucleus, restricting the possibilities for direct approaches of investigations. The major goal of this work is to introduce a new method for the visualisation of the folding of the chromatin structure throughout the cell cycle. We present evidence supporting the theory of a dynamic and flexible folding pattern.

Synchronized cells following reversible permeabilization are able to replicate in the presence of biotin-11-dUTP. Biotinylated deoxy-nucleotides do not disturb the DNA replication, but inhibit the chromatin folding leading to the accumulation of intermediates of the condensation. Chromatin structures were examined by fluorescent microscopy. The photographs were further studied by digital image analyser system. Using the computed technique, we managed to magnify and distinguish between chromatin structures, which seemed to be identical for the human eyes.

I007**CHROMOSOMAL IMBALANCES AND NUCLEAR MORPHOLOGY IN BREAST CANCER**

Friedrich K. 1, Scheithauer J. 1, Meyer W. 1, Dimmer V. 1, Theissig F. 1, Haroske G. 2, Baretton G. 1, Kunze K.D. 1

1) Dresden University of Technology, Institute of Pathology; Germany; Fetscherstr. 74; D-01307 Dresden, 2) Dresden-Friedrichstadt General Hospital; Germany; Friedrichstr. 41; D-01067 Dresden

The study aimed to detect differences in quantitative nuclear features in breast cancers, in relationship to changes in the genome.

Feulgen stained fine needle aspirates or imprints of fresh breast cancer tissue were measured by a high resolution image cytometry workstation. From each nucleus, 130 features were computed on a MicroVAX 4000 computer. Chromosomal imbalances were detected by CGH.

Breast cancer with a high number of chromosomal imbalances differ from their counterparts with a low number of imbalances in features of the shape and of the texture, indicating a higher nuclear polymorphism. A high number of imbalances of whole chromosome arms and of chromosomal parts, with at least one border outside of the centromere or telomere, were associated with changes of the nuclear texture, compared with cases with a low number of imbalances, in these chromosomal parts. Tumors with gains at 8q, losses at 18p and 18q exhibited a higher irregularity in the chromatin distribution than tumors without these imbalances. In tumors with a loss at 18p, additional differences in the shape of nuclei were found. Further differences in the nuclear texture were detected in correlation to gains at parts of 17q. Changes in the nuclear morphology were associated with the occurrence of imbalances in two chromosomal regions together, too.

On the other hand, some copy number changes, like gains at 1q, at 11q13, at 20q and losses at 8p, 9p, 17p were not mirrored by the nuclear morphology.

In summary, the results confirm the correlation between changes in the genome and the nuclear morphology and emphasize the role of specific chromosomal regions for the nuclear morphology.

J001**TOWARDS THE COMPUTER MODELLING OF DYNAMIC NUCLEAR ORGANIZATION**

Kreth G. 1,2,+, Edelmann P. 1,2, Cremer T. 3,2, Cremer C. 1,2

1) Kirchhoff Institute of Physics, University, D-69120 Heidelberg, Germany, 2) Interdisciplinary Center for Scientific Computing (IWR) (+ Graduate College), University, D-69120 Heidelberg, Germany, 3) Institute of Anthropology and Human Genetics, University, D-80333 München, Germany

An approach was developed for a computer simulation of large scale nuclear organization, allowing quantitative, experimentally testable predictions. For a simplified model calculation, the reciprocal interactions of chromosomal foci in the chromosome territories were approximated by substituting them by volume equivalent enveloping spherical domains of 500 nm diameter, each of them assumed to contain a chromatin domain with a DNA content of about 1Mbp (Spherical 1-Mbp Chromatin Domain model). Different experimentally testable quantities were calculated, such as the size and spatial distribution of "chromosome territories" in the model nuclei; "telomere-centromere" and "telomere-telomere" distances; nearest neighbor distances of "R and G band domains"; or the spatial distribution of "Double Minute chromosomes" (DMs) in model nuclei with a shape corresponding to neuroblastoma cell nuclei.

J002**APPLICATION OF PROLIFERATION CONTROL NETWORK MODEL TO THE SIMULATION OF EPITHELIAL HOMEOSTASIS**

Morel D., Marcelpoil R., Brugal G.

Equipe RFMQ Lab. TIMC-IMAG, Domaine de La Merci, Faculté de Médecine, Institut Albert Bonniot, 38706 La Tronche Cedex, France

Homeostasis defines the conditions of a system when it is able to maintain its essential variables within limits acceptable to its own structure and function in the face of unexpected disturbances. Because of the complexity of the biological processes involved, computer simulation represents a powerful tool to investigate the field of homeostasis regulation networks in silico.

Our approach combines a spatial representation of cells in 2D using the Voronoi graph and a model of cell proliferation and differentiation controls. The Voronoi graph associates a polygon to every cell and the set of these polygons defines the tissue architecture. The model for cell proliferation and differentiation regulation network includes intracellular (Cyclins, Cyclin Dependent Kinases, Rb, E2F family transcription factors, CDKs inhibitors) and extracellular controls (growth and differentiation factors, integrins). A software was developed to feed the model with as much parameters as wanted and to design possible control networks for cell proliferation and differentiation. This system, which integrates the spatial representation of cells, permits a quantitative modulation of the extracellular signals as a function of the cell neighbourhood during time dependent simulations.

Our results show the role of CDKs inhibitors (mainly p27) in the Rb dependent G1 to S phase control pathway. It is also possible to model the different kinetic behaviours of stem and transit amplifying cells of the epithelium basal layer. 2D simulations illustrate the influence of the microenvironment on cell proliferation in basal layers of stratified epithelia and of differential adherence in keratinocytes differentiation and related upward migration.

J003

ARCHITECTURAL ANALYSIS OF BRONCHIAL INTRA-EPITHELIAL LESIONS: A STOCHASTIC APPROACH TO STANDARDIZE ARCHITECTURAL FEATURES BASED ON A HOMOGENEOUS POISSON PROCESS

Guillaud M. 1, MacAulay C. 1, Korblic J. 1, Dawe C. 1, Le Riche J.C. 2, Lam S 3

1) Department of Cancer Imaging, British Columbia Cancer Agency and the University of British Columbia, 2) Department of Pathology, British Columbia Cancer Agency and the University of British Columbia, 3) Department of Respiratory Medicine, British Columbia Cancer Agency and the University of British Columbia

Bronchial carcinomas are preceded by a series of morphological and architectural changes. Numerous papers have shown the potential of graph theory derived algorithms to describe changes in tissue architecture and eventually as surrogate endpoints

biomarkers for chemoprevention studies. Nevertheless, the use of any architectural features is highly questionable when dealing with strips of epithelium of only a few hundred cells. Furthermore, in pseudo-stratified epithelium, pre-neoplastic process is characterized by a significant increase of the epithelium thickness (and the number of cells).

We have developed an algorithm that measures changes in the tissue architecture as a function of the number of cells, but also as a function of the area and the shape of the region under analysis. The idea is to use a theoretical point pattern (the homogeneous Poisson Process or Complete Spatial Randomness (CSR) with respect to which other empirical point patterns are compared).

Each biopsy is characterized by a bounded region B of area A, of shape S and by n, the number of cells in this region. About 25 architectural features are extracted from this sample. By Monte-Carlo simulations, we generate 500 homogeneous spatial point patterns, with n, A, and S as parameters and extract architectural features from each of these simulations. The mean and the standard Deviation of the probabilistic theoretical distribution of any feature are then used to transform raw architectural features into standardized features (z-score).

We have performed these simulations on more than 3000 bronchial pre-neoplastic lesions. We will show the potential of this approach to quantify the intrinsic tissue architecture changes in bronchial intra-epithelial lesions.

J004

QUANTITATED TISSUE ARCHITECTURE OF THE INVASIVE FRONT OF EARLY STAGE CARCINOMAS GIVES A TOOL FOR TREATMENT DECISION

Sudbø J. 1, Marcelpoil R. 2, Reith A. 1

1) Dpt of Pathology, The Norwegian Radium Hospital, Oslo, Norway, 2) Universite Joseph Fourier, Grenoble, France.

Several studies on oral squamous cell carcinomas (OSCC) suggest that the clinical value of traditional histological grading is limited both by poor reproducibility and low prognostic impact. However, the prognostic potential of a strictly quantitative and highly reproducible assessment of the tissue architecture in OSCC has not been evaluated.

Using image analysis, we retrospectively investigated the prognostic impact of 2 graph theory derived

structural features -average Delaunay Edge Length (DEL_av) and average homogeneity of the Ulam Tree (ELH_av) - in 193 cases of T1-2 (Stage I-II) OSCCs. Both structural features were derived from subgraphs of the Voronoi Diagram (VD). The geometrical centers of cell nuclei were computed, generating a two-dimensional swarm of pointlike seeds from which graphs could be constructed. The impact on survival of the computed values of ELH_av and DEL_av was estimated by the method of Kaplan and Meier, with relapse free and overall survival as considered end-points. The prognostic values of DEL_av and ELH_av as computed in the invasive front, the superficial part of the carcinomas, the total carcinoma and normal appearing oral mucosa were compared.

For DEL_av significant prognostic information was found in the invasive front ($P < 0.001$). No significant prognostic information was found in superficial part of the carcinomas ($P = 0.34$), in normal appearing mucosa ($P = 0.27$) or in the carcinoma as a whole ($P = 0.35$). For ELH_av significant prognostic information was found in the invasive front ($P = 0.01$) and, surprisingly, in putatively normal mucosa ($P = 0.03$). No significant prognostic information was found in superficial parts of the carcinomas ($P = 0.34$) or in the total carcinoma ($P = 0.11$).

In conclusion, strictly quantitative assessment of tissue architecture in the invasive front of OSCC yields highly prognostic information.

K001

IMPROVED CONFOCAL CHARACTERIZATION OF TARGETS IN NUCLEI

Kahn E. 1, Coullin P. 2, Frouin F. 1, Todd-Pokropek A. 1, Bernheim A. 2

1) INSERM U494, CHU Pitié-Salpêtrière, 75634 Paris Cedex 13, France, 2) CNRS UMR 1599, Institut Gustave Roussy, 94805 Villejuif, France.

The purpose is to show that cellular preparations requiring depth analysis of different domains stained by molecular cytogenetic methods (FISH, PRINS, HISOMA) can be processed by factor analysis of medical images (FAMIS), to isolate fluorescent probes by means of intensity depth profiles of fluorochromes. FAMIS was applied to preparations containing spots (centromeres, cosmids, telomeres) inside human cell nuclei to visualize depth differences and we used a confocal microscope

(SARASTRO CLSM 1000 Molecular Dynamics) to improve the visualization of images. 3D sequences of images obtained by depth displacement were first analyzed by the regular FAMIS algorithm. Resulting factor images were further processed by regularization methods which improve signal/noise ratio while preserving targets contours. Results showed that factors and regularized images could help to analyse targets inside nuclei. The study leads us to process preparations containing numerous spots on possible different planes to differentiate stained targets, to investigate depth differences and to improve visualization and detection.

K002

CYTOGENETIC CHARACTERIZATION OF CHROMOSOMAL REARRANGEMENT ACTIVATING THE MDR1 GENE IN A VINBLASTIN-RESISTANT CEM CELL LINE

Strusky S. 1, Cornillet-Lefebvre P. 1, Doco-Fenzy M. 1, Dufer J. 3, Ulrich E. 2, Gruson N. 2, Masson L. 2, Michel N. 2, Potron G. 1

1) Laboratoire d'Hématologie, EA2070, IFR53, 2) Laboratoire de Cytogénétique, Centre Hospitalier Régional, Reims, 3) Unité MÉDIAN, CNRS FRE2141, IFR53, Faculté de Pharmacie, Reims, France

In order to identify genomic changes associated with a drug-resistance acquisition, we performed R-banding karyotype, fluorescence in situ hybridization (FISH) and comparative genomic hybridization (CGH), to compare a human T-cell lymphoblastic leukemia cell line the CCRF-CEM cell line, and a variant subline resistant to vinblastin (CEM-VLB). This CEM-VLB cell line overexpresses the P-glycoprotein, the product of the MDR1 gene. The CGH analysis showed that the CEM-VLB cell line carried chemoresistance-specific chromosomal abnormalities (amplification of 7q11-q22, losses of 2, 3, 5, 9, 10, 16, and deletion of 4q13-qter). FISH identified a homogeneously staining region, on the short arm of the chromosome 2 translocated to 7q21 region, containing amplified MDR1 gene, and probably neighboring genes, as sorcin or MDR3. This chromosomal rearrangement occurred during drug selection and attested a resistance acquisition. According to previous reports, the translocation of the MDR1 occurs as the first step before amplification, leading to increased MDR1 expression.

K003
PATTERNS OF CHROMOSOMAL
ABERRATIONS ASSESSED BY
FLUORESCENCE IN SITU HYBRIDIZATION
IN HEAD AND NECK SQUAMOUS CELL
CARCINOMAS WITH DIFFERENT FLOW
CYTOMETRIC DNA CONTENTS

Hemmer J., Hauser C.

Division of Tumor Biology, University of Ulm, Germany

The prognosis of patients with flow cytometrically diploid head and neck carcinomas is excellent. Independent of the actual degree of DNA content aberration, the outcome of aneuploid tumours is poor. This, despite an increasing divergence of aneuploid DNA content from the normal diploid value, implies a corresponding gain in underlying karyotypic complexity. To analyse whether tumour clones with different DNA contents have chromosomal changes in common that may be critical for the acquisition of a similar malignant behaviour, FISH with 13 centromere-specific DNA probes was applied to 3 diploid and 11 aneuploid tumours with DNA indices ranging between 0.8 and 2.2. Disomic and monosomic cell populations were prevailing findings in DNA-diploid tumours. Polysomies were common in aneuploid tumours. Aneuploid tumours regularly contained cell populations with different degrees of aneusomy for identical chromosomes. Although FISH signal heterogeneity was identified for all chromosomes, there were remarkable differences. The mean number of aneusomic cell populations identified for DNA-aneuploid tumours ranged between 1.6 for chromosome 17 and 3.1 for chromosome 3. The inconsistencies between FISH signal heterogeneity and seemingly monoclonal FCM data may indicate that centromere-specific DNA probes identify gains and losses of marker DNA due to complex karyotypic rearrangements and the assembly of entirely new chromosomal entities rather than absolute changes in original chromosome numbers. Overall, there was no evidence of the critical involvement of particular chromosomes in the development of clones with different DNA contents.

K004
ACCUMULATION OF CHROMOSOMAL
CHANGES IN THE TRANSITION FROM
ADENOMA TO CARCINOMA DETECTED BY

CGH IN COLORECTAL MALIGNANT
POLYPS

Hermesen M. 1, Postma C. 1, Weiss M. 2, Meuwissen S. 2, Williams R. 3, Rapallo A. 4, Giaretti W. 4, Baak J. 1, Meijer G. 1

1) Department of Pathology, Free University Hospital, Amsterdam, The Netherlands, 2) Department of Gastroenterology, Free University Hospital, Amsterdam, The Netherlands, 3) Department of Pathology, University of Melbourne, Australia, 4) Laboratory of Biophysics and Cytometry, National Cancer Institute, Genoa, Italy.

Knowledge of genomic changes accompanying progression from colorectal adenoma to carcinoma within individual tumors is limited. In the present study, chromosome aberrations in pre-invasive (adenomatous) and invasive (carcinomatous) components of 40 malignant polyps were studied by comparative genomic hybridization.

In general, the invasive components showed more abnormalities and stronger signal amplitudes than the preinvasive ones, reflecting a lesser genetic heterogeneity in the former. As opposed to many other solid tumor types, losses were the most frequent events, at: 8p22-23, 11q13, 12q24, 15q11-15, 16p, 17p13, 18q12-21, 21q and 22q. Gains were observed at 8q22, 13q21-22 and 20q. In 5 cases, high level amplifications were seen both in the preinvasive and in the invasive components, at 1p34, 8q24, 13q34, 20q11 and 20q13. The carcinomatous parts of the malignant polyps showed a lower number of 8p loss and 8q gain than later stage carcinomas, suggesting that they are progression associated events. We detected a low incidence of K-ras mutations in these tumors, as opposed to single adenomas. Interestingly, we found an inverse correlation between K-ras mutation and 8q gain, where c-myc is located. It may be that both are capable of blocking the same pathway, one in the early stages of development, the other in the later.

When comparing the invasive with the pre-invasive components, we observed a clear increase in occurrence of losses at 15q11-15, 17p13, 18q12-21 and 21q. These events may be related to the acquisition of invasive behaviour. Taking p53 as a candidate gene on 17p13, we used immunohistochemistry to detect protein expression and indeed we found a significantly higher number of p53 positivity in the invasive components. We are currently working to identify other candidate genes

and proteins which may be involved in the transition from adenoma to carcinoma.

K005

CHROMOSOMAL CHANGES IN LARYNX AND PHARYNX SQUAMOUS CELL CARCINOMA DETECTED BY CGH SEEM UNRELATED TO TUMOR STAGE AND CLINICAL OUTCOME

Hermesen M.A.J.A. 1, Guervòs M.A. 2, Meijer G.A. 1, Baak J.P.A. 1, Van Diest P.J. 1, Marcos C.A. 2, Sampedro A. 3

1) Department of Pathology, Free University Hospital, Amsterdam, The Netherlands, 2) Department of Otolaryngology, Valle del Nalòn Hospital, Oviedo, Spain, 3) Cytometry Service, University of Oviedo, Spain

Chromosomal gains and losses in 34 larynx and 22 pharynx primary untreated carcinomas were investigated with comparative genomic hybridization (CGH) and results were related to a series of clinical parameters and follow-up information.

Flow cytometric analysis showed 18 out of 50 cases to be DNA diploid. CGH analysis on average detected 11.1 gains and 8.5 losses. The major chromosome arms showing gains were (in decreasing order): 3q, 7q, 8q, 5p, 11q13, 17q and 18p, and losses at 3p, 11qter, 4p, 18q, and 5q. Apart from low level gains, 35 tumours contained high level amplifications, with an average of 2.3 per case. The segment most frequently amplified was 3q26-qter (20 cases). Other recurrent regions were 11q13 (7 cases), 11q22 (5 cases), 3q12-13 (5 cases), 18p11.3 (5 cases), 18q11.2 (5 cases), and 8q24.3 (3 cases). Up to 36% of all chromosomal aberrations consisted of whole chromosome arms, in a substantial number of cases seen as a simultaneous gain of the one and loss of the other chromosome arm, indicative of isochromosome formation.

We found no specific chromosomal abnormality correlated with the clinical stage, the occurrence of positive lymph nodes, the DNA ploidy, or the degree of differentiation. When comparing cases of patients with favourable and unfavourable clinical follow-up, we found a relation to the stage and lymph node status, but not to the DNA ploidy or specific chromosome changes. This surprising result seems to indicate that genetic alterations on the level of DNA ploidy or chromosomes can not be used as prognosticators.

K006

COPY NUMBER ASSESSMENT OF CHROMOSOME REGION 3Q26 IN CERVICAL NEOPLASIA BY IN SITU HYBRIDIZATION

Macville M. 1, Wienk S. 1, Gemmink J. 1, Robben J. 1, Heselmeyer K. 2, De Wilde P. 1, Hanselaar A. 1.

1) Department of Pathology, UMC St Radboud Nijmegen, The Netherlands, 2) Genetics Department, Division of Clinical Sciences, NCI-NIH, Bethesda, MD, USA.

Molecular cytogenetic studies on paraffin-embedded cervical intraepithelial neoplastic (CIN) lesions and invasive carcinomas have revealed a positive correlation between a numerical gain of centromere of chromosomes (cen#) 1, 7, and X and CIN grade. CGH analysis identified a numerical gain for 3q24-26 as the sole genetic event marking the transition from severe dysplasia/CIS to microinvasive carcinoma, and, in tumor stages II-IV, a high copy number gain for 5p was the most prominent additional genetic imbalance. Interphase cytogenetic analysis based on specific genetic aberrations may be a useful new tool to discriminate progressive from regressive lesions in cervix cytology. We have developed conventional transmission light microscopic ISH protocols for a BAC probe specific for 3q26 on AgarCyto cell-blocks from cervical scrapings. Details for sampling, fixation, permeabilization treatments, hybridization conditions, immunocytochemical detection and screening will be discussed. Preliminary results of a study correlating numerical changes for 3q26 with CIN will be presented.

K007

METHODS FOR INTERPHASE CYTOGENETICS ON CYTOLOGICAL PREPARATIONS FROM CERVICAL SCRAPINGS

Macville M. 1, Wolf R. 1,2, Wichelo C. 1, Verbeek D. 3, Mravunac M. 3, Heselmeyer K. 4, Ried T. 4, De Wilde P. 1, Hanselaar A. 1

1) Department of Pathology, UMC St Radboud Nijmegen, The Netherlands, 2) Department of Pathology, Rijnstate Hospital Arnhem, The Netherlands, 3) Department of Pathology, Canisius-Wilhelmina Hospital Nijmegen, The Netherlands, 4) Genetics Department, Division of Clinical Sciences, NCI-NIH, Bethesda, MD, USA.

A key health care problem in cervical screening programs is the relative low specificity of the Pap-smear test to discern progressive and regressive intra-epithelial lesions. It has been estimated that 98% of the women who are treated for an abnormal Pap smear would never have developed cancer if left untreated. Therefore, ancillary methods to identify aggressive lesions in the first line of cytological diagnosis are highly demanded. Molecular cytogenetic studies on paraffin-embedded cervical intraepithelial lesions and invasive carcinomas have revealed a positive correlation between numerical gain of centromere of chromosomes (cen#) 1, 7, and X and CIN grade. Comparative genomic hybridization (CGH) analysis identified numerical gain of 3q24-26 as the sole genetic event marking the transition from severe dysplasia/CIS to invasive carcinoma, and, in tumor stages II-IV, a high copy number gain for 5p was the most prominent additional genetic imbalance. We have focused our diagnostic research on numerical aberrations of cen#1 and chromosome loci on 5p15 and 3q26 in histological and cytological patient material. We have developed ISH protocols on AgarCyto cell block material from cervical scrapings, and on two liquid-based cytology methods, AutoCyte Prep and ThinPrep. Preliminary results of a prospective study on cen #1 aneusomy by in situ hybridization in progressive and regressive lesions using cervix AgarCytos show that aneusomy for cen# 1 is a reliable marker for progression in women diagnosed with atypia or a low-grade squamous intraepithelial lesion (LSIL), and may be a potential parameter to triage patients with atypia and LSIL.

K008

CHROMOSOMAL INSTABILITY AND LOSS OF P53 FUNCTION IN PEYRONIE'S DISEASE MYOFIBROBLASTS

Shankey T.V., Branch J., Lubrano T., Mulhall J.P.
Department of Urology, Loyola University Medical Center, Maywood, IL, 60153, USA

Peyronie's disease is a focal fibromatosis of the penis of unknown origin. Previous studies have reported karyotypic abnormalities in Peyronie's and in similar fibromatoses.

Objective: This study was undertaken to investigate genetic abnormalities in Peyronie's cell cultures.

Methods: Fibroblast-like cells were cultured from Peyronie's plaque or normal tunical tissue from nine

Peyronie's patients. Cells established in tissue culture were characterized by immunofluorescence. Fluorescence in-situ hybridization was performed using centromere specific probes. DNA content and cell cycle analysis was performed using flow cytometry. Qualitative and quantitative expressions of p53 and related cell cycle proteins was measured using Western blot and flow cytometry, respectively.

Results: Low passage cell cultures demonstrated a IF pattern consistent with myofibroblasts (vimentin pos, cytokeratin and desmin neg, with low (20-30%) percentages of smooth muscle actin pos. cells). Low passage cells showed disomy for chromosomes 7,8,12,17, and 18, and monosomy for X and Y by FISH. Within 10 to 15 passages, the majority of cultures (plaque or normal) developed morphologically abnormal cells, with concomitant aneusomy for a number of chromosomes. Low passage (disomic) cells demonstrated low but elevated levels of p53 protein, compared to neonatal foreskin fibroblasts. Tests of p53 function demonstrated no significant increase in p53, mdm-2, p21 or Bak protein levels following 5 Gy irradiation. FISH analysis of these same low passage cells showed no evidence for loss of p53 loci (ratio of p53 loci to chromosome 17 centromere 1:1).

These results suggest a DNA virus may be involved in the development of Peyronie's disease.

K009

VIRTUAL INTERPHASE CYTOGENETICS

Cremer C. 1,2, Kreth G. 1,2

1) Applied Optics and Information Processing, Kirchhoff Institute for Physics (KIP), University Heidelberg, Albert-Ueberle-Str. 3-5, 69120 Heidelberg, Germany

2) Interdisciplinary Center of Scientific Computing (IWR) of the University, INF 368, 69120 Heidelberg; Germany

Molecular cytogenetics allows genome analysis on a „cell-by-cell“ basis, such as changes in chromosome number; tumor-relevant chromosome translocations; deletions and amplifications of individual chromosome regions; integration sites of DNA-vectors etc. Using metaphase spreads and spectral karyotyping (Speicher et al. 1996), the simultaneous measurement of hundred or more different genetic features appears to be possible. It should be highly desirable to transfer the spectral karyotyping approach to interphase nuclei. In doing this, however,

one has to cope with the problem that in contrast to metaphase spreads, it is much more difficult to separate optically the different genomic regions in such a way that multiple combinatorial labeling provides reliable results: In metaphase spreads, the 46 chromosomes are optically well separated from each other, and the fluorescence emission of each genome region in the size of a few megabase pairs (Mbp) can be detected independently from each other; thus, such regions can be identified due the combination of the different spectral emissions. In interphase nuclei, however, neighboring chromosome territories are not optically as well separated from each other as the metaphase chromosomes. The more chromosome territories, subterritories band regions, and still smaller units have to be discriminated by combinatorial spectral karyotyping, the more difficult an unequivocal assignment will become. For such an assignment, it is necessary that the distance between two nuclear sites A and B labeled by spectral combinations containing one or more identical spectral signatures (e.g. specs 1, specs 2, specs 3 for A; specs 1, specs 2, specs 4 for B) is larger (or at least equal) than the optical resolution of the system (as defined e.g. by the smallest distance discriminated using two „point like“ objects of the same spectral signature).

To resolve the problem, advanced methods of fluorescence microscopy with increased optical resolution will be essential. Recently, new methods of „Point Spread Function“ (PSF) engineering were introduced which allow an optical resolution of 100 nm and less in all three spatial directions. In many cases, however, even a considerably lower three-dimensional (3D) resolution realized in readily available commercial instruments will be sufficient, when an intelligent combinatorial labeling is performed, e.g., taking into account the actual knowledge about the distribution of chromosome territories in the nucleus (v. Hase 2000). To achieve such an intelligent labeling scheme, computer simulations of the nucleus with a "realistic" distribution of the chromosomes and virtual microscopy methods will be helpful (Cremer et al. 2000).

References :

Cremer, T., Kreth, G., Koester, H., Fink, R.H.A., Heintzmann, R., Cremer, M., Solovei, I., Zink, D., Cremer, C. (2000) *Chromosome territories, interchromatin domain compartment and nuclear matrix: an integrated view of the functional nuclear architecture*, *Critical Reviews in Eukaryotic Gene*

Expression, 12, 179-212.

v. Hase, J. (2000) *Quantitative Bildanalyse der DNA-Verteilung spezifischer Chromosomenterritorien im Zellkern*, *Diploma thesis, University of Heidelberg*.

L001

SENSITIVITY TO ANTI-CANCER DRUGS PREDICTED IN VITRO BY MEASURING CHANGES IN FLUORESCENCE INTENSITY AND POLARIZATION USING THE CELLSCAN: THE BASIS FOR A CLINICAL MODEL

Schiffenbauer Y.S. 1, Trubniykov E. 1, Zacharia B. 1, Gerbat S. 1, Berke G. 2, S. Chaitchik S. 3

1) Medis-El Ltd., Yehud, Israel, 2) Department of Immunology, Weizmann Institute of Science, Rehovot, Israel,

3) Sackler Medical School, Tel Aviv University, Ramat Aviv, Israel.

Tumor heterogeneity with respect to the response to chemotherapy is a major problem in the field of oncology. We have used the CellScan, a novel static cytometer equipped with a unique cell carrier, for the purpose of monitoring changes in fluorescence intensity (FI) and polarization (FP) in cancer cells affected by anti-neoplastic drugs. The novelty of the method is its end-point, which is independent of tumor proliferation, avoiding the complication of tumor culturing and reducing significantly the duration of the assay. Briefly, T47D and T80 human breast cancer cell lines were exposed to low and high doses of anti-neoplastic drugs and the FI and FP of fluorescein diacetate (FDA, indicator of cell viability) and rhodamine 123 (Rh123, indicator of apoptosis)-stained cells were measured.

Hyperpolarization of FDA as well as of Rh123 occurred in sensitive cells in conjunction with annexin V binding and propidium iodide exclusion, indicating that hyperpolarization is related to early apoptosis. The new experimental model presented here could serve as the basis for the development of a rapid clinical assay for anti-cancer drug action with small biopsies from solid human tumors.

L002

BIOCOMPATIBILITY / CYTOTOXICITY OF MEDICAL DEVICES : A DIRECT ASSESSMENT ON LIVING ADHERENT

**CELLS BY COLD LIGHT
CYTOFLUORIMETRY IN MICROPLATE**

Kaffy C. 1, Bruneau de la Salle S. 1, Rat P. 1,2, Warnet J.-M. 1,2

1) Unité de Pharmacologie Toxicologie Cellulaire, C.H.N.O. des XV-XX, 28, rue de Charenton 75012 Paris, France,

2) Laboratoire Toxicologie, Faculté de Pharmacie (Paris V), 75006 Paris, France

The purpose of this study was to investigate in vitro the cytotoxicity (necrosis, apoptosis) and cell proliferation induced by eluates extracted from different types of polymers: PMMA (PolyMethylMethacrylate), silicone and acrylic. Because these materials are used in Intra Ocular Lenses (IOLs), their cytotoxic potential must be evaluated according to the 10993-5 ISO norm with a new cytofluorimetric method. Biomaterials were immersed in culture medium for 24 hours at 37°C in 5% CO₂. IOL leachables, negative (Polystyrene for cell culture) and positive controls (phenol, latex extract) and cell control were incubated for 24 hours in a 96-well plate containing L929 mouse fibroblasts or human conjunctival cells.

The cytotoxic effect of each eluate was assessed by using a membrane integrity probe (fluorescent neutral red) and DNA probes (Hoechst 33342 / Propidium Iodide). This multilabelled assay allows to quantify different cellular stress : necrosis, apoptosis (chromatin condensation), cell proliferation and hormesis (chemical sensitisation) with a high sensitivity (pg/mL) using a microplate cold light cytofluorimeter (Fluorolite 1000-Dynex™). Results have shown that neutral red assay, although widely used, is not sufficient to evaluate the cytotoxicity of materials. Not only is there a necrotic aspect of the cell death but also an apoptotic one. Our in vitro results confirm the clinical observations about the use of such a medical device and side effects associated (secondary cataract).

To conclude, Microtitration Fluorimetric Assays on Live Adherent Cell (MiFALC tests)* should be very useful for the cytotoxicity screening and side effect prognostics of IOLs and to improve the actual ISO norm for all of the medical devices.

Reference :

* (*P.Rat, Methods Enzymol.,1995:252,331*).

**L003
OXIDATIVE STRESS ASSESSMENT
DIRECTLY ON LIVE ADHERENT CELLS IN
MICROPLATES USING COLD LIGHT
CYTOFLUORIMETRY. APPLICATION OF
FLUOROQUINOLONES**

Pouzaud F. 1,2, Rat P. 1,2, Christen M.-O. 3, Thevenin M. 2, Warnet J.-M. 1,2

1) Unité de Pharmacologie Toxicologie Cellulaire, CHNO des XV/XX - 75012 Paris 2) Laboratoire Toxicologie, Faculté Pharmacie (Paris V) 75006 Paris 3) Laboratoires Solvay Pharma Suresnes 92 - France

Fluoroquinolones (FQ) are widely used in clinics, but adverse effects (high tendon rupture risk) have been recently observed. To investigate oxidative stress associated to five FQ, Pefloxacin (PEF), Ofloxacin (OFX), Ciprofloxacin (CIP), Levofloxacin (LEV), Moxifloxacin (MOX) were directly incubated with Rabbit adherent tenocyte cell line, at their human blood (10⁻³-10⁻⁶M) concentrations. Cell viability, redox potential, Reactive oxygen Species (ROS) and O₂⁻ production and intracellular glutathione were assessed using neutral red, Alamar Blue (AB), H₂DCF-DA, dihydroethidium and monobromobimane probes. Fluorescence signal has been scanned directly in 96-well microplates with high sensitivity (pg/ml), using cold light cytofluorimeter (Fluorolite 1000-Dynex™). A high significant delayed tenotoxicity was detected after 48-72h, especially, for PEF, MOX and CIP. ROS overproduction was observed for all FQ, but O₂⁻ increase was only observed for PEF and CIP. AB test permits to discriminate intrinsic tenotoxicity potential of FQ. High redox potential decrease (-70, -80% vs control) was observed for PEF, MOX and CIP, whereas moderate redox potential decrease (< -30%) was observed with OFX and LEV. For all FQ, Anethole DithioleThione (ADT) can modulate oxidative stress (↑ ROS, - GSH). Our tenotoxicity models can easily separate 2 groups of FQ: PEF, MOX and CIP with high tenotoxicity compared to OFX and LEV. Consequently, microplate cytofluorimetry and Microtitration Fluorimetric Assays in Living Cells (MiFALC tests) can be alternative methods for FQ tenotoxicity evaluation.

L005
EFFECTS OF XENOBIOTICS ON A
MAMMALIAN CYTOCHROME P450
AROMATASE

Sipahutar H., Nativelle C., Simon M.-J., Séralini G.-E., Moslemi S.

EA2608, University of Caen, Esplanade de la Paix, 14032 Caen - France.

Aromatase is an enzymatic complex that catalyzes the conversion of androgens to estrogens. Estrogens play a role in promoting the growth of estrogen-dependent tumours like breast cancer. Considerable attention has recently been focused on the environmental chemical pollutants that may prompt the development of estrogen-dependent tumours or disrupt the endocrine balance necessary for normal development or glandular functions. In this study, we evaluate the impact of xenobiotics on the aromatase activity and estimate their cytotoxicity on the human fetal kidney cells (E293).

The IC₅₀ values of chlordecon, bisphenol A, nonyl phenol, diadzein, atrazine, alpha-endosulfan, vinclozolin, 4,4'-DDT, beta-endosulfan and aroclor 1254, calculated from dose-response curves with aromatase activity, estimated by ³H₂O release assay, were 0.42, 0.43, 0.45, 0.54, 0.75, 0.78, 0.78, 0.95, 0.95, 1.65 mM, respectively. The IC₅₀ values of *p,p*-DDE, *o,p*-DDT and lindane were more than 2 mM. In the same system of incubation, 4-androstene-3,6,17-trione, a well-known aromatase inhibitor, presents an IC₅₀ of 150 nM. MTT tests reveal that all compounds are cytotoxic at the IC₅₀ dose levels after 72 hrs of incubation with E293 cells.

The present work provides rapid means for *in vitro* screening of the endocrine potency for environmental chemical pollutants on the mammalian aromatase complex. Further examination to evaluate their mechanism of action would be necessary both *in vitro* and *in vivo*.

L006
EVALUATION OF THE BIOLOGICAL
SAFETY OF CONDOMS USING AN IN VITRO
CELL CULTURE METHOD

Pretorius E., Bester M.J., Motsoane N.A.

Department of Anatomy, Faculty of Medicine, BMW building, PO Box, 2034 Pretoria 0001, South Africa

Latex products have long been recognized as a cause of latex protein allergy. The increased usage of latex

gloves, with the consequent increased occurrence of latex allergies appears to have escalated with increasing awareness of the transmission of HIV-AIDS and other infections. The use of condoms as a means to prevent the transmission of STD's (sexually transmitted diseases) and HIV-AIDS has been widely promoted. Although extensive testing is done to evaluate the physical quality of condoms, no information is available regarding the biological safety of condoms. This study was undertaken to determine the effects of short-term exposure to physiological levels of condom surface material on cell viability (MTT assay) and cell growth (crystal violet assay). A direct contact cell culture testing method (FDA test method F813-83 used to evaluate the cytotoxic potential of medical materials and devices) was used. The cell line ATCC, L-929 was grown in media exposed to different concentrations of condom material. Three types of latex condoms were tested namely: without spermicide, with spermicide and flavoured condoms with spermicide. Cell studies revealed no significant decrease in cell viability or growth for condoms with and without spermicide. However, a significant decrease in cell viability was observed for flavoured condoms with spermicide and results indicate an effect on cell growth. The modified, FDA test method F813-83 was found to be a sensitive test system for the evaluation of the biological safety of condoms.

L007
IDENTIFICATION OF EFFECTOR CELLS
VERSUS TARGET CELLS IN CYTOTOXIC
CONJUGATES BY A MODIFIED COMET
ASSAY

Godard T. 1,2, Gauduchon P.1, Debout C.3

1) GRECAN / INSERM CJF 96-03, Université de Caen, Laboratoire de cancérologie expérimentale, Centre François Baclesse, 14 076 Caen cedex 05, France, 2) Agence Française de Sécurité Sanitaire des Aliments (AFSSA), la Haute Marche, Javené, 35 133 Fougères, France, 3) Laboratoire d'Histologie et de Biologie Cellulaire, UFR de Médecine, CHU côte de Nacre, 14 032 Caen cedex, France

DNA fragmentation is one of the most typical morphological modifications occurring during cell death by apoptosis. Different studies have already shown that the single cell gel electrophoresis assay (comet assay) is able to detect apoptotic cells through the presence of highly damaged cells. In our study,

the natural killer Kurloff cells, used as effector cells, recognize and bind to the tumoral L2C target cells. Formation of such conjugates lead to the death of the target cells by apoptosis, as previously described by different conventional techniques. With the comet assay, a conjugate could directly be visualized as an association of an undamaged cell joined to a highly damaged cell. Moreover, the specific labelling of Kurloff cells with immunomagnetic beads is visible as grey-dull spheres against the bright-red light of nuclear origin on the comet preparation. The use of such labelled effector cells demonstrate that highly damaged cells present in conjugates truly represent apoptotic death of the target cells.

M001

HEPATOCYTES OF RATS INFECTED WITH A PROTOZOAN INTESTINAL PATHOGEN CRYPTOSPORIDIUM PARVUM

Anatskaya O.V., Sidorenko N.V., Beyer T.V.
Institute of Cytology, Russian Academy of Sciences, St. Petersburg 194064, Russia

Cryptosporidium parvum is a leading cause of severe diarrhea, resulting in body dehydration and muscle dystrophy. In mammals, *C. parvum* is known as an intestinal pathogen, and actually there is no evidence about its possible influence on liver. In our experiments two groups of 10-12 day old rats were fed respectively, 3.5x100000 and 1x1000000 *C. parvum* oocysts to obtain a weak and heavy host infections for comparison. The rats were sacrificed 4 days after infection. The average liver weight in the infected rats exceeded the one in the control by 20%. It is the first signal of liver pathology to be reflected also at the cellular level. Hepatocytes are known to respond to pathological changes in the liver by cell hypertrophy and increase in its ploidy level. The cell ploidy levels were estimated cytofluorimetrically, on smears isolated cells. The hypertrophy was estimated by measuring cells protein contents using adsorption cytophotometry after Naphtol Yellow staining. In the control rats, the hepatocytes population was predominantly diploid with the share of 4c and 2cx2 cells only about 10%. Unlikely, in the *C. parvum* -infected rats, the share of polyploid cells was much higher and correlated with the severity of infection. In the weakly infected rats, the share of 2cx2 and 4c-hepatocytes increased by 25% whereas in the heavily infection, the corresponding increase was as much as 100%. In the heavily infected rats octaploid cells

made about 2%, being totally absent in the normal group. The hepatocyte protein contents, in the weakly and heavily infected animals increased by 10 and 30%, respectively. Thus, our first evidence suggested that the rats infected with *C. parvum*, may suffer, in addition, from pathological changes in their liver, proven at both organ and cellular level.

M002

ADJUVANT METHODS INCREASE DIAGNOSTIC ACCURACY IN EFFUSION CYTOLOGY

Friedrichs N., Motherby H., Pomjanski N., Böcking A.

Institute of Cytopathology, Heinrich-Heine-University, Moorenstr. 5, 40225 Düsseldorf, Germany

Aims: To increase diagnostic accuracy of effusion cytology which currently amounts to 58.0 % sensitivity and 97.0 % specificity.

Methods: DNA-image cytometry was applied to routine smears; abnormal stemline positions (<1.8c >2.2c, <3.6c >4.4c) and the occurrence of cells >9c were indicators of DNA-aneuploidy as markers for neoplastic cells. BerEp4, Calretinin and others were used as immunocytochemical markers, applying the ABC-method. AgNORs were counted per 100 cells as clusters and satellites.

Results: DNA-aneuploidy was detected in 95.4 % of carcinomas and 57.1 % of mesotheliomas, but never in tumorcell-negative, reactive effusions. In cytologically doubtful cases, the method detected tumor cells with a sensitivity of 82.9 % and a specificity of 94.7 %. 95.0 % and 14.0 % of carcinomas, resp. 8.0 % and 97.0 % of mesotheliomas were BerEp4- resp. Calretinin-positive. In cytologically doubtful effusions BerEp4 revealed a sensitivity to detect carcinomas of 77.8 %. Whereas 0 % of reactive mesothelial proliferations showed mean values of >4.5 AgNORs per nucleus; this was the case in 95.0 % of mesotheliomas and in 100.0 % of carcinomas. Applying adjuvant methods for routine diagnostics, we were able to increase overall sensitivity by 7.6 %, specificity by 5.4 % and diagnostic accuracy by 6.4 %. In all cases, we correctly differentiated between carcinomas and mesotheliomas. 48.0 % of malignant mesotheliomas were cytologically diagnosed in stage 1 and in 73 % at first by cytology.

Conclusions: Adjuvant methods help to increase diagnostic accuracy in effusion cytology and to early identify malignant mesotheliomas.

M003

DIFFERENTIATION BETWEEN MALIGNANT AND BENIGN FOLLICULAR ADNEXAL TUMORS OF THE SKIN BY DNA IMAGE CYTOMETRY (DNA-ICM)

Vogelbruch M. 1, Böcking A. 2, Kapp A. 1, Kiehl P. 1

1) Department of Dermatology and Allergology, Hannover Medical University, Germany, 2) Institute of Cytopathology, University of Düsseldorf, Germany.

We could demonstrate in previous studies that DNA-ICM can be helpful in detecting (prospective) malignancy in sebaceous tumors and sweat gland tumors, but little is known about DNA-ICM in follicular adnexal tumors of the skin. In the present study, a series of 13 malignant and 55 benign follicular tumors was analysed by DNA-ICM. All cases were clear-cut malignant or benign, respectively, on histopathological criteria. DNA-ICM was performed according to the current recommendations of the ESACP. The stemline interpretation according to Böcking was performed in all cases. 5c-exceeding events (5cEE) and the 2c deviation index (2cDI) were calculated in all cases with the exception of one benign tumor which revealed euploid polyploidization. A 2cDI threshold of 0.24 proved to be the most reliable marker for the differentiation between malignant and benign follicular tumors. On the basis of this feature, 13/13 malignant and 54/54 benign tumors were correctly classified. The use of the 2cDI was superior to the analysis of 5cEE (sensitivity 77%, specificity 100%) and to the stemline interpretation (sensitivity 23%, specificity 100%). Yet, 2cDI cannot be applied if euploid polyploidization can be recognized revealing a second stemline at 4c. In conclusion, ICM-DNA may be helpful in distinguishing between malignant and benign follicular tumors, especially if this distinction is difficult on morphological grounds alone.

M004

IMAGE CYTOMETRIC AUER-I CLASS IDENTIFIES A REAL LOW-RISK GROUP

AMONG LYMPH NODE NEGATIVE PREMENOPAUSAL BREAST CANCER PATIENTS

Baldetorp B., Bendahl P.-O., Fernö M., Knutsson Y., Lindén T., Malmström P., Åkerman M.

Departments of Oncology and Pathology/Cytodiagnosics, University Hospital, Lund, Sweden.

Histological grade and flow cytometric S-phase fraction (SPF) are established prognostic factors in breast cancer. DNA content as measured with image cytometry (ICM) has by several groups also shown to provide prognostic information.

Aim: To evaluate the prognostic value of ICM DNA content, in addition to the one obtained by histological grade and SPF.

Patients and methods: The DNA content was analysed with ICM on imprints from 224 patients. Definitions: 1) Auer classes (I-IV), 2) ICM ploidy (peridiploid, peritetraploid, multiploid and remaining cases) and 3) fraction of DNA 5c exceeding events.

Histological grade and SPF were available in 215 and 200 of these cases, respectively. After a median follow-up time of 45 months, 34 patients had developed distant recurrences.

Results: Patients with Auer I tumours (n=70) had a longer distant recurrence-free survival compared to those with Auer II-IV tumours (n=154; p=0.004, log rank test). The 5-years distant recurrence free survival was 94% vs. 76%. In two separate multivariate analyses, including either histological grade or SPF, the independent prognostic value of Auer classes remained (hazard ratios: 3.7 and 3.6, respectively; p=0.04 in both). The two other classification systems were in neither uni- nor multivariate analysis significantly prognostic.

Conclusion: DNA content, analysed with ICM, identifies a group of patients [Auer I tumours (diploid/peridiploid) with a low "S-phase"] with a very low risk to develop distant recurrences within 5 years.

M005

CLINICAL IMPLICATIONS OF DNA PLOIDY FINDINGS IN ORAL PREMALIGNANCIES

Sudbø J., Kildal W., Reith A.

Dpt of Pathology, The Norwegian Radium Hospital, Oslo, Norway

It is important to identify patients at risk of developing oral squamous cell carcinomas, because these patients may benefit from treatment with

systemic agents with documented biological effects on the oral mucosa. DNA ploidy analysis predicts the occurrence of oral squamous cell carcinomas from oral leukoplakias with a considerable degree of certainty, but the prognostic impact in oral erythroplakias has not been investigated.

Fifty-seven biopsies from 37 patients diagnosed with dysplastic oral erythroplakias were evaluated histologically and by DNA ploidy in epithelial cells. DNA ploidy was measured by image cytometry, and the results interpreted according to an established protocol. The primary end-point was cancer-free survival as estimated by the method of Kaplan and Meier and the log-rank test. Two sided P values for tests of independence were based on Fisher's exact test.

A total of 57 dysplastic red lesions of the oral cavity from 37 patients were investigated. Forty-one lesions from 25 patients, were classified as aneuploid, of which 23 patients (92 %) later developed a carcinoma in the oral cavity (after a mean observation time of 53 months, range 29-78 months). Sixteen lesions from the other 12 patients were classified as DNA diploid (normal DNA content). None of these 12 patients later developed a carcinoma (mean observation time 98 months, range 23 to 163 months, $P < 0.001$). In multivariate analysis, DNA ploidy was a significant prognostic factor ($P < 0.001$), while histological grade, gender, current use of tobacco, size and location of lesions, or the presence of multiple lesions were not ($P = 0.33, 0.12, 0.09, 0.11, 0.07$ and 0.09 , respectively).

DNA ploidy is a significant prognostic marker in patients with oral erythroplakias. These findings are in keeping with recent data obtained from oral leukoplakias, and indicates that DNA ploidy may serve as a tool for treatment decisions in lesions of the oral mucosa.

N001

DETECTION OF CHROMOSOMAL ABERRATIONS IN CANCER SCREENING SAMPLES BY INTERPHASE CYTOGENETICS WITH TUMOR AND TUMOR STAGE SPECIFIC PROBES LEADS TO EARLY AND REFINED DIAGNOSIS

Heselmeyer-Haddad K.M. 1, Fehm T. 2, Djavidan M. 1, Ghadimi B.M. 3, Wilber K. 4, Morrison L. 4, Sherman M. 5, Uhr J. 2, Auer G. 6, Ried T. 1

1) NCI, Bethesda, NIH, MD, 2) Southwestern Medical Center, Dallas, TX, 3) University Medical

Center, Göttingen, Germany, 4) Vysis, Downers Grove, IL, 5) Johns Hopkins University, Baltimore, MD, 6) Karolinska Institute, Stockholm, Sweden

CGH screening for chromosomal aberrations in precancerous and cancerous lesions showed patterns specific for tumor types and tumor stages. In cervical carcinogenesis, we detected a 3q gain (over 80% of the carcinomas) at the transition to invasive disease. Breast carcinomas showed frequent gains of 1q, 8q, 17q, and 20q, while benign fibroadenomas did not show any aberrations. We identified candidate genes in the regions of interest, screened BAC libraries and generated probes for interphase cytogenetics. The pilot study for the cervical material comprises 30 Cytyc thinpreps with normal or CIN 3 morphological diagnosis (masked). So far, we evaluated 8 samples of which 5 were CIN 3 lesions and 3 normal smears. In 4 of the 5 CIN 3 lesions, we detected nuclei with increased signals for 3q compared to the ploidy of the cells. The normal specimens and 1 CIN 3 lesion did not show cells with 3q gain. The breast material comprises normal tissue, fibroadenomas and carcinomas in form of fine-needle aspirates and will be hybridized with 3 different probe panels. Another possibility for the application of these markers is the use of interphase cytogenetics on peripheral blood samples enriched for circulating epithelial cells by ferrofluid coated with antibodies against epithelial markers. Using FISH we detected chromosomal aberrations in cells isolated from patients with organ-confined breast cancer. Interphase cells from the primary tumor showed the same aberrations which strongly suggests that the tumor cells detected in the peripheral blood are derived from the primary tumor. This approach could be used as a cancer screening tool in risk groups and as a monitor device of patient treatment. The results of our studies indicate that aberrant cells in cancer screening samples can be genetically characterized and distinguished with the help of specific interphase probes or probe panels which will lead to improved early detection and refined diagnosis.

N004

QUANTITATIVE FLUORESCENCE IN SITU HYBRIDIZATION ON INTERPHASE NUCLEI OF DIPLOID BREAST CANCERS SUGGESTS THE EXISTENCE OF DIFFERENT EVOLUTIONARY PATHWAYS

Truong K. 1,2, Guilly M.N. 3, Vielh P. 4, Sastre-Garau X. 5, Soussaline F. 1, Dutrillaux B. 2, Malfoy B. 2.

1) IMSTAR SA, Paris, France, 2) UMR 147-CNRS, Institut Curie, Paris, France, 3) DRR, DSV, CEA, Fontenay-aux-Roses, France, 4) Cytopathologie et Cytométrie Clinique, Institut Curie, Paris, France, 5) Service de Pathologie, Institut Curie, Paris, France

DNA ploidy measurements are quite often used for diagnostic and prognostic purposes in the evaluation of breast cancer samples. DNA aneuploid cells indicate presence of tumor cells whereas DNA diploid cells do not exclude the existence of malignant cells. A more sensitive approach to analyze aneuploidy is the Fluorescence in situ hybridization (FISH) on interphase nuclei. Interphase FISH allows immediate and sensitive detection of chromosome rearrangements. We have developed an approach using interphase FISH and image cytometry for the detection of chromosome 1 imbalances within breast cancer cells. Here, we show the result of a study focused on diploid samples determined by flow cytometry and selected from a series of 227 breast cancers. Imbalances between the long and short arms, indicating the presence of malignant cells, were found in 55% of these tumors. Comparison with histological data showed that imbalances were mainly found in low grade tumors and that high grade tumors did not show these imbalances in their majority. The data suggest that these two groups progress with separate genetic patterns. In addition, it indicates different genetic origins of the two groups.

O001

RAPID DIAGNOSIS OF LYMPHOMA IN LYMPH NODE ASPIRATION USING MORPHOLOGY, PHENOTYPING AND DNA ANALYSIS

Lorand-Metze I., Costa F.P.S., Pereira F.G.
Department of Internal Medicine, Faculty of Medicine, State University of Campinas, Brazil

The recently proposed REAL classification emphasizes the importance of the phenotype, besides morphology, in the diagnosis of lymphomas. We analysed, in material obtained from lymph node aspiration, the utility of a combination of routinely stained smears (morphology), a panel of monoclonal antibodies and DNA analysis. The panel comprised:

CD19, CD10, CD20, CD5, CD23, anti-kappa, anti-lambda, CD3, CD4 and CD8. The final diagnosis was confirmed by lymph node biopsy. We studied 26 cases: 4 mantle cell NHL, 4 follicular NHL, 2 immunocytomas, 2 Burkitt's NHL, 1 lymphoblastic NHL, 12 diffuse B large cell NHL, and 1 anaplastic NHL. Diagnosis was concordant with biopsy in 24/26 cases. Cytology provided a good screening but phenotype was confirmatory in all cases except for anaplastic lymphoma. S phase fraction was important in the diagnosis of B large cell NHL (median 13.2%; 6.5%-43%) whose phenotype was less specific. Lymph node aspiration is less invasive, may be repeated if necessary (relapse) and permit a fast diagnosis. Morphology, phenotype and S phase fraction give complementary information. S phase fraction had a relationship to survival.

O003

DIAGNOSTIC DNA-FLOW- VS. IMAGE-CYTOMETRY IN EFFUSION CYTOLOGY

Böcking A., Motherby H., Pomjanski N., Kube M.
Institute of Cytopathology, Heinrich-Heine-University, Moorenstr. 5, D-40225 Düsseldorf, Germany

Aims: To determine sensitivity and specificity of flow- and image-cytometry for detection of DNA-aneuploidy as a marker for malignant cells in effusions.

Methods: 200 effusions (80 tumor cell-positive, 74 - negative and 46 cytologically equivocal) were stained with DAPI-SR for DNA-flow- and with Feulgen-Pararosaniline for -image-cytometry. They were measured using a PAS-flow-cytometer and an AutoCyte-QUIC-DNA-workstation according to the ESACP consensus reports for DNA-flow- and -image-cytometry, resp..

Results: Sensitivity of DNA-aneuploidy for the identification of malignant cells was 32.1 % for DNA-flow- and 75.0 % for -image-cytometry. Specificity of DNA-euploidy in benign cells was 100.0 % for both methods. Positive predictive value of DNA-aneuploidy for the identification of malignant cells was 100.0 % for both techniques, negative predictive value of DNA-euploidy was 48.6 % for DNA-flow- and 72.0 % for -image-cytometry.

Conclusions: Single parameter DNA-flow-cytometry of effusion reveals an insufficient sensitivity for the detection of DNA-aneuploidy in neoplastic cells. Multiparameter flow-cytometry seems to be a

promising alternative, revealing higher rates of DNA-aneuploidy in tumor cell-positive effusions when only epithelial marker-positive cells are measured.

O004**DETECTION OF AROMATASE PROTEIN IN BOVINE LUTEIN CELLS BY FLOW CYTOMETRY**

Torsten Viergutz, Berthold Loehrke, Marion Spitschak, Falk Schneider, Wilhelm Kanitz
Research Institute for the Biology of Farm Animals
D-18196 Dummerstorf- Germany

Introduction: Ovarian follicular theca and granulosa cells differentiate after ovulation into small and large lutein cells to produce pregnancy-maintaining steroids (progestins). Progesterone production requires estrogens. A key enzyme of estrogen synthesis is P450 aromatase (P450arom). However, P450arom expression in bovine lutein cells is thought to be lacking. The aim of the study was to examine expression of P450arom in small and large lutein cells as their steroidogenic activity is known to be differing.

Methods: Lutein cells were obtained from corpora lutea on day 5 and 12 of the ovarian cycle. Cell-specific P450arom protein was detected by flow cytometry and immunofluorescence microscopy, total protein through immunoblotting. Steroids were measured with RIA and EIA for progesterone and estradiol.

Results and Conclusions: P450arom was detectable by immunoblotting, microscopic imaging and flow cytometry. The latter enabled specific detection and quantification of P450arom in small and large lutein cells. The large cells (day 5) expressed at least threefold the enzyme amount of small cells. Decrease in the amount per cell occurred at day 12 in both cell types. Expression correlated with steroidogenesis. The results demonstrate that bovine lutein cells express P450arom, the expression is dependent on the developmental stage of the corpus luteum, and estradiol production is correlated with expression rate of P450arom. The findings may be important for side-effects on female reproductive cycle in treatments of estrogen-dependent diseases.

O005**FLOW CYTOMETRIC STUDIES OF APOPTOTIC CELL MEMBRANE DAMAGE IMPROVED BY DUAL UV/BLUE EXCITATION**

Mazzini G. 1, Ferrari C. 2, Göhde W. 1

1) CNR Histochemistry Study Center, Dept. of Animal Biology, 2) Dept. of Surgery, University of Pavia - Italy.

Cell death (apoptosis/necrosis) is playing, in these last few years, an important role in many aspects of the biomedical area. Nowadays, a large variety of methodological approaches has been proposed to detect and enumerate apoptotic cells by flow cytometry. Among others, those based on the cell membrane modifications induced in the early phases of the apoptotic process are the most established and applied. The dye pair Hoechst 33342 (HO) and Propidium Iodide (PI), thanks to their peculiar characteristics to be respectively permeable and impermeable to the intact cell membrane, seems to be very useful. Unfortunately, the spectral interaction of these dyes generates a consistent "energy transfer" from HO to PI. Therefore, the co-presence of the dyes in a nucleus results in a modification in the intensity of both emitted fluorescence. In order to correlate the apoptotic cells (red fluorescence) to the cell cycle phases (blue fluorescence) we have tested different staining protocols aimed to reduce as much as possible the interference of the involved dyes. In a DHD/K12TRb colon carcinoma cell culture model, we had been able to detect apoptotic cells as well as their location in the cell cycle phases, using a very low PI concentration. By means of a flow cytometer Partec PAS, equipped with HBO lamp and argon ion laser, a double UV/blue excitation has been performed, able to discriminate blue (live) cells from the damaged (blue-red) ones, even at 0.1 microg/ml PI. The same instrumental setting is going to be used to test other red fluorescent dyes, having very limited absorption in the UV/blue spectral region, to be coupled with HO.

O006**POSSIBLE IMMUNOPHENOTYPE OF T-LYMPHOCYTE CELLS IN T-GAMMA-LYMPHOPROLIFERATIVE DISEASE (T-G-LPD)**

Kardum M.M. 2, Siftar Z. 1, Kardum-Skelin I. 2, Sustercic D. 2, Planinc - Peraica A. 2, Nazor A. 1, Borovecki A. 2, Jaksic B. 2

1) Institute of Clinical Chemistry, University Hospital "Mercur" Zagreb, Croatia, 2) Department of Medicine, University Hospital "Mercur" Zagreb, Croatia

T-gamma-lymphoproliferative disease (T-g-LPD) as a particular clinical and pathological entity inside a large group of lymphoproliferative disorders, often develops in a chronic disease with recurrent infections, but the very rarely neoplastic clone of T-g-lymphocytes infiltrates the peripheral blood (PB) or/and bone marrow (BM). For two years, in the University Hospital "Mercur", three cases of T-g-LPD were found. A complete medical examination including morphology of bone marrow aspirate, histology, serology and ultrasound of the abdomen was done. In PB and BM smears, the infiltration with a neoplastic clone of T-g-lymphocytes, containing azurophilic granules in their cytoplasm, was found and flow cytometric immunophenotyping of PB and BM samples was necessary. Inside a homogenous population of lymphocytes (medianPB =70.0%; medianBM =81.0%), the extent of T-lymphocytes subpopulations was determined. Immunophenotyping by FCM proved the T-origin of the cells and presumed of possible phenotype of a neoplastic clone of T-g-lymphocytes: CD2+CD3+CD7 +CD8+CD4-CD57+CD56- with aberrant CD5 membrane marker expression (positive on 41% CD3+BM and 37% CD3+PB mature T-lymphocytes). Dominancy of cytotoxic-suppressor T-lymphocyte subpopulation in BM and PB was found (CD3+CD57+;CD3+CD8+>>CD3+CD4+), but the sum of T-lymphocytes subpopulations in PB ((CD4+)+(CD8+)@79%) was lower than measured positivity of CD3 membrane marker (CD3+=90.4%). As the majority of T-g-LPD is cytologically and morphologically homogenous, it is necessary in the future to investigate whether the aberrant expression of membrane marker CD5 and the reduced sum of mature T-lymphocytes are the rule or may be an exception of the immunophenotypic profile of T-g-lymphocytes which also could assume possible existence of more "atypical" T-lymphocytes inside a group of T-g-LPD.

O007

THE APOPTOTIC EFFECT OF FCM IN B-CLL MEASURED BY ANNEXIN V

Benito L. 2, Álvarez B. 3, Martín I. 1, Oña F. 1, García Marco JA 4, García Vela JA 1

1) Department of Hematology, Hospital Universitario de Getafe, Madrid, Spain, 2) AECC., Madrid, Spain, 3) Shering España. Puerta de Hierro, Madrid, Spain, 4) Clínica Puerta de Hierro, Madrid, Spain.

There is an increasing interest in assessing whether the results obtained with fludarabine in B-CLL could be improved by combining it with other drugs. *Objective* : To analyse the in vitro effect of fludarabine alone and in combination with cyclophosphamide and/or mitoxantrone on B-CLL cells. *Method* : Mononuclear cells from 13 patients (11 typical/2 atypical B-CLL) were incubated with fludarabine (FAMP) alone and in combination with mitoxantrone, and/or mafosfamide. Quantification of apoptotic B CD19+CD5+ lymphocytes was analysed after 48 hours of drug incubation, with annexin-V-FITC. The drug concentrations used were 1µg/mL for FAMP, 1µg/mL mitoxantrone and 1µg/mL mafosfamide. *Results* : The mean of spontaneous apoptosis was 27.2%. Fludarabine produced a significant increase in the apoptotic effect on B-CLL cells (46.7%). Mafosfamide and mitoxantrone increased in the apoptotic effect of fludarabine in all the patients studied, after 48 hours of incubation (60.5 and 79.9%, respectively) (p<0,001). The addition of mitoxantrone to the combination of FAMP plus mafosfamide increased the apoptotic effect of this combination (86.3% vs 60%, p=0,001) but it was not superior to the combination of FAMP plus mitoxantrone. *Conclusion* : These results support that fludarabine in combination with mitoxantrone and/or cyclophosphamide can be highly effective in the treatment of B-CLL and the combination of these drugs could improve the results obtained with fludarabine alone.

O008

APOPTOSIS-REGULATORY PROTEINS IN B-CLL

Alvarez B. 2, Benito L. 3, Martín I. 1, Oña F. 1, García Marco JA. 4, García Vela JA. 1

1) Department of Hematology, Hospital Universitario de Getafe, Madrid, Spain, 2) Shering

España, Madrid, Spain, 3) AECC, Madrid, Spain, 4) Clinica Puerta de Hierro, Madrid, Spain.

The combination of mafosfamide (Mafos) and/or mitoxantrone (Mitox) with fludarabine (FAMP) improves the apoptotic effect on B-CLL cells. *Objective* : To analyse the in vitro effect of FAMP in combination with Mafos and/or Mitox on apoptosis-regulatory proteins in B-CLL. *Method* : B-CLL cells from 14 patients were incubated with FAMP alone and in combination with Mafos and/or Mitox. The intracellular expression of Bcl-2, Bax, Bcl-x and Mcl-1 was analysed by flow cytometry. *Results* : FAMP produced a significant increase in the apoptotic effect on B-CLL cells. This effect was increased with the combination of Mitox or Mafos. The addition of Mitox to the combination of FAMP plus Mafos increased the effect of this combination, but it was not superior to the combination of FAMP plus Mitox. The levels of Bcl-2 decreased with fludarabine ($p=0.038$) and this decrease was higher with the combination FAMP plus Mitox ($p=0.021$) or with the three drugs ($p=0.020$). Fludarabine did not produce by itself any change in the expression of Bax and this was only after the addition of Mitox that we observed a decrease in its level. Then, the ratio Bcl-2/Bax decreased with fludarabine (0.036) and with all the combinations that contained Mitox, which correlated with apoptosis ($r=-0.32, p=0.08$). Bcl-X and Mcl-1 decreased with all drugs, but no modification was observed in response to these combinations. *Conclusion* : The apoptotic effect of the combination fludarabine plus Mitox could be explained, in part, by the decrease in the ratio bcl-2/bax.

O009

CELL ANALYSIS SYSTEM BASED ON IMMUNO-FLUORESCENT ANALYSIS OF IMMUNO-MAGNETIC SELECTED AND ALIGNED CELLS WITH COMPACT DISK TECHNOLOGIES

Tibbe A.G.J. 1, De Grooth B.G. 1, Greve J. 1, Terstappen L.W.W.M 2, Dolan G.J. 2

1) University of Twente, Faculty of Applied Physics, Biophysical Techniques Group, P.O. Box 217, 7500 AE Enschede, The Netherlands, 2) Immunicon Corporation.

The Cell Tracks system is based on the immunomagnetic selection, followed by magnetic separation

and aligning of the selected cells along ferromagnetic lines of nickel (Ni).

Whole blood is incubated with ferromagnetic nanoparticles labeled with monoclonal antibodies, as well as fluorescent-labeled monoclonal antibodies. After incubation, the blood mixture is placed in a specially designed chamber that is placed in a strong magnetic field. The magnets create a gradient moving the magnetically labeled cells up-wards to the top of the chamber. The optically transparent upper surface of the chamber contains ferromagnetic lines of nickel (Ni) deposited by lithographic techniques. When the cells reach the top of the chamber, they become subject to a high local internal gradient induced by the Ni lines and aligned in between them. The cells that are not magnetically labeled slowly move down under the influence of gravity. In this way, the cells labeled by the immunomagnetic particles are well aligned at the upper surface of the chamber.

After the aligning process, a 635 nm laser is focused on the aligned cells with a regular CD-objective. By moving the chamber in the direction of the Ni lines, the cells pass the laserfocus one after the other. For each cell, the fluorescence signals generated are analyzed and the cell position recorded. The fluorescence intensity and color identify the aligned cells.

This cell analysis method is significantly less complex than current cell analysis equipment and provides additional functionality through its ability to subject cells to repeated and varied analysis while they remain in their natural environment, i.e., whole blood.

O010

DNA PLOIDY AND S-PHASE DETERMINATION BY FLOW CYTOMETRY (FC) IN 50 PATIENTS WITH MULTIPLE MYELOMA (MM): INTEREST OF THE DNA/CD38 DOUBLE STAINING PROCEDURE

Salaün V., Truquet F., Macro M., Malet M., Troussard X.

Laboratoire d'hématologie, CHU Caen, France.

Patients with MM have in the bone marrow a variable number of tumoral plasma cells with a very low proliferation rate. By conventional cytogenetic analysis, chromosomal abnormalities are detected in only 30% to 50% of cases. In MM, the impact on prognosis of chromosomal abnormalities is now well

established. DNA ploidy and S-phase determination by FC could be an alternative procedure.

We initially analysed DNA index (DI) in 40 MM patients using propidium iodide (PI) (DNA con 3 kit, DAKO). An hyperdiploid (DI>1), diploid (DI=1) and hypodiploid (DI<1) pattern was observed in 57% (23/40), 40% (16/40) and 2,5% (1/40) cases, respectively. However, this technique does not allow to quantify the S-phase in diploid samples. Then, we developed a CD38/PI double staining and gated specifically on CD38+ plasma cells. Thirty patients were studied : 20 with both procedures and 10 exclusively with CD38/PI. We detected a DI>1 in 77% (20/30) and a DI=1 in 33% (10/30) of cases. When using both tests, we found 3/20 (15%) of discrepant results: in all cases, plasma cells were < 5% and the DI equal to 1 with PI was >1 with CD38/PI. The aneuploid GO/G1 peak was in all cases located in S-phase of residual non plasma cells. CD38/PI staining appears much more sensitive than PI and has to be used for the cell cycle study in MM patients.

O011

MULTIPARAMETER FLOW CYTOMETRY (MP-FCM) AS A TOOL FOR THE DETECTION OF MICROMETASTATIC TUMOR CELLS IN THE SENTINEL LYMPH NODE PROCEDURE

Leers M. 1, Schoffelen R. 1, Theunissen P. 1, Oosterhuis J. 2, Bijl H. 2, Rahmy A. 3, Tan W. 3, Nap M. 1

1) Atrium Medical Centre Heerlen, Dept of Pathology, P.O. Box 4446, 6401 CX Heerlen, The Netherlands, 2) Atrium Medical Centre Heerlen, Dept of Surgery, P.O. Box 4446, 6401 CX Heerlen, The Netherlands, 3) Atrium Medical Centre Heerlen, Dept of Nuclear Medicine, P.O. Box 4446, 6401 CX Heerlen, The Netherlands

Aim of the present study & Methods: We investigated the use of MP-FCM for the detection of micrometastasis in sentinel lymph nodes (SLN) in breast cancer. Sentinel lymph nodes from 98 patients (n= 238) were analysed. H&E and immunohistochemical (IHC) sections for cytokeratin (MNF116 1:50; DAKO) were cut at three levels with a distance of 500 µm. Intervening two levels were used for MP-FCM. Cells were immunostained for MNF116 (1:50), followed by an incubation with goat-anti-mouse Ig-FITC. DNA was stained using

propidium iodide. Of each lymph node 100000 cells were analysed on a DAKO Galaxy flow cytometer.

Results: 38/98 patients showed metastatic tumor in the SLN by one or more of the three methods. In 37/38 cases where metastatic cells were seen in the routine H&E and/or IHC, more than 1% cytokeratin positive cells were detected by MP-FCM. In 14/38 these foci were smaller than 2 mm (micrometastasis). In 3 of these 14 cases MP-FCM revealed positive SLN whereas this was not observed at first glance in the H&E or IHC. After revision of the slides, 1/3 mentioned above remained negative. However, MP-FCM analysis of the cytokeratin-positive cells showed an aneuploid DNA peak which was almost identical to the primary breast tumor. Duplicate measurements, done in 41 cases showed a 99% reproducibility. All micrometastasis except for the one mentioned above showed only diploid tumor cells, despite the fact that their primary tumors did contain both diploid and aneuploid tumor cells. In primary tumors with more than 60% aneuploid cells, predominantly aneuploid macrometastasis were found whereas diploid primary tumors only showed diploid micro- or macrometastasis in their SLN.

Conclusion: MP-FCM was in all cases sufficient, and even superior to H&E and IHC, to detect micrometastatic tumor cells in a large volume of lymph node tissue from SLN. Approximately 30% of SLN micrometastasis prove to have additional non-SLN metastasis. The size of the aneuploid fraction (>60%) in the primary tumor may influence the risk of having both SLN and non-SLN metastasis.

P001

DETECTION OF A LARGE NUMBER OF ANTIGENS USING SEQUENTIAL IMMUNOFLUORESCENCE STAINING

Erlandsson F. 1, Wählby C. 2, Bengtsson E. 2, Zetterberg A. 1

1) Department of Oncology-Pathology at the Karolinska Institute, Stockholm, Sweden, 2) Centre for Image Analysis at the Uppsala University, Uppsala, Sweden.

The cell cycle is regulated by a large number of proteins, most of which are located and/or active in the cell nucleus. The complex relationships between the expression patterns of these proteins in tumours in vivo have previously been impossible to study, since only the presence of two or three proteins can be visualized simultaneously by classic

immunohistochemistry. We have developed a protocol that allows the removal of the immunofluorescence stains applied to a tissue section, and subsequently the tissue section can be stained again. The protocol involves denaturation of the primary antibodies, photo bleaching of the fluorophores, as well as elutriation of the secondary antibodies. The process can be repeated several times, allowing the staining of a large number of antigens in the same tissue section. When the emitted fluorescence is imaged after each turn of staining, the approximate amount of each of the antigens in each of the cell nuclei can be evaluated. Thus the complicated relationships between the proteins regulating the cell cycle can be studied *in vivo*. The immunofluorescence staining steps can be followed by an HTX-eosine staining to allow the study of the morphology of the investigated tissue. We have applied the described method to investigate the expression patterns of a large number of proteins in tissue sections of cervical carcinoma. The described method relies heavily on 3D image analysis, which is further described by C. Wählby.

P002

MICROSPECTROFLUOROMETRY OF AUTOFLUORESCENCE EMISSION FROM HUMAN LEUKEMIC LIVING CELLS UNDER OXIDATIVE STRESS

Kibangu Bondza P., Millot C., Millot J.M., Dufer J. Unité MÉDIAN - CNRS FRE2141, IFR53, UFR de Pharmacie, 1 rue du maréchal Juin, 51100 REIMS, France

UV-laser microspectrofluorometry was applied to study the intracellular localization of autofluorescence and the influence of an oxidative stress on this emission. Under a 363 nm excitation, all spectra from K562 erythroleukemia cancer cells show equivalent profiles with a 455 nm maximum emission, near of reduced nicotinamide adenine dinucleotide-(Phosphate) solution (NAD(P)H,H⁺) (465 nm maximum emission). The intracellular locations of the autofluorescence emission and of the specific mitochondrial probe rhodamine 123 (R123) were matched, showing that the spatial distribution of autofluorescence is homogeneous and different from that of R123. Hydrogen peroxide (H₂O₂) (200 µM) and menadione (Men) (5 µM) induce a weak spectral change and a decrease in autofluorescence intensity, down to 40% of the initial emission. Doxorubicin

(Dox) induces a dose-dependent decrease in autofluorescence emission and a release of intracellular free radicals. When cells were pre-treated with 1 mM glutathione (GSH), Dox induces a lower free radicals release, no significant variation of autofluorescence intensity and a lower growth inhibitory effect. Image cytometry of autofluorescence suggests that the intracellular NAD(P)H would not be restricted to mitochondrial compartments. The release of free radicals was associated with a decrease in autofluorescence intensity, mainly attributed to NAD(P)H oxidation both inside and outside mitochondria.

P003

TWO-COLOUR FLUORESCENCE CYTOMETRY FOR NUCLEAR FINE STRUCTURE ANALYSIS OF RESTING AND PROLIFERATING BREAST CANCER CELLS

Haroske G. 1, Meyer W. 2, Friedrich K. 2, Kurth-Franke E. 2, Kunze K.D. 2

1) Dresden-Friedrichstadt General Hospital, Institute of Pathology, Germany, 2) Dresden University of Technology, Institute of Pathology, Germany.

Aim: The study was aimed to develop a methodology for an automated two-colour fluorescence measurement of cell structures, and to apply that method to the study of proliferating versus resting tumour cells in human breast cancers.

Methods: Paraffin-embedded tissue sections from 43 breast cancers as well as from 10 normal esophageal mucosae were double-stained with a DTAF-labelled MIB-1 antibody and with the DNA stain Hoechst 33342. For staining control, rat liver imprints and normal mucosae were used. Each of the 400 tumour cells per case were cytometrically measured by a motorized microscope, equipped with a 3CCD camera, a x63 objective and the Zeiss filter sets 02 and 24. From each nucleus, 130 morphometric and densitometric nuclear features were derived from the Hoechst image.

Results and Conclusions: After the Hoechst images were segmented, the spectral emission was measured in both colors, calibrated by internal reference lymphocytes. A thresholding between proliferating and resting tumor cells was based on the green fluorescence of the internal reference, too. For each of the features, mean and standard deviation in the proliferating and resting subgroup of each case was used for the discrimination by different statistical

procedures. A paired discriminant analysis was best suited to elaborate those features being statistically different, as well as having discriminatory power for a high level accuracy in reclassification. The results demonstrated that an automated approach in fluorescence cytometry is feasible, thus opening new perspectives in biological marker studies on a cell-by-cell level.

P004
ANATOMICAL AND FUNCTIONAL
EVIDENCES FOR THE EXISTENCE OF AN
INNERVATION OF RAT
CEREBROVASCULAR VESSELS BY
GALANIN

Marchalant Y., Barbelivien A., MacKenzie E.T., Dauphin F.

University of Caen, UMR 6551 CNRS, Cyceron, IFR47, Caen, France.

Based on the putative role of galanin in the regulation of cerebral blood flow (CBF), we aimed to characterize, in the rat, the existence of an innervation of intracortical (frontal, parietal, temporal, occipital) vessels by galaninergic fibers, through immunohistochemistry, associated with optical, confocal and electronic microscopy. In each cortex, 29% of the 4808 vessels visualized were associated (in a 5µm distance) with galaninergic fibers, and in the frontal cortex, these innervations were sensibly more important in the layer II. More than 50% of the innervated vessels were small ones (<15µm). Additionally, 70% of the innervating fibers were in close apposition with the vessel walls (<2,5µm); this, in association with the presence of 125I-galanin binding sites on microvessels, suggests a functional role of this innervation. Following an excitotoxic lesion of the substantia innominata, the source of the cholinergic ascending pathway to the cortex, we observed a decrease in the density of this innervation in the deep layers (-35%), and an increase in the superficial layers (+50%) of the cortex. Overall, these results, when compared to data related to the association of a dysfunction of the cholinergic system and an overexpression of the galaninergic system in cerebral ischemia and Alzheimer's disease, allow us to propose a pivotal implication for this galaninergic innervation on the physiological or pathophysiological control of local cerebral blood flow.

P005
QUANTITATIVE FLUORESCENCE IMAGING
IN SITU APPLIED TO FRESH APPPOSITIONS
OF BREAST TUMOUR BIOPSIES:
INFERENCES ON MATERIAL ADEQUACY
AND CLINICAL RELEVANCE

Michels J.J. 1, Chassoux D. 2, Chasle J. 1, Denoux Y. 1, Duigou F. 1, Linares-Cruz G. 3

1) Centre François Baclesse, Caen, 2) INRA 806, IBPC, Paris, 3) Lab. pharm. Exp. IGM St-Louis, Paris, France

In a previous work, we reported the strong relationship between proliferative activity and breast cancer prognosis (Breast Cancer Res Treat, 2000, 62; 117). Such observations were based on SPF measurement by FCM in more than 600 node negative cancer patients. The work described herein is focused on the DNA content analysis on fresh appositions of breast tumour biopsies. DNA content may be assessed on a small number of cells in situ by fluorescence imaging and computer assisted image analysis (Anal Quant Cytol Histol, 1999, 21, 489). Rapidity, precision of measurements and structural conservation of subcellular compartments are the inherent advantages of this approach.

Fresh breast cancer appositions were found to constitute an adequate material for DNA quantitative measurements and by this fact allow cell cycle analysis useful for prognostic purposes. The minimum number of cells required to perform iterative analysis in a reproducible manner and to get relevant information was around 400 (identification of high SPF cases).

Such a fast and simple approach is proposed in complement of, or in replacement of FCM, when the latter is not possible (technical difficulties, sample size, etc.). Moreover, it opens a large scope of in situ topological analysis by multilabeling. The detection of a given marker and its assignment to a specific cell cycle phase may be performed at a single cellular level.

The analysis of nuclear matrix associated proteins (i.e. PML) is being explored by our team. Changes in the topological distribution were described for PML in breast tissues (ranging from normal breast to invasive breast cancer).

(Oncogen, 1995, 10, 1315). DNA contents and PML patterns relationships are under characterisation. Such parameters may be put forward for clinical purposes.

P006
MONITORING THE EFFICACY OF
ADJUVANT THERAPY IN BREAST CANCER
BY QUANTIFYING CIRCULATING TUMOR
CELLS USING THE MAINTRAC ANALYSIS
(LASER SCANNING CYTOMETRY OF
MAGNETIC BEAD ENRICHED CELLS)

Pachmann K., Tulusan A.H., Lobodasch K., Dengler R., Pachmann M., Pachmann U.
 Friedrich-Schiller University Jena and TZB
 Transfusion medical center Bayreuth, Germany

Aim : Until now, there has been no method available to directly monitor the success of adjuvant chemotherapy in early stage breast cancer. We describe here a method that allows direct quantitative determination of circulating tumor cells in blood and bone marrow during adjuvant chemotherapy. The white blood cells and the tumor cells from whole blood were incubated with HEA-coated magnetic beads and FITC- conjugated HEA-antibody (Miltenyi). The cells were run over a magnetic column attached to a strong magnet. Labelled cells were retained and most squeezed out and measured in a laser scanning cytometer (Compucyte). Positive events could be rescreened for intactness of the cells and specificity of staining. We established the sensitivity of the MAINTRAC approach by spiking tumor cells into normal peripheral blood to be 1 cell in 108 normal leukocytes, with a recovery rate of 90% with the possibility to retrieve every positive event and a good correlation between expected and obtained values ($R^2 = 0.98$) in a model system. We have now analysed more than 300 breast cancer patients, 50 of which were monitored twice or more during the course of adjuvant chemotherapy. Changing numbers of cells during different chemotherapy regimen are shown. Correlation to two prognostic factors (Ki 67 and PAI1 in stroma) is emerging. *Conclusion* : Combining automated immunofluorimetry with visual evaluation of the relevant events enables detection and quantitative evaluation of circulating suspicious cells in breast cancer. This allows for the first time monitoring of tumor cells, during adjuvant therapy, in early stage cancers, in a timely fashion and thus real time monitoring of the efficacy of chemotherapy.

P007
MULTICOLOR IMMUNOPHENOTYPING OF
TISSUE SECTIONS BY LASER SCANNING
CYTOMETRY (LSC)

Tárnok A. 1, Gerstner A. 1, Trumpfheller C. 2, Racz P. 2, Tenner-Racz K. 3

1) AT, Pediatric Cardiology, Cardiac Center, Univ. of Leipzig, Germany, 2) AG, Otorhinolaryngology, Univ. of Leipzig, Germany, 3) CT, PL, KTR, Bernhard-Nocht-Institute, Univ. of Hamburg, Germany

Quantitative analysis of leukocytes in solid tissues is difficult to perform but would yield important data in a variety of clinical and experimental settings. In lymphatic organs the analysis of their spatial distribution would give relevant information about alterations during diseases (leukemia, HIV, AIDS) and their therapeutic regimen. We have established an automated analysis method for LSC suitable for archived or fresh biopsy material of human lymph nodes and tonsils. Sections are stained with PI for DANN and up to three antigens using direct or indirect immunofluorescence staining. Measurement is triggered on DNA-fluorescence (Argon Laser). Due to the heterogeneity in cell density measurements are repeatedly performed at different threshold levels (low threshold: regions of low cellular density, germinal centers; high threshold: dense regions, mantle zone). Data are acquired by single- (Ar) or dual-laser excitation (Ar-HeNe) in order to determine from single- (FITC), up to triple-staining (FITC/PE-Cy5/APC). Percentage and cellular density of cell-subsets is quantified in different structural regions of the specimen. The results obtained by the LSC could be verified by manual analysis of the sections. With LSC a semi-automated operator-independent rapid and simultaneous immunophenotyping of lymphatic tissues with up to four antibodies is possible. This technique should yield new insight into processes during diseases and should help to follow up and quantify the success of therapeutic interventions.

Q001
RELATIONS BETWEEN HYPOXIA-
INDUCIBLE FACTOR-1 (HIF-1), THE
NITROIMIDAZOLE PROBE EF5 AND
EPENDORF PROBE MEASUREMENTS IN
CERVIX CANCER

Nickle T., Haugland H.K., Vukovic V., Hedley D.W.

Ontario Cancer Institute/Princess Margaret Hospital, 610 University Avenue, Toronto, Ontario M5G 2M9, Canada

The presence of hypoxia is associated with poor prognosis in cancer patients. Currently, direct oxygen measurements using the Eppendorf electrode remain the gold standard for clinical assessment of hypoxia. An alternative is the use of nitroimidazoles such as EF5. These probes bind to hypoxic tissue and can be detected in biopsies using immunohistochemistry. The alpha subunit of the HIF-1 transcription factor is rapidly degraded under oxic conditions, but accumulates in hypoxic tissue.

We examined the tissue distribution of HIF-1 α in relation to hypoxia in cervix cancer xenografts, using dual fluorescence labeling for HIF-1 α and EF5 in combination with wide field fluorescence image analysis. The two markers were highly correlated. In a parallel experiment, quantitative immunohistochemical measurements of HIF-1 α expression were made in a series of 42 biopsies obtained from cervix cancer patients at the time of Eppendorf probe measurements. There was a significant positive correlation between HIF-1 α expression and tumour oxygenation ($p < 0.01$). These results indicate that HIF-1 α expression has the potential to provide a useful indicator of hypoxia in biopsies obtained from human solid tumours.

Q002

A NEW INDEX FOR INTRATUMORAL HETEROGENEITY IN BREAST CANCER

Sharifi-Salamatian V., Rigaut J.P.

Analyse d'Images en Pathologie Cellulaire (AIPC), Hôpital St. Louis, Université Paris 7, 75475 Paris, France

The aim of this work is to investigate intratumoral heterogeneity in breast cancer and its relationships with breast cancer grading. A novel methodological approach to measure heterogeneity is used here and, farther, an estimation of the three histological grades of Scarff, Bloom and Richardson are proposed. The geostatistical method used here lies upon notions of asymptotic behaviour, dispersion variance, ergodicity and integral range. After computing the integral range, the estimation of the convergence "speed" of the spatial average to the statistical mean of the spatial point process (α) was obtained. The more the process is heterogeneous, the slower the convergence

of the dispersion variance to zero and the smaller the value of α . Very recently, we realized that the use of the asymptotic slope of the Hurst (H) parameter (related to fractals) bears a relationship with dispersion variance and procures more robustness to the estimations. Twenty tumours were obtained and paraffin sections stained by MIB-1 (Ki-67). The results were expressed through α as an index of heterogeneity. There were significantly different grades for 1 and 2 than for 3. Similar discrimination was obtained with the same sections using the Hurst parameter (H). Thus heterogeneity, as measured by α or H, clearly bears a relationship with grading. We use an index of heterogeneity which might have better individual prognostic value than the current grading system. The final proof of an improved grading using these parameters will of course require a confrontation with the results of survival studies, which are in progress.

R001

MORPHOLOGICAL PROPERTIES OF HUMAN THROMBOCYTES. A COMPUTERIZED MORPHOMETRIC STUDY

Korobova F.V., Kozinets G.I.

National Research Center for Hematology of Russian Academy of Medical Sciences, Moscow, Russia

Whole blood platelets from 40 normal subjects were prepared for light microscopy followed by computerized morphometric analysis. The complex of morphometric parameters automatically measured from each platelet included eight geometrical and six optical attributes. It is concluded that: (1) Blood platelets are quite suitable for morphometric study. (2) Area and diameter of spreaded platelets can serve as a criteria of an estimation of heterogeneity of these cells on size. Form factor illustrates the ability of platelets to produce pseudopodia. (3) Specific optical density of green colour and share of red colour describe a degree of saturation of platelets by granules. Share of blue colour reflect tinctorial properties of platelet cytoplasm. The reduction of ratio of these parameters can testify insufficiency of granules' components, on the one hand, or reduction of number of granules, on the other hand. (4) Appropriate and valid statistical analyses are essential to determine the character of changes of platelet attributes and connections between them. (5) The measurement of optical and geometrical features of patients platelets with essential thrombocythemia has shown their significant difference from normal

meanings. After the course of treatment, morphometric properties of platelets came near to those of healthy people. (6) Computer-assisted morphometry of blood platelets allows to essentially expand opportunities of the clinical analysis of thrombocytes and should ultimately find an important place in clinical hematology.

R002

NUCLEAR TEXTURE ANALYSIS IN COLORECTAL CARCINOMAS: ASSOCIATION WITH MITOSIS, APOPTOSIS, IMMUNOSTAINING OF P53, P21, MDM2, BCL-2 AND PATIENT PROGNOSIS

Elkablawy M.A. 1, Diamond J. 1, Maxwell P. 1, Bartelsi P.H. 2, Hamilton P.W. 1

1) Quantitative Biomarker Group, Department of Pathology, Cancer Research Centre, Queen's University of Belfast, UK, 2) Optical Sciences Centre, University of Arizona, Tucson, Arizona, USA.

On a series of 47 colorectal carcinomas, immunoeexpression of p53, p21, mdm2 and bcl-2 was carried out using a standardised semi-quantitative protocol. In addition, the mitotic index (MI) and apoptotic index (AI) were calculated for each case using quantitative cell counts. Finally, sequential 4µm sections were taken and stained using the Feulgen reaction for the demonstration of DNA. Digital images were recorded from each case using a x100 (n.a.=1.4) objective and a calibrated videophotometer system. From each case, 60 individual nuclei were segmented using KS400 software (Carl Zeiss) and analyzed for chromatin texture using purpose written software. Twenty out of 60 nuclear texture features were significantly associated with tumour progression as measured by Dukes' stage. A series of 30 nuclear texture features was significantly associated with the mitotic index, while only two features were significantly associated with the apoptotic index. Four nuclear texture characteristics were significantly associated with p53, bcl-2 and mdm2 expression. A statistical comparison with five-year survival revealed that cluster_shade ($p<0.004$), upper quartile OD ($p<0.02$), lower quartile OD ($p<0.02$), most frequent OD ($p<0.02$) and maximum OD ($p<0.04$) were significantly associated with survival. Using multivariate Cox survival analysis, cluster_shade ($p<0.004$) was the only significant independent

prognostic nuclear texture factor. The relationship between nuclear texture and immunostaining is likely to reflect an overall phenotypic change in the protein profile of the cell and altered chromatin pattern. While nuclear texture abnormalities have a role in predicting long term survival in colorectal cancer, their role is somewhat limited.

R003

MULTI-DIMENSIONAL IMAGE ANALYSIS OF SEQUENTIAL IMMUNOFLUORESCENCE STAINING

Wählby C. 1, Erlandsson F. 2, Zetterberg A. 2, Bengtsson E. 1

1) Centre for Image Analysis at Uppsala University, Uppsala, Sweden, 2) Department of Oncology-Pathology at the Karolinska Institute, Stockholm, Sweden

By combining immunohistochemistry with digital image analysis, properties of specifically stained cells in culture or tissue sections can be quantified. Biological systems are controlled by a very large number of interacting molecules. Visualization of more than one antigen simultaneously by multicolor immunostaining is therefore often desirable or even necessary, both for quantitative studies and to explore spatial relationships of functional significance.

We have developed a novel method for sequential immunofluorescence staining, which, in combination with 3D image registration and segmentation, can be used to increase the number of antigens that can be observed simultaneously in single cells in tissue sections. Sequential application and removal of fluorescence markers greatly increase the number of different antigens that can be visualized and quantified in single cells simultaneously. Quantification and efficient objective analysis of the image data require digital image analysis. We present a method for 3D image registration combined with 2D and 3D segmentation and 4D extraction of data. Registration of 3D images of tissue sections is required for quantitative, fast, objective and automatic analysis of the image data. A semi-automatic 2D segmentation method and its automatic extension to 3D is also presented. The staining technique, as well as an application where proteins involved in the control of transition events in the cell cycle are studied, is further described by F. Erlandsson.

R004**PRELIMINARY STUDY OF COMPUTER ASSISTED EVALUATION IN SCARFF BLOOM - RICHARDSON (SBR) HISTOLOGICAL GRADING**

Narozni M. 1, Lachard A. 2, Martin P.M. 1, Dussert C. 1, Palmari J. 1

1) Laboratoire de Cancérologie Expérimentale, IFR Jean Roche, Faculté de Médecine Nord, Bd. P. Dramard, 13326 Marseille cedex 20, France, 2) Service d'Anatomie Pathologique et Cytogénétique, Centre Hospitalier Intercommunal de Toulon, La Seyne / Mer, BP 1412 83056 Toulon, France

Morphological tumour differentiation has been shown in numerous studies to give a good prognosis in breast cancer. SBR histological grading is based upon a subjective assessment of microscopical appearances. Three histological factors are examined and scored from 1 to 3: the degree of tubule formation, the pleomorphism and the mitotic activity. From the total scores, a grade is established as follows: Grade I (3-5 points), Grade II (6-7 points) and Grade III (8-9 points).

Histological grading may be criticised because its reproducibility is poor. There is also an unequal distribution of patients among the three grades with over 50 % of the patients in Grade II and insufficient prognosis separation between Grade II and Grade III. The aim of this work was to develop a quantitative test equivalent to the grading by using automated image analysis. To perform this task, we used the skill exercised by the histopathologist in interpreting images.

On a first step segmentation algorithms were carried out to extract structures taken into account by the pathologist. To do so, we combine histogram methods and mathematical morphology. Tubular differentiation and nuclear morphometric parameters (densitometry and geometry) were measured. On a second step, a learning sample was constructed by using discriminant factorial analysis with an a priori classification according to SBR grades. Using the decisional discriminant analysis made it possible to ascertain the grades for a test sample with a correct classification rate of 95 %.

These preliminary data confirm the role of quantitative image cytology in objectively determining the SBR grade, although further studies will be needed to validate the method in a larger sample.

R005**EVALUATION OF MACS IN THE ORAL CAVITY USING PAIRED MULTIVARIATE DISCRIMINANT ANALYSIS**

Meyer W. 1, Friedrich K. 1, Haroske G. 2, Theissig F. 1, Baretton G. 1, Kunze K.D. 1

1) Dresden University of Technology, Institute of Pathologie, Germany, Fetscherstr. 74, D-01307 Dresden, 2) Dresden-Friedrichstadt General Hospital, Germany, Friedrichstr. 41, D-01067 Dresden

The use of paired data is a good method to show differences in features values: Individual variations of the "normal" or "reference" state are excluded by using feature differences in each individual. The paired t-test is well known for its univariate analysis. We adapted the multivariate discriminant analysis in order to use the difference of the features between reference and analysis cells in one individual. Furthermore, we developed a complete search for feature combinations most effectively discriminative. 29 tissue sections from oral cavity cancers were measured at the positions "normal", "MAC" and "tumour". At each position and in each slide, about 250 nuclei were measured. From those nuclei, each of 133 features was generated, leading to 133 means and 133 standard deviations for each position in the slide. The error probabilities where Bonferoni adjusted (number of independent features are given by the minimum of the number of slides or the number of features as a pessimistic approach). The following results are shown for the "conventional" and the "paired" multivariate discriminant analysis, referring to a MAC problem: Single slide classification quality, given in %:

discriminant analysis:	"normal"	"paired"
"normal" vs. MAC: 1 feature	76	94
"normal" vs. MAC: 2 features	85	100
"normal" vs. MAC: 3 features	n.s.	100
"normal" vs. MAC: 4 features	n.s.	100

The results demonstrate the considerable improvement in discrimination and accuracy of classification not only between normal and tumour tissue, but also in detecting the subvisual MACs.

R006**CORRELATION BETWEEN AGNORS SIZE AND CELL CYCLE TIME SHOWED BY IMAGE CYTOMETRY AND CGH**

Canet V., Montmasson M.P., Giroud F., Brugal G.
Laboratoire TIMC-IMAG UMR CNRS 5525, Institut
Albert Bonniot, Université Joseph Fourier Grenoble
I, Domaine de la Merci, 38706 La Tronche Cedex,
France

Although the correlation between AgNORs and other so-called proliferation markers (MIB-1/Ki-67, PCNA, p53) remains debatable, most authors agreed that AgNORs size, or AgNORs number, is related to the proliferation activity. Using different cell lines differing by their respective doubling times in vitro, a linear relationship between interphase AgNORs size and cells doubling time was observed: the larger was the interphase AgNORs, the shorter was the cell population doubling time. Nevertheless, the question remains whether such differences resulted from either biological differences between the cell lines used or from actual differences of the respective cell populations kinetics.

The first aim of this study was thus to analyze the relationship between the population doubling time and the quantity of AgNORs interphase proteins in one and the same cell culture (MCF-7) at various temperatures used to modulate the cell cycle time. After MIB-1 and AgNORs combined staining, the quantity of AgNORs proteins was measured in cycling cells by image cytometry. The AgNORs relative area (ratio of AgNORs area to nuclear area) was inversely proportional to the population doubling time thus supporting the hypothesis that the cell cycle time and the size of the ribogenesis machinery are co-regulated. Complementary experiments with three cell lines of same tissular origin but with different doubling time confirmed that the cell cycle time and the AgNORs size were inversely correlated.

Finally, CGH (Comparative Genomic Hybridization) was used to investigate why different cell lines of same tissular origin differ by their cycling time. Several chromosomal regions showed obvious differential deletion / amplification which might be related to the transcription / traduction ribogenesis machinery accounting for difference in AgNORs content and cell cycle speed. Results will be discussed with respect to the set of genes potentially affected.

R007
QUANTITATIVE IMAGE ANALYSIS OF
IMMUNOSTAINING AS A TOOL FOR THE

EVALUATION OF TISSUE EOSINOPHILIA IN
ATOPIC DERMATITIS

Kiehl P., Falkenberg K., Vogelbruch M., Kapp A.
Department of Dermatology and Allergology,
Hannover Medical University, Germany

Background: Eosinophilic granulocytes are major effector cells in allergic inflammation, but little is known about frequency, amount and distribution of tissue eosinophilia in skin lesions of atopic dermatitis (AD).

Objective: To give a quantitative description of tissue eosinophilia in AD based on morphometric data.

Methods: 31 lesional skin biopsies of AD were evaluated using our recently described method for the quantification and localization of eosinophilic granule protein (EGP) based on automated image analysis of highly sensitive immunostaining. Using the antibodies EG1, EG2, MBP and EPO, amount and distribution of EGP deposition were determined by calculation of the immunopositive area fraction at different levels of depth from epidermis and compared to neutrophil elastase (NE).

Results: EGP was found in nearly all biopsies (30/31). Significantly more EGP than NE was detected with EG1, EG2 and MBP, respectively. Superficial EGP distribution with less than 10% (median) of total EGP below a depth of 1.39 mm from epidermis was found. Significantly more EGP was measured in lesions exhibiting epidermal hyperplasia than in biopsies without this histopathological indicator of chronicity.

Conclusion: Superficial deposition of relevant amounts of EGP was regularly found in lesions of AD. EGP deposition may be especially involved in the development of chronicity.

R008
QUANTITATIVE METHOD OF
DETERMINATION OF GLUCOSE-6-
PHOSPHATASE ACTIVITY IN
HEPATOCYTES

Bezborodkina N.N., Kudryavtseva M.V.,
Kudryavtsev B.N.
Institut of Cytology RAS, Tikhoretsky av.4, 194064
St.Petersburg, Russia

Activity of glucose-6-phosphatase (G6Phase) was studied by a histochemical method in the portal and central zones of the rat liver in normal time and experimental cirrhosis. G6Phase was detected by

refixation of cryostat sections in a fixative with addition of glutaraldehyde and by a subsequent prolonged (18-24 hr) incubation of the sections in a chilled standard medium. To visualize the reaction final product, precipitate of lead phosphates, it was necessary to replace the anion by sulfide, which provided conversion of colorless products into the stained ones. Activity of G6Phase was determined using a videotest image analyzer that allowed combining cytospectrophotometric analysis of the content of the cell compound with determination of its precise localization in the tissues. It has been shown that in normal liver activity of G6Phase in the portal zone was 1.5 times higher than in the central zone of hepatic lobule. The ratio of the G6Phase activity in the periportal and pericentral (P/C) hepatocytes is on average of 1.4. In rats with liver cirrhosis, G6Phase activity in the portal zone was decreased by 26%. The P/C ratio in this case is 1.09. Thus, in the cirrhotically altered liver, the zonal heterogeneity of G6Phase is preserved, although it is changed significantly as compared with norm.

R009

ANALYSIS OF THE COMPONENT "TREE" AS A NEW TOOL FOR ANALYTICAL CELLULAR PATHOLOGY

Metze K. 1, Souza Filho W. 2, Adam R.L. 1, Lorand-Metze IGH. 3, Leite N.J. 2

1) Department of Pathology, Faculty of Medicine, State University of Campinas, 2) Institute of Computing, State University of Campinas, 3) Department of Internal Medicine, Faculty of Medicine, State University of Campinas, Campinas, Brazil

The number of components of a digitalized image can be described based on its gray values. Comparing the images of successively decreasing gray levels, changes of the components are observed, such as decrease of the size of the whole component or its "splitting" into sub-components. According to graph theory, we can regard the whole set of these successive images for a certain component as a "tree" and consider the number of some of its parameters, such as "nodes", "ramifications" and "leaves". We developed a software to determine these new parameters in a digitalized image. The method is especially useful for a very detailed characterization of nuclei or their components. The use of topological information has the advantage that the whole

structure of the component trees is invariant even under deformation-(bending, stretching and squeezing). Segmentation of regions of interest at different (although nearby) gray levels may provoke alterations of parameters, such as area, form factors or entropy, whereas this is not the case for many parameters of the component tree, which may be used for discrimination. For instance, a good separation is achieved between the AgNOR stained nuclei of normal lymphocytes and cells of chronic lymphocytic leukemia (CLL). Furthermore in a discriminant analysis (between four randomly chosen patients with CLL) it was possible to assign correctly about 80% of the cells to one particular patient based only on the analysis of the component tree of the AgNORs.

Supported by FAEP, CNPQ, FAPESP

R010

SPECTRAL ANALYSIS USING DISCRETE FOURIER TRANSFORMATION FOR THE STUDY OF NUCLEI: SOFTWARE DESIGN AND APPLICATION ON CARDIOMYOCYTES DURING PHYSIOLOGICAL DEVELOPMENT

Adam R.L. 1, Leite N.J. 2, Metze K. 1

1) Department of Pathology, Faculty of Medicine, State University of Campinas, 2) Institute of Computing, State University of Campinas, Campinas-SP, Brazil

The Fourier analysis has mainly been used in order to study diffraction patterns or nuclear contours in histologic or cytologic preparations. It has been yet rarely applied to nuclear texture features in digitalized images. The aim of this study was to improve the practical use of the fast Fourier technique in routine preparations and to investigate the discriminative values of power spectrum features derived from the transformed image. In segmented images of nuclei, the difference of the gray levels at the boundary between the nucleolemma and the background, provokes concentric (Airy) rings in the frequency domain. In order to minimize this effect, an algorithm was developed which defined the mean of the nuclear gray values as the background and smoothed the nuclear edges. This procedure was applied to cytologic preparations of KOH-treated and hematoxylin stained nuclei of cardiomyocytes of rats during physiological development (the 9th day of gestation – the 60th day after birth). In fetal cardiomyocytes, the transformed images revealed a

large component of information located in the high spatial frequencies. After birth, however, an increase of low spatial frequencies was observed. Furthermore, inertia and several Haralick features derived from the transformed image (e.g. angular moment, cluster prominence) discriminated between nuclei of rats of different ages. Therefore we think that the nuclear image transformed by the Fast Fourier algorithm may provide useful information on the chromatin features.

Supported by FAEP, FAPESP, CNPQ

R011

NUCLEAR MORPHOLOGY AND TUMOR PROGRESSION IN BREAST CANCER

Friedrich K. 1, Rothert F. 1, Meyer W. 1, Dimmer V. 1, Theissig F. 1, Haroske G. 2, Baretton G. 1, Kunze K.D. 1

1) Dresden University of Technology, Institute of Pathology; Germany; Fetscherstr. 74; D-01307 Dresden, 2) Dresden-Friedrichstadt General Hospital; Germany; Friedrichstr. 41; D-01067 Dresden

The aim of the study was the quantitative analysis of nuclear morphology in breast cancers with different features of tumor progression, like the clinicopathological features, the hormone receptor stage, the proliferative activity, the occurrence of local recurrences and metastases.

Feulgen stained sections of 68 primary breast cancers, their lymph node metastases and their local recurrences were examined by high resolution image cytometry. From each nucleus, 130 features were computed on a MicroVAX 4000 computer. The proliferation activity was detected immunohistochemically for the Ki-67 antigen by the MIB-1 antibody.

Breast cancers with one to four lymph node metastases differ from the tumors with more than four metastases in the nuclear texture. The comparison of cases with different Bloom-Richardson grade revealed a lot of changes in the nuclear morphology, not only indicating a high polymorphism in grade 3 tumors. Differences in the nuclear shape and the chromatin distribution were detected in correlation to the hormone receptor stage. A high proliferation activity was associated with changes of the nuclear shape and texture. The lymph node metastases differ from their primary tumors in features describing the chromatin amount.

In summary, the prognostically relevant clinicopathological features lymph node stage and Bloom-Richardson grade are accompanied by some characteristics in the nuclear morphology. Functional features, like hormone receptor stage and proliferation activity are as well reflected by the nuclear morphology. The lymph node metastases differ from their primary tumors in quantitative nuclear feature, indicating a further evolution of the metastasizing tumor cells.

R012

AUTOMATED IMAGE ANALYSIS BASED DETECTION AND ANALYSIS OF CYTOKERATIN-POSITIVE DISSEMINATED TUMOUR CELLS IN BLOOD OR BONE MARROW

Beliën J.A.M. 1, Gouwenberg Y. 2, Brakenhoff R.H. 2, Van Diest P.J. 1

1) Dept. of Pathology, Academic Hospital Vrije Universiteit, Amsterdam, The Netherlands, 2) Dept. of Otolaryngology, Academic Hospital Vrije Universiteit, Amsterdam, The Netherlands

Since early dissemination of tumour cells in patients with small, curatively resected tumours is one of the leading causes of relapse at distant sites and of death from cancer, it is clinically relevant to detect possible obscure metastatic cells. For several cancers, it has been shown that the presence of these cells in bone marrow influences the prognosis.

Imaging techniques like CT, MRI and PET are not sensitive enough for detecting small numbers (1 in 1 million) of disseminated tumour cells in blood or bone marrow. Other techniques like RT-PCR and immunohistochemistry are more promising.

In this study, we have developed an automated rare event detection system that can be used for the recognition of (disseminated) immunohistochemically positive stained tumour cells in blood or bone marrow. The system includes an automated transmission light microscope, a black and white CCD camera and a PC for software based image analysis.

We have used cytokeratin-specific monoclonal antibodies to identify epithelial cells in blood and bone marrow. The system scans a single specimen with 1.5 million cells within 4 hours. Besides screening for positive cells, the system can also produce a total cell count. Suspicious cells are

digitally stored and can be displayed for reviewing. Since the X,Y coordinates are also stored, each cell can be relocated for inspection, analysis at higher magnification or dissection using a laser-dissection microscope.

Initial results showed a 5% false negative rate mainly due to faint staining. Future improvements in staining and image processing software may improve the results found so far.

R014
IMMUNOHISTOCHEMICALLY STAINED
BREAST CARCINOMA CELL NUCLEI
SEGMENTATION OF NEURAL NETWORKS

Hwang H.G. 1, Lee B.I. 1, Cho N.H.2, Choi H.K. 1

1) School of Information and Computer Engineering, Inje University, Korea, 2) Department of Pathology, Yonsei University, Korea

The breast carcinoma cell tissue images were stained by Diaminobenzidine(DAB) and counterstained with Hematoxylin. An accurately cell nucleus segmentation is prerequisite to diagnosis and prognosis for breast cancer patients. However, the immunohistochemical color tissue images hold with a lot of variations and noises. To overcome this problem, we used texture features and a back-propagation neural network algorithm to segment and classify breast carcinoma cells into positive nuclei, negative nuclei and background. First, we generated pixel positions using a Markov Random Function(MRF) and selected to each 90 pixels respectively the three regions in an image. The total 900 pixels we trained on 10 images. From each selected pixel we took 80 neighbors (9x9 mask). The mask was normalized and calculated the 18 co-occurrence texture features. In the next place, we input the calculated texture features to the back-propagation neural networks i.e. 18 nodes in input layer, 12 nodes in hidden layer and 3 nodes in output layer. To make the desired net approach and to reduce the value of the error rate (10⁻⁶), we continually trained the neural networks. Finally, we correctly obtained 95.3 % classification e.g., 90 % for positive cell nuclei, 98 % for negative cell nuclei and 98 % background. The results of the immunohisto-chemically stained breast carcinoma cell nuclei segmentation for the color images have a good correlation with visual inspection by pathologist.

R015
QUANTITATIVE STUDY OF HUMAN
BUCCAL MUCOSA CELLS : EFFECT OF
SMOKING AND SEX-DEPENDENT
DIFFERENCES

Lavrencak J. 1, Zganec M. 2, Flezar M. 1, Us-Krasovec M. 1

1) Institute of Oncology, Dept. Cytopathology, Ljubljana, Slovenia, 2) Faculty of Electrical Engineering, Ljubljana, Slovenia

The effects of cigarette smoking on clinically normal buccal mucosa as well as sex and age-dependent differences have been assessed in several morphologic, but only a few quantitative studies using flow and image cytometry. The equivocal results, obtained mostly on small study groups, indicate the need for further studies based on larger groups.

Therefore, we collected buccal mucosa cells from 151 healthy subjects. The cells were scrapped with wooden spatula and suspended in transport medium. Membrane filtration method and filter imprint technique were used for smear preparation. All smears were fixed in Delaunay fixative. For image analysis, the slides were stoichiometrically stained by modified Feulgen-thionin method. Image acquisition was performed by high-resolution image cytometer (Cyto-SavantTM, Oncometrics Imaging Corp., Vancouver, Canada). The probability distribution for each of 62 nuclear features (NF) was calculated. The statistical analysis of NF was done for the group of 65 smokers (n=56547 nuclei) versus the group of 86 non-smokers (n=79052 nuclei) and for the group of 68 female (n=51454 nuclei) versus the group of 60 male (n=42297 nuclei).

Discriminative ability of NF was constantly below 55%. Our study suggests that smoking and sex do not have a significant influence on cell nuclei of buccal mucosa.

R016
ESTIMATING ACUTE AND CHRONIC
HYPOXIA IN CANCER PATIENTS:
QUANTITATIVE

IMMUNOHISTOCHEMISTRY OF VESSELS,
PIMONIDAZOLE AND IODODEOXYURIDINE

Begg A. 1, Haustermans K. 1,2, Hofland I. 1, Hoebbers F. 1, Blyweert E. 2, Raleigh J. 3, Varia M. 3, Sciot R. 2, Van Velthuysen L. 1, Delaere P. 2, Balm A. 1

- 1) The Netherlands Cancer Institute, Amsterdam, 2)
- University Hospital Gasthuisberg, Leuven, Belgium,
- 3) University of North Carolina, USA

Purpose: To assess immunohistochemical methods to measure human tumor hypoxia and perfusion.

Background: Tumor hypoxia is a known negative prognostic factor for patients undergoing radiotherapy, chemotherapy or surgery. Hypoxia occurs through both diffusion and perfusion limitations, both likely to be important in determining therapy response. Pimonidazole, an hypoxia marker, and iododeoxyuridine (IdUrd), a cell kinetic marker, are being used to measure hypoxia and perfusion respectively. Our hypothesis is that low IdUrd labeling indicates temporary reduction in IdUrd supply resulting from a perfusion reduction.

Material and methods: 20 SCC head and neck patients treated with primary surgery were given pimonidazole and IdUrd i.v. 16h before surgery. Paraffin embedded sections were double stained for either CD31 and pimonidazole or CD31 and IdUrd. Whole sections were digitized using a stepping microscope stage. Tumor areas were delineated from non-tumor areas, and the proportion of tumor tissue greater than a fixed distance (80-150 μ) from the nearest vessel, called diffusion limited fraction (DLF), calculated using "SCIL-image" software. Tumor areas stained for pimonidazole were also quantified. Finally, IdUrd labeling of tumor cells around individual blood vessels was scored visually using a scale from 0 to 5.

Results: There was a wide variation between and within tumors in all parameters. Pimonidazole areas were significantly smaller than the DLF for all tumors, although there was a statistically significant correlation between them ($r=0.29$, $n=237$, $p<10^{-5}$). Estimates of the fraction non-perfused vessels (based on no surrounding IdUrd labeling) ranged from 1-33% (mean 15%).

Conclusion: Measuring chronic and acute hypoxia and perfusion in human tumors appears feasible by immunohistochemistry.

R018
THE PRESS-PRO21 SLIDE : A REFERENCE
TOOL FOR CALIBRATION OF ICM
INSTRUMENTATION

Giroud F.

Equipe RFMQ-TIMC-IMAG, Université Joseph Fourier, Grenoble, France.

The PRO21 slide is a microscopic test slide dedicated to calibration of image cytometry instrumentation. It has been developed during the PRESS* project in the frame of the "Measuring and Testing" program (DGXII-CEE). The slide exhibits a set of various densitometric features : 11 columns of different transmission values from 5% to 100%, and 5 different test patterns organized according to 5 different lines. The test patterns are either 10 microm diameter circles or 10 microm side squares, regularly arranged on black or transparent background. Additionally, various geometric features are materialized as an horizontal and a vertical graduated scale in the center of the slide, and (x,y) coordinates marks regularly arranged on the whole slide area. Due to its large range of features, the slide enables you to perform :

- camera and stage alignment,
- stage motion calibration,
- sampling density calibration,
- electro-optical system evaluation (Optical Transfer Function),
- segmentation robustness (from square or circle particles),
- geometric distortion evaluation,
- illumination calibration (checking for electronic noise, drift during time, shading phenomenon),
- densitometric calibration (linearity, density object measurements).

The different features of the PRO21 slide will be presented and corresponding calibration tests will be documented. Services of QACODIC server dedicated to assurance and quality control of ICM instrumentation and densitometric measurements of segmented density objects will be illustrated. The microscopic slide is actually commercially available ; contact at the following electronic address : Francoise.Giroud@imag.fr

* PRESS : Prototype Reference Standard Slides for quantitative cytometry of nuclear

R019
EXTRACTION OF SIGNIFICANT FEATURES
FOR CREATING AN OPTIMIZED
CLASSIFIER OF BLADDER CARCINOMA
CELL HISTOLOGICAL SECTIONS

Choi. H.J. 1, Lee. B.I. 1, Yang. Y.I. 2, Choi. H.K. 1

1) Department of Computer Science, Inje University, 607 Abang-dong, Kimhae, Kyungnam 621-749,

Korea, 2) Department of Pathology, Inje University, 607 Abang-dong, Kimhae, Kyungnam 621-749, Korea

The main task of this study is to develop an objective and reproducible classification method for malignancy grading of Feulgen stained bladder carcinoma. To create an optimized classifier, it is needed to extract the features that describe accurately order/disorder of the nuclear variations, chromatin intensity variations and morphological variations. The developed algorithms are as follows. First, we acquired 40 representative bladder carcinoma cell histological images from each of the four groups (Grade1, Grade2A, Grade2B, Grade3). Then, we extracted 9 morphological features, 6 textual features and 18 Wavelet textural features. Second, we evaluated the significance of the extracted features using variance analysis(ANOVA). Third, we created 4 classifiers respectively of the three category classifiers and their combination set using multivariate discriminant analysis(MANOVA). Finally, we compared and analyzed the correct classification rate of each classifier. In the test set, we obtained 55% correct classification rate for the morphological classifier, 80% correct classification rate for the texture classifier, 90% correct classification rate for the Wavelet texture classifier and 95% correct classification rate using of all features. It was represented a higher correct classification rate than the one of the classifier created by a category features. The result of this study was a combination of features. We conformed that the correct classification rate was determined by feature extraction and feature evaluation. We expect that the proposed method in this paper could be available as an objective pathology diagnosis assistant tool for bladder carcinoma patients.

R020
GRADING AND STAGING OF OVARIAN SEROUS ADENOCARCINOMAS USING IMAGE CYTOMETRIC NUCLEAR TEXTURE FEATURES

Flezar M. 1, Lavrencak J. 1, Zganec M. 2, Us-Krasovec M. 1

1) Institute of Oncology, Dept. Cytopathology, Ljubljana, Slovenia, 2) Faculty of Electrical Engineering, Ljubljana, Slovenia

Image cytometric nuclear texture features (NTF) could be used for objective and reproducible determination of malignant potential of ovarian cancer, which is conventionally defined by clinical staging and histological grading.

The purpose of our study was to find out whether NTF could discriminate between different grades and stages in the group of ovarian serous adenocarcinomas.

In our study we analysed NTF of 67 ovarian serous adenocarcinomas. Archival tissue samples of the tumors were used for the preparation of single cell suspensions, according to the modified Hedley's method. Cell monolayer slides were stained according to the Feulgen-thionin method. Image cytometric analysis was performed by an automated high resolution image cytometer, namely Cyto-Savant. The discrimination analysis was accomplished using all the acquired nuclear images of a tumor, subsequently only nuclear images of the diploid peak were used for the discrimination analysis.

The results of our study showed that different conventional grades and stages of ovarian carcinomas could not be reliably discriminated using a single NTF. However, the combination of three NTF could correctly classify 82% (all tumor nuclei included) or 83% (nuclei of diploid peak only) of carcinomas according to their histological grade. Furthermore, a combination of NTF could discriminate between low and high FIGO stage in 85% (all tumor nuclei included) and 86% (nuclei of diploid peak only).

We showed that the combination of NTF could discriminate between different grades and stages of ovarian carcinoma. However, the discrimination by NTF does not match exactly the conventional classification. Therefore, we believe that NTF should be correlated with survival data, so that more objective and reproducible grading and staging systems could be built.

R021
CELLS OF THE BLOOD SYSTEM: DIGITAL IMAGE CAPTURING AND PROCESSING

Boev S.F., Sazonov V.V., Vinogradov A.G., Verdenskaya N.V., Ivanova I.A., Pogorelov V.M., Naumova I.N., Levina T.N., Sarytcheva T.G., Kozinets G.I.

Mints Radotechnical Institute, 8th March Str. 10, Moscow, 125083 Russia, Haematological Scientific

Centre, Novozykovsky pr. 4-a, Moscow, 125167 Russia.

An automated instrument for blood cell analysis is designed. The instrument is based on computer microscopy and cell analysis in dry blood smears colored according to the standard Romanovskii-Gimza procedure. In comparison with the well-known haematological analysers, our instrument provides more detailed information on cells morphology and shows final results not only in the form of the standard filled-in blank of blood analysis, but also in the form of cell galleries. The instrument consists of a light microscope equipped with an automated object table, digital videocamera and computer. Additionally, the instrument can be added with an instrument for preparation of monolayered smears required for automatically analysing smears. Software of this instrument is based on digital image processing and image recognition procedures. The instrument can be used as a fairly universal tool in scientific research and public demonstrations in medical treatment and education processes. In addition, it may appear to be very useful in telepathology applications. The principle used as the basis of the instrument appeared adequate for creating an instrument version serviceable during space flights where standard manual procedures and flow cytometry systems fail.

R022

CELLS OF THE BLOOD SYSTEM: DIGITAL IMAGE CAPTURING AND PROCESSING

Pogorelov V.M., Kozinets G.I., Sazonov V.V.
Haematological Scientific Centre, Novozykovsky pr. 4-a, Moscow, 125167 Russia, Mints Radotechnical Institute, 8th March Str. 10, Moscow, 125083 Russia

During this decade, the usage of computers and workstations in haematological laboratory has become as ubiquitous as slides and microscope are now. For the purpose of our discussion, we may subdivide haemacytology computerization into:

- The automated microscopy system for peripheral blood cells (ASPBC)
- The monitoring of acute leukaemia patients
- Discrimination and automated classification apoptotic lymphocytes in silver-stained peripheral blood smears

-The automatic analysis of AG-granular structure of nucleolus in lymphoproliferative disorders (LPD)

-The computerised standardisation of the diagnosis LPD.

Briefly, ASPBC can be used as an automated microscope for quantitative analysis of dry stained smears of blood, for morphometric parameters of leukemic cells to characterise their maturity and it may be used in acute leukaemia patient monitoring. The size of lymphocytes and the nucleoli segregation demonstrated the highest correlation with apoptotic cell death. In more complicated cases when there is no agreement between different observers, our computer estimation of Ag-granules number is reliable. Computer image analysis is convenient for standardisation of the diagnosis of mature B-cell lymphoproliferative disorders.

R023

QUANTITATIVE DESCRIPTORS OF THE LYMPHOCYTES

Angulo J. 1, Serra J. 1, Flandrin G. 2

1) Centre de Morphologie Mathématique, Ecole des Mines de Paris, 35 Rue St. Honoré, 77305 Fontainebleau, France, 2) Laboratoire Central d'Hématologie, Hôpital Necker-Enfants Malades, 149 Rue de Sèvres, 75743 Paris, France

Recent literature in methodology about diagnosis on lymphoproliferative disorders still considers the lymphocyte morphology as the principle basis for the identification of lymphoid neoplasm. In lymphocyte quantitative description, the nuclear size and shape are essential. However, there are also other important features that require a complete description: shape of cytoplasm profile, nucleus/cytoplasm ratios, cytoplasm color-texture, texture of nuclear chromatin, detection of nucleolus, etc. Motivated by the consideration that the choice of shape, color and texture description parameters remain a difficult problem, we have put much emphasis in the design of a new global approach that allows us an objective and complete quantification of the lymphocytes. After segmenting each lymphocyte image into three meaningful regions: nucleus, cytoplasm and background (using a classical method of the Mathematical Morphology: watershed with markers), the proposed approach calculates the values of each parameter that has been defined, and builds a feature vector that will be used in the subsequent

classification. The ability of discrimination of this descriptor is shown by means of an image base of 50 lymphoproliferative cases (about 1500 images with a uniform coloration).

R024

AUTOMATIC CELLULAR RECOGNITION IN SEROUS CYTOLOGY

Lezoray O., Cardot H., Elmoataz A.

LUSAC EA 2607, Site Universitaire, BP 78, 50130 Octeville, France

We propose a system as an assistance to screening using image analysis cellular classification. It is called ARCTIC and proceeds to the recognition of cells from serous cytology. The structure of the system is threefold : extraction of the color cells, quantitative analysis, classification of the cells using artificial intelligence techniques. The extraction of the cells in the images is based on a color mathematical morphology scheme which enables a finer segmentation of the cells even clustered. Segmentation results have been visually inspected by three different experts on a database of 2000 cells. The nuclei and the cytoplasm of the cells of the database have been segmented with an accuracy of 94.5% and 93% which is very good for this microscopic application. Once segmented, cells are characterized by 46 different attributes among size, color, shape and texture criteria. The final step of our system consists in the classification of the cells in 18 different classes. First, a decision tree is used to set whether the object to recognize is a cell, a cluster of cells or a debris. This is performed with an error rate of 6.3%. Cells are then classified using an architecture of neural networks and a wrapper feature selection method for the selection of relevant attributes among the 46 computed ones. A database of 3630 segmented cells was used, 80% of this latter for training of the networks and 20% for test. The global recognition rate of the system for the 18 different classes is 60,3%. With a merging of the different classes in normal and abnormal cells, respectively 99% and 96% are recognized. Since our system is conceived to operate in post-screening, abnormal cells which have been missed by a cyto-technician during a conventional screening, might be recognized by our system allowing a better quality control of slides from serous cytology.

R025

EVALUATION OF THE VOLUME FRACTION OF OVARIAN CANCERS' STROMAL COMPARTMENT BY AUTOMATIC IMAGE PROCESSING OF THE WHOLE HISTOLOGICAL SECTION

Elie N. 1, Tran K. 1, Plancoulaine B. 2, Coudrey T. 3, Denoux Y. 4, Herlin P. 4, Chermant J.-L., Coster M. 5

1) GRECAN EA 1772, CJF INSERM 96-03, CRLCC François Baclesse – Caen, France, 2) Institut Universitaire de Technologie, département de Mesures Physiques – Caen, France, 3) GREYC-ISMRA, UPRES-A CNRS 6072, F - 14032 Caen cedex, France, 4) Laboratoire d'Anatomie Pathologique, CRLCC François Baclesse – Caen, France, 5) LERMAT-ISMRA, UPRES-A CNRS 6004, F-14032 Caen cedex, France, 1-5) Pôle Traitement et Analyse d'Images de Basse Normandie.

Several studies have demonstrated that the relative abundance of stroma in ovarian cancers informs about the future of the tumor : the less abundant is the stromal compartment the poorest is the prognosis (Schueler et al, 1993). The introduction of this prognosis parameter in routine practice requires the development of a simple and reliable evaluation method. The estimation of the stromal volume fraction is classically done thanks to stereology tools applied to sampled microscopical fields. Interactive point counting is reputed tedious and sampling strategy difficult to adapt to heterogeneous tumors as ovarian carcinomas (Brinkhuis et al, 1996).

We propose here to evaluate the stromal compartment by fully automatic image processing of the whole histological section. The acquisition method consists in scanning a "representative" histological section as a whole, thanks to a high resolution slide scanner, provided with a glass slide holder (Polaroid). The colour image is then analysed using a specifically developed chaining of image processing operators (Aphelion-ADCIS). Two staining procedures were compared and applied to 5 μm and 9 μm thick sections : the classical Hematoxylin-Erythrosin-Saffron staining (HES) and a simplified Hematoxylin-Saffron staining (HS). The comparison of the results obtained with interactive drawing underlines the superiority of HS staining both in terms of the simplicity of the procedure and of the reliability of the results.

References :

Schueler, J.A. et al (1993) Prognostic factors in well-differentiated early-stage epithelial ovarian cancer. Cancer, 71, 787-795.

Brinkhuis, M. et al (1996) Value of quantitative pathological variables as prognostic factors in advanced ovarian carcinoma. J.Clin.Pathol., 49, 142-148.

Mr. Elie was recipient of a MESR fellowship.

R026

ABOUT PLOIDY OF PATHOLOGICAL MONONUCLEARS IN INFECTIOUS MONONUCLEOSIS

Shilov B.V.

Solyanoi pereulok, 34, 2 Tomsk, Russian federation, 634003

The purpose of this study was to analyze with ICM (Imaging Cytometry) some morphological classes of mononuclears from 60 young patients with Infectious Mononucleosis. Morphological features of pathological mononuclears stained by Azur-II-Eosin and Feulgen. Some basic forms of nucleated cells were defined, such as: cells with normal circular nucleus; cells with weak nucleus deformation; cells with fabiform of nucleus; cells with 1-, 2- and polylociniate; cells with angular nucleus; cells with sharply deformed nucleus. Using ImageJ (W.Rasband, NIH, USA) quantitative shape parameters, histogram parameters were considered. After that conclusion, about probable content of DNA of atypical mononuclears in different morphological forms were made.

R027

AUTOMATED IDENTIFICATION OF DIPLOID REFERENCE CELLS IN CERVICAL SMEARS USING IMAGE ANALYSIS

Van der Laak J., Siebers A., Cuijpers V., Pahlplatz M., De Wilde P., Hanselaar A.

Department of Pathology, University Medical Center St Radboud, Nijmegen, The Netherlands

Acquisition of DNA ploidy histograms by image analysis may yield important information regarding the behavior of premalignant cervical lesions. Accurate selection of nuclei for DNA measurement is an important prerequisite to obtain reliable data. Traditionally, manual selection of nuclei of diagnostic and reference cells is performed by an

experienced cytotechnologist. In the present study, a method for fully automated identification of nuclei of reference cells is described. This method consists in a decision tree implemented on the measurement device, containing nodes with feature threshold values and multivariate discriminant functions. Nodes were constructed to recognize debris and inflammatory cells, and to recognize non-diploid cells and diploid intermediate squamous cells. Evaluation of the classifier was performed by comparing resulting diploid integrated optical densities with those from manually selected reference cells. On average, automatically acquired values deviated 2.4% from manually acquired values, indicating that the method described in this paper may be useful in cytometric practice.

R028

A UNIFIED APPROACH TO LOW DIMENSIONALITY ADAPTIVE TEXTURE FEATURE EXTRACTION APPLIED TO OVARIAN CANCER PROGNOSIS ESTIMATION

Albregtsen F. 1, Nielsen B. 1,2, Danielsen. HE 2

1) Group for Signal Processing and Image Analysis, Department of Informatics, University of Oslo, Norway, 2) Division of Digital Pathology, The Norwegian Radium Hospital, Montebello, Oslo, Norway.

Texture features used for classification are often selected from a large number of rather ad hoc features. Whatever sophisticated selection algorithm we use, the risk of purely coincidental "good" feature sets may become alarmingly high, particularly if the available data set is limited, and separate training and test sets are not used.

For a number of texture analysis methods, we have constructed parametric class distance matrices to extract a minimum number of features. We have used the squared class distance matrix elements as weights and the sign of the class difference matrix elements as a bit map in a weighted summation of the frequency matrix entries.

The 10 most difficult Brodatz textures have been used to evaluate the new adaptive features. We have also constructed class difference and distance matrices from 10 000 monolayer cell nuclei taken from 40 patients of two classes (good and bad prognosis) of early ovarian cancer. Using a "peel-off-scanning", we have made separate estimates of

texture features in the periphery and center of the images.

The new adaptive features outperform the predefined features when applied to all 45 possible Brodatz texture pairs. We notice that there is a marked difference between the matrices computed from the peripheral 30% and the central 70% segments of the cell nuclei. These subtle texture differences are very hard to discern from the images.

Consequently, we have computed the new adaptive features for each cell nucleus, separately for the peripheral and central segment. We have used the mean, standard deviation and 10 and 90 percentiles of the features to characterize each patient. The best feature pairs then gave less than 25% classification error.

We note that by using this low dimensionality feature extraction approach, we have substantially reduced the risk of selecting good feature pairs by pure coincidence.

R029

THE EXTRACTION OF LOW DIMENSIONALITY ADAPTIVE FEATURE VECTORS FROM THE PERIPHERY AND CENTER OF OVARIAN CELL NUCLEI FROM MONOLAYERS AND HISTOLOGICAL SECTIONS

Nielsen B. 1,2, Albrechtsen F. 1, Kildal W. 2, Danielsen H.E.

1) Group for Data Analysis, Signal and Image Processing, Department of Informatics, University of Oslo, P.O.Box 1080 Blindern, N-0316 Oslo, Norway,
2) Division of Digital Pathology, The Norwegian Radium Hospital, Montebello, N-0310 Oslo, Norway.

In order to quantify the chromatin structure of cell nuclei from patients with early ovarian cancer, low dimensionality adaptive fractal and Gray Level Cooccurrence Matrix feature vectors were extracted from nuclei images from monolayers and histological sections. Each light microscopy nucleus image was divided into a peripheral and a central part, representing 30% and 70% of the total area of the nucleus, respectively.

A major problem in texture analysis is that we often have a large number of feature combinations to choose from, and that the features are static and predefined. Thus, the individual features do not adapt to the problem at hand, but we may still get over-

optimistic results. Identifying a few consistently valuable features is important for many applications as it improves reliability and enhances our understanding of the phenomena that we are modelling.

Earlier, we have therefore proposed a low dimensionality adaptive feature extraction based on class difference and class distance matrices.

Class difference and distance matrices were useful to illustrate the difference in texture between the good and bad prognosis classes of ovarian samples. Homogeneous areas in the darker part of the image were more probable for the bad prognosis class, while homogeneous areas in the lighter part of the image were more probable for the good prognosis class. Class difference and distance matrices also clearly showed the difference in texture between the peripheral and central parts of nuclei. Both when working with nuclei images from monolayers and from histological sections, it seems useful to extract separate features from the peripheral and central part of the nuclei images.

R030

AUTOMATIC SEGMENTATION OF OVERLAPPING NUCLEI IN LUNG BIOPSY IMAGES

Kemp R., Lam S., MacAulay C.

Cancer Imaging Department, British Columbia Cancer Research Center, 601 West 10th Avenue, Vancouver, BC, V5Z 1L3, Canada

The identification and segmentation of nuclei in images of tissue biopsies and specifically lung biopsies is a difficult task. The high degree of nuclear overlap and presence of nuclear fragments pose a challenge for any algorithm to segment correctly.

We describe an automated technique to separate clustered objects in such images. The method uses watershed, Hough transform and adaptive contour techniques with prior knowledge of nuclear parameter statistics in order to obtain the most likely arrangement of nuclei to have formed the cluster image. This system makes possible the clinical application of architectural and morphological measurements in epithelial and other sectioned material.

We will present the results of this system applied to images of bronchial epithelial tissue taken from the central bronchus. The seven micron thick sections are Feulgen-stained in order to highlight the nuclear

features and exhibit various degrees of hyperplasia, metaplasia and dysplasia.

R031

LOW RESOLUTION IMAGE CYTOMETRY FOR QUANTIFICATION OF TUMOUR BLOOD VESSELS

Tran T.K.N. 1,2, Thuillier J. 1, Lebeau C. 1, Herlin P. 1, Chermant J.-L., Coster M. 2

1) Centre F. Baclesse, Caen, France, 2) LERMAT, ISMRA, Caen, France, 1-2) Pôle Traitement et Analyse d'Images de Basse Normandie.

Quantification of structures on histological sections, such as blood vessels, are frequently subject to several constraints. First of all, measurements are often limited to a restricted microscopical field, visually selected and regarded as reflecting the whole tumour, whatever heterogeneous pattern of the biomarker may be. Furthermore, these measurements, even manual or semi-automatic, require the involvement of the observer, resulting in poor data reproducibility and to interobserver variability, inconsistent with routine clinical use.

We here propose the use of a slide scanner for acquisition of low resolution images of the whole histological section. These large images, or the selected fields of interest (such as "hot spots") which can be easily delineated, are processed as a whole, at once, thanks to a fully automatic image analysis programme. Density of blood vessel sections estimated on scanner images were compared to manual counting, stereological method and measures obtained from microscopical mosaic images of exactly the same fields.

This work was supported by grants from the "comités départementaux de la Manche et du Calvados de la Ligue Nationale de Lutte contre le Cancer". Miss Tran was recipient of a "Ligue de Lutte contre le Cancer" fellowship.

R032

AN ADAPTATIVE GENERALIZED REGION GROWING OPERATOR : APPLICATION TO COLOR IMAGES

Belhomme P. 1, Gougeon G. 1, Herlin P. 2

1) LUSAC, Site Universitaire, Rue Louis Aragon, B.P. 78, F-50130 Cherbourg-Octeville, France, 2) Lab. d'anatomie pathologique, Centre Baclesse, route

de Lion/Mer, BP 5026, F-14076 Caen cedex 05, France

Analysis of medical images from histological sections is a complex problem. However, the automatic processing of a great number of clinical cases can only be done after a reliable image segmentation. To reach this point, contour based methods or region based methods are usually used; combining these two families is in practice much more efficient. Among the region based methods, the watershed transformation implemented with ordered queues is a powerful tool in mathematical morphology. It relies on an optimal scanning of a fixed potential function (usually a gradient image), under the constraints of objects and background markers, for the detection of its watershed lines. The main drawback of this tool, with color images, is that obtaining such a fixed potential function yields to reduce a color image into a single object-representative component and, by consequence, only one local criterion is taken into account.

We propose to extend this algorithm in order to integrate many other local criteria but, much more, some global criteria which can be expressed as statistical parameters iteratively computed. We will see that our extension allows to simulate many region growing methods and pay attention to the criteria that can be used, to the way they can be combined and to the way their respective weight may be tuned. We thus result in a Generalized REgion Growing Operator (GREGO) with optimal scanning. To show its adaptiveness, it will be applied onto histological color images of cancer.

R033

MEASURES OF BONE ARCHITECTURE BY IMAGE ANALYSIS ON HISTOLOGICAL SECTION

Schupp S. 1, Elmoataz A. 1, Herlin P. 2, Levasseur R. 3, Marcelli C. 3., Bloyet D. 1

1) GREYC, Groupe de Recherche en Informatique, Image et Instrumentation de Caen-UMR CNRS 6072, 6 Bd Marechal Juin, 14050 Caen cedex, France, 2) Centre de Lutte Contre le Cancer François BACLESSE, Route de Lion sur mer 14076 Caen, France, 3) Département de rhumatologie, CHU de Caen, 14033 Caen, France, 1-2) Pôle Traitement et Analyse d'Images de Basse Normandie

Histological sections were performed on femur of rats which had received a treatment causing an osteoporosis disease. Several sections were obtained at different stages. These slides were stained to color in green trabecular and cortical bone.

Image segmentation is a strategy in three steps with tools based on Partial Differential Equation (PDE), integrating the statistical information. The first step is a preprocessing by PDE, in order to filter out the noise, while enhancing contours. The second step is the initialization of the third step : localization by active contours. Initialization is achieved by a fuzzy classification of seeds obtained by mathematical morphology operators. For localization, we used the non-regularized model of geometric approaches implemented by fast marching methods.

Measurements of trabecular bone are performed inside an area of interest. A first class of measures concerns area and perimeter of trabecular bone. These measures are obtained on segmented images. In order to get the second class of measures which characterize trabecular bone architecture, we need to compute a skeleton on the binary image. This image analysis operation allows us to obtain an average diameter of pillar bone and to account for junctions and terminal points. With these preliminary measures, significant indices are calculated.

These measures show that the kinetic of evolution of bone mass is of importance and needs a regular follow-up of the patient. A great bone mass which damages very quickly and a small bone mass which damages slowly, go in the same time to a critical bone mass, threshold of potential fracture.

R034

STRATEGY OF AUTOMATED SEGMENTATION BASED ON PDE AND ON FUZZY CLASSIFICATION FOR AUTOMATIC COMPUTING OF IMMUNOSTAINING INDEX

Schüpp S. 1, Elmoataz A. 1, Herlin P. 2, Bloyet D. 1
1) GREYC, Groupe de REcherche en Informatique, Image et Instrumentation de Caen - UMR CNRS 6072, 6, Bd Maréchal Juin, 14050 Caen cedex, France, 2) Centre de Lutte Contre le Cancer François, BACLESSE, Route de Lion sur mer 14076 Caen, France, 1-2) Pôle Traitement et Analyse d'Images de Basse Normandie

Immunohistochemistry is now largely introduced in prognosis pathology for tumor growth assessment. Quantitative Immunohistochemistry for proliferation

using image Cytometry is a promising tool for the evaluation of cancer prognosis and potential responses of tumors to therapy. By immunodetection of a protein (Ki67), the nuclei in proliferation can be stained in brown, and the non proliferating nuclei counterstained in blue. The objectives is to determine the volume fraction of brown nuclei. The color information is a deciding factor for extraction (segmentation) and characterization of objects of interest. We present a new method of image segmentation. This method is a three steps strategy which uses tools based on Partial Differential Equation (PDE), integrating the statistical information. The first step is a preprocessing by PDE, in order to filter out the noise, while enhancing contours. The second step is the initialization of the third step dedicated to localization by active contours. Initialization is achieved by a fuzzy classification of seeds obtained by mathematical morphology operators. For localization, we used the non-regularized model of geometric approaches implemented by fast marching methods. The fuzzy classification uses mainly the color information and brings an obvious enhancement in comparison with other segmentation strategies. The principle is the following : from a known number of classes and an initializing image of classes centroids, an iterative process assigns a membership degree of a class to each pixel until convergence criterion is reached. The binary image of objects is obtained by taking the maximum of each class. We illustrate the use of fuzzy classification on different examples of immunostained histological sections.

R035

STUDY OF THE TEXTURE OF CELLS IN SEROUS CYTOLOGY BY IMAGE ANALYSIS

Lezoray O. 1, Lecluse M. 2, Elie H. 2

1) LUSAC, EA 2607, IUT Saint-Lô, 120, rue de l'exode, 50000 SAINT -LO, France, 2) ANAPATH, CHLP, 46, Rue du Val de Saire, 50102 Cherbourg, France

To perform a classification of cells in cytological images, quantitative descriptors are needed to describe the cells extracted by a segmentation scheme. Usually, size, shape and textural features are used for the characterization of cells. We have studied textural features based on four different methods for texture characterization (statistical, watershed clustering, texton extraction, top-hat

method). For each of these methods, respectively 8,7,13 and 6 different features were designed to describe the texture of the cells [1]. The study was based on a pool of 2000 labeled cells from serous cytology ranging from normal to abnormal cells. To know if the computed features enable a good discrimination between normal and cancerous cells, all the pairs of combinations of one texture parameter with the area of the cells were analyzed and the most relevant parameters were retained. They allow the distinction of normal and abnormal populations in a range of 60% to 90% according to the relevant features used. To increase the distinction between the populations, two parameters were designed using combinations of the existing parameters in order to describe cytological malignancy criteria [2]. The former represents the size of the chromatin and parachromatin in the nuclei and the latter represents the same quantity versus the nucleus area. Pair combination of these parameters with the most relevant ones enables a better separation of the normal and abnormal populations (70% to 95%). These two last parameters might be useful to discriminate cells in an automatic system based on image analysis.

References :

- [1] O. Lezoray, "ARCTIC: a cellular sorting system", VI'98, pp 312-319, 1998
 [2] C. Rouselle & al, "Chromatin texture analysis in living cells", *The histological journal*, Vol 31, pp 63-70, 1999.

R036

REGULARIZED FUZZY C-MEAN: APPLICATION IN MEDICAL IMAGE SEGMENTATION

Coudrey T. 1, Schupp S. 1, Elmoataz A. 1, Herlin P. 2, Bloyet D. 1

- 1) GREYC-ISMRA, UPRES-A CNRS 6072, F - 14032 Caen cedex
- 2) Laboratoire d'Anatomie Pathologique, CRLCC François Baclesse – Caen

Image analysis is able to provide pathologists with stable and reproducible measuring methods. The critical step of image analysis is the segmentation step which leads to the extraction of objects of interest to be measured. Segmented objects are then characterized by many parameters for automatic cell sorting for example in cytopathology. In histopathology, it is the study of the relationships

between segmented objects (for example nuclei) which is able to characterize tissue architecture. The here presented segmentation method is based on the fuzzy set theory. It leads to a fully automatic pixels classification algorithm which decides the suitable number of clusters according to the selected parameters. The fuzzy image partitions are regularized thanks to a filtering procedure based on the partial derivative equations allowing to take into account the spatial constraints. This method finds applications in many domains. The results of the segmentation algorithm are illustrated mainly on two segmentation problems encountered on colour images, the detection of mitosis figures and the detection of immunostained nuclei.

S001

REFRACTIVE INDEX OF DIABETIC PATIENTS ERYTHROCYTES AT DIFFERENT PH LEVEL OF EMBEDDING MEDIUM

Mazarevica G., Freivalds T., Jurka A.

Institute of Clinical and Experimental
Medicine, Riga, Latvia

The aim: to characterize hemoglobin and red blood cells (RBC) membrane properties changes for diabetic patients.

The microscopic investigation was carried out for intact and fixed RBC. For refractive index (RI), measurements smears of peripheral blood were air-dried and fixed for 3 min in methanol. Mixtures of polyvinylpyrrolidone and buffer of different pH (1:1) were used as embedding media. Intact RBC were mixed with buffered embedding medium, put on a slide and overlaid with coverslip. An interference microscope was used for the RI measurements at 19 different pH (pH=2-13).

Resulted curves of the RI of diabetic patients and control group were of similar configuration having the branch in the acid part, a middle part with maximum and two minimums and the branch in the alkaline part of the pH scale. The curves of the individuals from the control group overlapped each other. On the contrary, the curves of the diabetic patients within the group showed distinct dispersion of their middle part and the alkaline branch. The middle part of the curves of the diabetic patients was shifted to the alkaline end of the pH scale and RBC RI curves are lower in comparison with the control curves: the central maximum of the curves of diabetic patients corresponded to pH=6,6 whereas the

central maximum of the control group curves was at pH =6.2-6.8. Contrary to diabetic patients intact RBC RI curves the control group's central part contains only one significantly different minimum at pH 7,2. Using this method, it is possible to show phenotypic differences between uniform type intact and fixed cells - erythrocytes in diabetic patients and in healthy donors.

S002

AUTOFLUORESCENCE-BASED CLASSIFICATION OF BACTERIA: A STUDY USING CONFOCAL LASER MICROSCOPY ON MICROCOLONIES

Lamfarraj. H. 1, Sockalingum. G.-D. 1, Pina. P. 2, Allouch. P. 2, Manfait. M. 1

1) Unité MÉDian, CNRS FRE 2141, IFR 53, UFR Pharmacie, 51 rue Cognacq Jay 51096 Reims Cedex, France, 2) Hôpital Mignot, CH de Versailles, 78157 Le Chesnay, France

In this study we have used confocal laser microspectrofluorometry in the UV (excitation wavelength = 360 nm) and visible (excitation wavelength = 457 nm) to acquire autofluorescence signals from bacterial microcolonies. Data have been collected from 6h, 12h and 24h old colonies of *E. coli* and *S. aureus* reference strains using two different culture media (Mueller- Hinton and Trypticase Soja agar) in order to standardise the method. Autofluorescence in the visible (emission wavelength = 528-545 nm) is mainly due to flavin molecules and staphyloxanthin (for *S. aureus*) and in the UV (emission wavelength = 445-466 nm) it originates from co-enzymes NADH or NADPH in their reduced form and also other pigments. Statistical methods combining discriminant analysis and principal components analysis (PCA) have been applied to the data set for classification of the spectra. Results show that for 6-12h cultures on MH there was a good separation between *E. coli* and *S. aureus* when excited in the visible. By using spectral imaging we also found some biological heterogeneity at the level of a single microcolony and spectra could be separated into three groups: centre, intermediate and periphery. A study on clinically-relevant strains is on-going.

S003

SPECTRAL IMAGING AND HSD-ANALYSIS OF CO-LOCALIZING CHROMOGENIC DYES IN IMMUNOSTAINED SPECIMENS

Van Der Laak J. 1, Macville M. 1, Kerstens H. 1, Katzir N. 2, Pahlplatz M. 1, De Wilde P. 1, Hanselaar A. 1

1) Department of Pathology, University Medical Center St. Radboud, Nijmegen, The Netherlands, 2) Applied Spectral Imaging, Migdal Ha'Emek, Israel.

For analysis of single- and double-immunostaining signals in transmitted light microscopy, we compared the HSD color model with Fourier-transform spectral imaging (SpectraCube). Spectral imaging is used extensively for spectral karyotyping analysis in fluorescence microscopy, and makes use of full spectral information. The HSD model is based on images acquired by a 3-CCD RGB camera, and thus uses only limited spectral information. Expectedly, the availability of full spectral information will favor the use of spectral imaging for multicolor analysis. A number of different combinations of enzyme precipitates, with and without counterstain, was used to study the potential of both techniques.

Recognition of a single stain was possible with both methods. A single immuno-signal and a counterstain could be discriminated for almost all combinations of stains by both techniques. When the spectra of immuno-signal and counterstain showed a high degree of resemblance (e.g. Fast Red and Nuclear Red), both spectral imaging and HSD analysis misclassified a large number of pixels. Immuno-double staining of co-localizing antigens expressed in the same cellular compartment could be discriminated under certain staining conditions by spectral imaging, and to a lesser degree by HSD analysis. Overstaining and variability in staining quality hampered recognition by both techniques to a large degree, underlining the need for quality assurance in the laboratory.

We conclude that with these new techniques, automated assessment of expression patterns of molecular markers in tissue sections and cytology is feasible. Future research will concentrate on object recognition based on pixel classifications defined in this study. Subsequently, we may conclude whether full spectral information is needed for accurate object recognition and quantification of expression patterns, or that a 3-CCD RGB camera suffices.

S004**BUILDING OF A MICROSCOPICAL IMAGE ACQUISITION DEVICE DEDICATED TO CLINICAL ONCOLOGY**

Thuillier J. 1, Plancoulaine B. 2, Lezoray O. 3, Herlin P. 1, Bloyet D. 3

1) Centre François Baclesse – Caen, France, 2) Institut Universitaire de Technologie, département de Mesures Physiques – Caen, France, 3) GREYC - ISMRA, UPRES-A CNRS 6072, 6 boulevard Maréchal Juin, 14050 Caen cedex, France, 1-3) Pôle Traitement et Analyse d'Images de Basse-Normandie

To improve the reliability of tumor prognosis evaluation, quantitative analysis of structures on histological sections must report the global behaviour of the frequently heterogeneous tumor. More often, the subjective choice of a Region Of Interest (ROI) to be measured is responsible for the poor reproducibility of the results obtained from a team to another. Furthermore, because of the current computer tool limitation in terms of speed and available memory, it is difficult to work on the whole histological section at any microscope magnification. In this context, we developed a software based on the combination of a microscope (Olympus) and a moving stage (Märzhaüser) with a high-resolution slide scanner (Polaroid). After an interactive overlay drawing of the ROI on the scanner image of the whole histological section, the tool drives the stage onto the selected area and grabs the corresponding fields. An autofocus algorithm is used to produce uniformly focused fields during the stage movement. Then, thanks to the chaining of image processing operators (ADCIS), the programme creates the resulting mosaic image. This last operation consists in the image assembly, but includes also correction of luminosity and overlapping of the neighbouring images.

This tool is first dedicated to the quantification of structures on histological sections (such as counting of blood vessel sections) but it can also be introduced in telepathology as an easy to use remote microscope control system.

This work was supported by grants from the “Comité Régional pour l'Image et les Technologies de l'Information et de la Communication”.

S005**UNIQUE CAPABILITIES OF LASER SCANNING CYTOMETRY (LSC) THAT COMPLEMENT FLOW CYTOMETRY (FC)**

Bedner E. 1, Smolewski P. 2, Darzynkiewicz Z. 2

1) Department of Pathology, Pomeranian Medical University, Szczecin, Poland, 2) Brander Cancer Research Institute, New York Medical College, Valhalla, NY, USA

There are limitations of FC for some applications inherent to the fact that cells are measured in flow. The LSC combines advantages of FC and image analysis and therefore may be used in these applications. The following capabilities of LSC make this instrument useful for the applications in which FC cannot be used: (a) the cells located on slides may be measured repeatedly and time is one of the recorded parameters. Kinetic curves constructed for individual cells can be matched with the respective cells classified by their position on the slide, fluorescence intensity, or image by light microscopy; (b) analysis of the same cell populations can be carried out sequentially using immuno-, or cytogenetic probes. Following the data merge, a correlation between cell immunophenotype, functional parameter, expression of particular protein, DNA ploidy, cell cycle position, and/or cytogenetic profile can be analyzed; (c) the measured cell can be relocated and examined by fluorescence or light microscopy. This capability is of special value when cell morphology is required to positively identify the measured cell; (d) cell loss during specimen preparation and staining is minimal and therefore the samples with too few cells to be measured by FC can be analyzed by LSC; (e) tissue sections can be analyzed by LSC; (f) the specimens analyzed by LSC can be stored for archival preservation or further studies using new probes; (g) LSC allows for morphometric analysis of fluorescence distribution within the cells or cell aggregates (colonies). This capability of LSC has been already utilized in FISH analysis, to identify apoptotic cells, to distinguish mitotic from interphase cells, to measure translocation of Bax from cytosol to mitochondria, activation of NF- κ B, for multiparameter analysis of phenotype of a progeny of individual cells (cell clones) and in the micronuclei assay.

S006
REFLECTION CONTRAST MICROSCOPY
USED FOR MORPHOMETRY

Ploem J.S.

Leiden University, The Netherlands

With reflection contrast microscopy (RCM) of thin tissue sections (embedded in resins) optimal light microscopic images can be obtained for morphometry. RCM meets all requirements for high definition microscopy (HDM): (1) high lateral resolution, (2) high vertical resolution (no interference of pre- and postfocal images with the image obtained from the layer in focus, when objectives of high NA are used), and (3) high contrast between cytochemical stains, counterstains and the image background. Routine transmitted-light microscopy generally does not meet HDM criteria. Most routine biomedical specimens give rise to pre- and post focal images because of their (required) thickness (2-3 micron) needed for sufficient colour (absorption) contrast. In routine fluorescence microscopy the image contrast is often better than with transmitted-light microscopy. It is, however, not optimal for morphometry since interference by pre-focal and post-focal images with the main image may occur. Only confocal scanning fluorescence microscopy avoids such interference. The efficiency of morphometrical procedures is enhanced by the possibility to obtain precise thresholding (segmentation in a binary image) of only cytochemically stained cellular structures. The surprisingly large image contrast obtained with reflection contrast microscopy between immunostained cellular structures, counterstained tissue elements and background enables stable thresholding of the signal.

T001
SKY ANALYSIS OF CHROMOSOMAL
ABNORMALITIES IN 10 COLON CANCER
CELL LINES REVEALS COMPLEX,
IMBALANCED ABERRATIONS BUT NO
RECURRENT TRANSLOCATIONS

Hermesen M. 1, Alonso Guervòs M. 1, Tänzer S. 2, Baak J. 1, Meijer G. 1, Schröck E. 2

1) Dept. Pathology, Free University Hospital, Amsterdam, The Netherlands, 2) Institut für Molekulare Biotechnologie, Jena, Germany.

Chromosomal instability is the most important type of genetic instability in sporadic colon cancer. In a previous study using CGH, we found recurrent chromosomal imbalances in colorectal carcinomas, the most frequent being losses on chromosome arms 8p, 17p and 18q, and gains on 8q, 13q and 20q. These imbalances must be related to structural chromosomal changes, however, hardly anything is known about chromosomal translocations in these tumors. Recently, Spectral Karyotyping (SKY) has been developed using 24 chromosome specific probes that are combinatorially labeled with 5 different fluorochromes. Thus, all chromosomes are visualized with distinct fluorescent colors and are automatically classified, based on their characteristic spectra. We studied 10 colon carcinoma cell lines in order to better understand the role of chromosomal translocations and imbalances in colon cancer.

We found an average number of 12 rearrangements (range 3-31) in these cell lines. All types of balanced and unbalanced aberrations were found: isochromosomes and whole arm translocations (which have the breakpoints within the centromere), translocations of small genomic regions, deletions, duplications, inversions and insertions. The majority consisted in complex, non-centromeric and imbalanced translocations. Interestingly, no recurrent translocations were found, as characteristic for hematological and mesenchymal tumors. This supports the idea that the possible biological role of reciprocal translocations in colon cancer is not the formation of fusion protein products, but perhaps rather gene inactivation and altered gene expression. A number of specific chromosome regions was frequently involved: 1q, 3cen, 3q, 5p, 6q, 7q, 8p, 9p, 12q, 13cen, 15q, 19p. Some of these genomic regions were not previously known to be involved in colon cancer. We will continue our SKY analyses studying fresh, primary colon tumors, in order to obtain more clinically relevant information.

T002
CHROMOSOMAL IMBALANCES IN BREAST
CARCINOMA

Farabegoli F. 1, Hermesen MAJA. 2, Ceccarelli C. 3, Santini D. 3, Weiss M.M. 2, Meijer GA. 2, Van Diest P.J. 2

1) Dept. Experimental Pathology of the University of Bologna, Italy, 2) Dept. Pathology, Free University Hospital, Amsterdam, The Netherlands, 3) Institute

of Anatomic and Histologic Pathology of the University of Bologna, Italy

We have investigated 47 primary breast carcinoma samples by Comparative Genomic Hybridization (CGH) in order to detect chromosomal imbalances involved in breast cancer development and progression. Forty-three samples were Invasive Ductal Carcinoma, 3 were Invasive Lobular Carcinoma and 1 was a Mucinous carcinoma. Lymph-node invasion was found in 31 samples.

Chromosomal imbalances were detected in all but one samples to a different extent. High incidence of DNA gains was found at chromosome 1q (79%), 8q (72%), 3q (38%), 5q (36%), 17q (30%). Consistent gains (greater than 20%) were also found at chromosome 2p, 3p, 4q, 5p, 6q, 7q, 8p, 9p, 11p, 12q, 12p, 13q, 14q, 16p, 18q, Xq. The most frequent DNA loss was found at 17p (72%), followed by 16q (59.5%) and 1p (53%). DNA losses greater than 20% were also found at chromosome 8p, 11q and 17q.

The present results are in agreement with data already published by using CGH. In contrast with other reports, we found DNA gains at chromosome regions not often found to be affected in breast carcinoma: 9p, 12q, 12p and 13q. Since breast carcinoma is a very heterogeneous disease, the detection of these abnormalities might be important in disclosing additional chromosome regions harbouring genes critical for breast cancer development in a subset of patients.

F. Farabegoli was recipient of a short-term EMBO fellowship (ASTF 9620)

U001

LASER MICROBEAM MICRODISSECTION AND LASER PRESSURE CATAPULTING: THE FORCE OF FOCUSED LIGHT IN DIFFERENT AREAS OF MEDICINE AND BIOLOGY

Burgemeister R. 1, Hitzler H. 1, Clement-Sengewald A. 2, Friedemann G. 1, Schütze K. 1

1) P.A.L.M. MicroLaser Technologies, Bernried, Germany, 2) Women's hospital of the Ludwig-Maximilians, University Munich, Germany

Laser micromanipulation systems are the state of the art technologies for non-contact manipulations of single cells or small cell areas. Recent advances in molecular methods to analyze genes and their transcripts asked for the development of technologies

to extract specimen of morphologically defined origin for subsequent genetic or proteomic analysis without any contamination. It is very important to procure wanted cells from unwanted bystander cells to obtain pure preparations. Therefore, the combined micropreparation techniques of Laser Microbeam Microdissection (LMM) and Laser Pressure Catapulting (LPC) increasingly gain importance in a wide field of molecular medicine and biology. With LPC, the selected specimen are ejected from the object plane with the only force of light and are directly catapulted into the cap of a common microfuge tube. Subsequent molecular genetical examinations can be carried out after centrifugation of the catapulted material into the bottom of the PCR tube. Any kind of tissue from different sources (also archival samples) and even subcellular structures can be captured using this laser method. Wherever precise optical micromanipulation is required or where the procurement of homogenous samples is mandatory for the subsequent analysis of cell or chromosome specific genetic alterations, the P.A.L.M. MicroLaser system is a key technology. LMM and LPC are the state of the art tool for quick and pure sample preparation for a variety of applications.

U002

MOLECULAR DIAGNOSTICS OF CANCER DISPOSITION IN ADENOMAS OF HNPCC PATIENTS THE IMPORTANCE OF LASER-MICRODISSECTION

Renke B. 1, Giuffre G. 2, Richter C. 1, Heinmöller E. 1, Tuccari G. 2, Rüschoff J. 1

Institutes of Pathology, 1) Klinikum Kassel, Germany, 2) University of Messina, Italy

Whereas almost 90% of hereditary non-polyposis colorectal cancers (HNPCC) are characterized by instabilities in simple repetitive sequences (microsatellite instability, MSI) current data show much lower frequencies of MSI in HNPCC related adenomas. We hypothesized that the lower detection rate of MSI in adenomas reflects not only the degree of dysplasia (Iino et al. Gut 2000); it might also be influenced by the manner of tissue sampling.

We studied 11 HNPCC associated adenomas from the same number of patients according to the degree of dysplasia (D1-D3). Various areas of the same lesion were harvested by laser-microdissection

(PALM) and PCR was performed using the MSI markers recommended by NIH (Boland et al. 1998). MSI status was defined as high (MSI-H), low (MSI-L) and stable (MSS).

When tissue sections of the whole adenoma were analysed only 6 of 11 cases were MSI-H, 2 were MSI-L and 3 MSS. In contrast MSI was found in all cases when laser microdissection was used for sampling. All but one case were classified MSI-H, the remaining was MSI-L. BAT40 showed instability in all cases. Although there was a tendency towards higher MSI rates in high grade dysplasia laser microdissection revealed instabilities in all lesions with low grade dysplasia at least at one marker.

Thus, MSI is an early event in HNPCC adenomas that is easily underdiagnosed if whole tissue sections are analysed. We therefore recommend that MSI testing in adenomas should be performed by using laser-microdissection.

U003

PITFALLS IN DIAGNOSTIC MOLECULAR PATHOLOGY. SIGNIFICANCE OF SAMPLING ERROR

Heinmöller E. 1, Renke B. 1, Beyser K. 1, Dietmaier W. 2, Rüschoff J. 1

Institutes of Pathology, 1) Klinikum Kassel, and 2) University of Regensburg, Germany

Today, polymerase chain reaction (PCR) based techniques are routinely used in molecular diagnostic tests in clinical medicine. In tissue specimens, however, false positive and false negative results can be obtained if pathomorphological and processing aspects are not considered.

We therefore studied the impact of tissue sampling in two widely-used diagnostic tests: Assessment of clonality in B-cell non-Hodgkin's lymphoma and demonstration of tuberculosis hominis species. Tissue sections of routinely formalin-fixed and paraffin-embedded diagnostic specimens were taken and the significance of sampling was systematically investigated by laser-microdissection or by processing the entire section. PCR analyses were done according to standard protocols.

False positive pseudo-monoclonality was obtained in small gastrointestinal biopsies as well as in laser microdissected lymph follicles of non-neoplastic tonsils. False negative results could be demonstrated in a case with tuberculosis where a fresh frozen lymph-node specimen gave a clearly positive result.

In formalin fixed material, however, PCR was negative if only few tissue sections were analyzed.

In molecular pathology, sampling error is an important source of false positive and false negative diagnosis particularly if disease and tissue specific morphological features such as sample size, type of fixation and intralesional heterogeneity are ignored.

U004

MOLECULAR GENETIC ANALYSES IN LASER MICRODISSECTED SINGLE OR FEW CELL SAMPLES. APPLICATIONS AND PITFALLS

Rüschoff J. 1, Renke B.1, Sommer S. S.2, Heinmöller E.1

Institute of Pathology, 1) Klinikum Kassel, Germany and 2) Cancer Center, City of Hope, Duarte, USA

Laser microdissection has opened an avenue to precise molecular analysis of histologically defined subcompartments of normal or diseased tissues. This directly enables insights into the molecular basis of dynamic processes such as carcinogenesis. Thereby, PCR-based whole genome amplification (WGA) prior to specific PCR enable multiple genetic analyses from sample sizes as low as a single cell. We have developed a technique of tissue fixation using ethanol and EDTA which allows immunohistochemical staining of two proteins (p53 and PCNA) simultaneously. From these tissues, single positive stained cells can be investigated for TP53 mutations. In addition, we have optimised WGA to enable successful multiple molecular genetic analyses of more than 50% of single cells dissected. However, allele drop out (ADO) is an important pitfall in the molecular analysis of templates consisting of 10 cells or less if the presence of a heterozygote sequence change or loss of heterozygosity (LOH) is of diagnostic interest. In our experiments, we found ADO-rates up to 78% when single cells prone to oxidative damage were analysed for heterozygote base changes. In formalin fixed tissue samples from pancreatic cancer or preneoplastic duct changes we demonstrate multiple molecular genetic analyses in genes like *p16INK4*, *TP53* and *DPC4* using WGA prior to specific multiplex PCR. From one microdissected sample, we demonstrate analysis of LOH and genomic sequence analysis of particular genes simultaneously. This approach will greatly facilitate future studies of early changes or progression in neoplastic disease.

V001
SOCIOLOGIC BEHAVIOR OF NON INVASIVE AND INVASIVE BRONCHIAL EPITHELIAL CELLS

Zahm J.M., Matos M., Raby B., Polette M., Birembaut P., Bonnet N.
 Inserm U514, Université de Reims, 45 rue Cognacq-Jay 51092 Reims, France

Tumor invasion is in part related to alterations of the cellular cohesiveness which can be studied through the analysis of the cell to cell behavior. We have developed a model of cellular cohesion, allowing the in vitro study of the spatial and temporal distribution of two human bronchial cell lines characterized by a different invasive capacity. Using a software developed in our laboratory, different models, based upon a graphical representation, describe the neighborhood of a cell population. The cell lines were plated at 40000 cells/cm² density. Videorecordings, performed twice a day until the cells reached confluency, allowed to analyze the variation of the cell spatial distribution versus time. The graphical representation of the cell behavior showed that the non-invasive 16HBE14o- cell line rapidly formed clusters with a cohesive organization, whereas the invasive BZR cells remained isolated each other and were characterized by a non cohesive organization. By using videomicroscopic and image analysis techniques, we quantified the cell migration speed and the proliferation rate of the cells. The results obtained from these experiments suggest that the migration speed and the proliferation rate are likely not to be involved in the different spatial organization of the cell lines. However, an evident relationship exists between the sociologic behavior of the cell lines and their invasiveness. The in vitro model of cellular cohesion, associated to the image analysis techniques that we have developed, would be useful to evaluate the aggressive capacity of tumor cells in relation with the clinical diagnostic of patients with cancer.

V002
A NEW APPROACH USING VIDEOMICROFLUOROMETRY AND DISCRIMINANT FACTORIAL ANALYSIS FOR CCRF-CEM LYMPHOBLASTOID CELL CYCLE STUDIES. APPLICATION TO DRUG EFFECTS INVESTIGATIONS

Savatier J., Rocchi E., Salmon J.M.

UPRES 1947 : Biologie Physico-Chimique des Systèmes Intégrés, Université de Perpignan, 66860 Perpignan cedex, France

Single living cells are labelled with three fluorescent markers : Hoechst 342 for nuclear DNA, Rhodamine 123 for mitochondria and Nile Red for plasma membrane. Numerical image analysis allow us to obtain, for each cell, morphological parameters (cell and nuclear sizes, nucleo-cytoplasmic ratio, shape factor) and functional information by fluorescence intensity (nuclear DNA content, level of mitochondria energetic state, amount and properties of plasma membrane) with total value, mean and standard error. These parameters are used in a typological analysis (dendrogram method) which separates control cells into three groups. A discriminant factorial analysis confirms these groups : G1, S and G2/M, and indicates which parameters levels are associated with and the cell probability to belong to each one. These control cells define a learning population. The populations of treated cells (with several concentrations of two laxaphycins and adriamycin) are analysed as supplementary individuals in a discriminant factorial analysis using control cells as learning population. They are classified into G1, S and G2/M groups. A new discriminant factorial analysis with the only treated cells confirm this classification, with an error lower than 5%. Furthermore, such an approach allows to accurately evidence the changes of some cellular parameters values.

W001
DIFFERENTIAL GENE EXPRESSION IN HUMAN MESOTHELIOMA CELLS USING ARRAYS TECHNOLOGIES

Mohr S., Rihn B.H.

Institut National de Recherche et de Sécurité (INRS), P.O. Box 27, 54501 Vandoeuvre, France.

Although asbestos has been banned in most industrialized countries, it is still a major public health concern. Asbestos fibers are considered as mutagenic and carcinogenic for humans. In France, asbestos is thought to be responsible each year for many pulmonary diseases : pleural plaques, bronchogenic carcinomas and mesotheliomas (malignant tumor of pleura). In order to better understand the transformation process of pleural cells, we compared the gene expression of

mesothelium cells (Met-5A) and mesothelioma cells (MSTO-211H). Using high-density filter array and cDNA microarray, we assessed expression levels of more than 6,500 genes. Data analysis with Gemtools 2.4 software allows a hierarchical classification of genes of known functions by enzyme, function and pathway clusters and leads to characterize both malignant and normal phenotypes. Interestingly, of the fewer than 300 genes that differed between cell lines, most functioned in i) macromolecule stability, ii) cell adhesion and recognition, iii) cell migration (invasiveness), iv) vascular switch and v) extended cell division. Expression levels of several genes were confirmed by quantitative RT-PCR and in situ hybridization. This study provides new markers of mesothelioma and mesothelial cells, useful for diagnostic, prognostic, therapeutic that could now be tested on clinical specimens.

W002
MICROARRAY COMPARATIVE GENOMIC
HYBRIDIZATION REVEALS A NARROW
GAIN AT 20Q13 IN HUMAN GASTRIC
CARCINOMAS

Weiss M.M., Snijders A.M., Albertson D., Pinkel D., Meijer G.A., Meuwissen S.G.M., Baak J.P.A., Kuipers E.J.

Depts. of Gastroenterology and Pathology, Free University Hospital, Amsterdam, The Netherlands, UCSF Cancer Center, San Francisco, California, USA.

As detected by comparative genomic hybridization (CGH), gains of chromosome 13 and 20 are frequent aberrations in gastric carcinomas (Van Grieken, J. Pathol, 2000). In order to investigate these chromosomes with a higher resolution and sensitivity, we performed microarray CGH in a series of 26 gastric cancers. As targets, 57 clones on chromosome 13, 23 clones on chromosome 20, and 52 clones randomly dispersed throughout the genome, were used. The integrated tumor to reference fluorescence ratio was calculated per spot. Thresholds of 0.8 and 1.2 were used for losses and gains, respectively. To confirm the microarray CGH data, FISH has been performed on selected cases for 11q13 and 20q13.

Microarray CGH results were technically of high standard. The technique indeed showed a higher sensitivity, by detecting (high-level) gains that had gone undetected by chromosome CGH. Gains on

chromosome 20q were detected in 10 out of 26 cases (38%). Of these 10 cases, 7 showed a whole chromosome arm gain and 3 showed a gain restricted to 20q13. No region-specific gains were detected at 13q, which probably indicates that only whole arm aberrations occur at this chromosome in gastric cancer. (High-level) gains on 11q13 were detected in 7 out of 26 cases (27%). Immunohistochemically overexpression of cyclin D1 was seen in 3 of 7 cases. These 3 cases indeed showed the highest microarray CGH ratios. In general, the microarray CGH data correlated well with conventional CGH, as well as with the FISH data.

W003
CGH-MATRIX ARRAY: HIGH RESOLUTION
APPROACH FOR DETECTION OF
CHROMOSOMAL ABNORMALITIES IN
BREAST CARCINOMA

Aubele M. 1, Smida J. 2, Zitzelsberger H. 3, Höfler H. 1,2, Werner M. 2

1) Institute of Pathology, GSF-Research Center for Environment and Health, Neuherberg, Germany, 2) Institute of Pathology, Technische Universität München, Germany, 3) Institute of Radiobiology, Ludwig Maximilians Universität, München, Germany

Aims: Chromosomal CGH has been broadly applied to identify chromosomal gains and losses in breast cancer. The limited resolution of events -involving regions of about 10 to 20 Mb of the genome- can be overcome using an array of mapped sequences instead of metaphase chromosomes.

Methods: Chromosomal regions relevant in progression of breast carcinoma have been already identified by chromosomal CGH. In order to narrow these regions of interest, we established the CGH-Matrix array technique for detailed determination of imbalances. A microarray using STS-mapped YAC clones was constructed achieving more than double coverage of the entire regions of interest. Each of the YAC clones has been verified by FISH hybridisation on normal metaphases. Differentially labelled total genomic DNA from 'normal' and formalin fixed, paraffin-embedded (FFPE) tumour tissue probes, n=10) are cohybridized to the CGH-Matrix array.

Results: So far more than 500 YAC clones were identified to match to the regions of interest and were spotted onto slides. About 400 STS-mapped YAC's (Whitehead Contigs) spanning the region from 2 to

47 cM match the region 3p14- p24, which was frequently found amplified by chromosomal CGH. DNA gain in tumorous DNA samples was found for about 30 of these YAC's, spanning a region from 30 to 36 cM.

Conclusions: We demonstrate the ability of CGH-Matrix arrays to measure DNA copy number changes with high precision in the human genome, and to analyse routine FFPE tissue samples by obtaining new information on chromosomes.

X001

EVALUATION OF IMMUNOHISTOCHEMICAL SCORING SYSTEMS IN COLORECTAL CARCINOMAS: ASSOCIATION WITH TUMOUR STAGE AND PATIENT SURVIVAL

Elkablawy M.A., Maxwell P., Williamson K., Anderson N., Hamilton P.W.

Quantitative Biomarker Group, Department of Pathology, Cancer Research Centre, Queen's University of Belfast, UK.

Several methods have been proposed to assess immunohistochemistry (IHC) staining scores. Our aim was to evaluate the effect scoring systems have on the interpretation of apoptotic and cell cycle proteins and their prognostic value in colorectal carcinoma. In a series of 52 colorectal carcinomas, immunolocalization of p53, p21 and bcl-2 was carried out using six IHC scoring protocols, firstly by semi-quantitative scoring system of stained tumour cell percentage score multiplied by staining intensity score, and secondly by quickly estimating threshold values of 10%, 20%, 25%, 50% and median of stained tumour cell percentage. Immunoreactivity of the proteins showed variability between scoring protocols. No significant difference was detected between the 10% and 20% scoring results for all assessed parameters. p21 associations with other parameters in the study were correlated in the 10%, 20%, 50% and the semi-quantitative scoring methods. Similarly, bcl-2 associations with other parameters showed high correlation between the 50% and the semi-quantitative scoring methods and between the 25% and the median scoring methods. p53 associations were highly correlated between the 25% and the median scoring methods. Bcl-2 overexpression was associated with more favourable patient survival using the semi-quantitative and the 50% scoring methods in univariate analysis ($p < 0.03$)

and multivariate Cox survival analysis ($p < 0.016$). In conclusion, the methods of evaluation can affect the interpretation of protein expression level with false positives influencing the significance of results. The quick 50% scoring method could be used instead of the semi-quantitative scoring method in predicting patient survival in colorectal carcinoma.

X002

INTEGRATED USE OF QUALITY CONTROL FEATURES IN INDIVIDUAL DNA IMAGE CYTOMETRY MEASUREMENTS

Haroske G. 1, Meyer W. 2, Giroud F. 3, Oberholzer M. 4, Böcking A. 5

1) Dresden-Friedrichstadt General Hospital, Institute of Pathology, Germany, 2) Dresden University of Technology, Institute of Pathology, Germany, 3) Université Joseph Fourier - Grenoble, Laboratoire RFMQ TIMC-IMAG, France, 4) University of Basle, Institute of Pathology, Switzerland, 5) Heinrich-Heine-University Düsseldorf, Institute of Cytopathology, Germany

The biological information desired from DNA image cytometry measurements in clinical specimens is folded by "artificial" influences from preparation and the technology of measurements. Quality control tools have been developed to separate some of those influences from the biological information. Although their use seems to be easy, the interpretation of an individual DNA measurement in terms of artefacts and biological effects can be very difficult.

In some thousand clinical DNA cytometric measurements from different sources, the effects of optical limitations of the cytometry devices as well as of sampling in correlation with the diagnostic or prognostic implications were studied by means of a standardized application of quality control tools provided by the EUROQUANT server.

With highly precise and stable measurements, the diagnostic conclusions can be reliably drawn. The lower the quality of a measurement in one or several quality-sensitive variables is, the more complicated is its interpretation, and the lower is its reproducibility. The results show the comparatively high complexity of quality control and diagnostic interpretation.

X003**INFLUENCE OF DIGITISING CONDITIONS ON IMAGE ANALYSIS MORPHOMETRIC PARAMETERS**

Boudry C. 1, P. Herlin P. 2

1) URFIST/Ecole nationale des chartes. Paris, 2) Laboratoire d'Anatomie Pathologique. Centre de Lutte contre le Cancer F. Baclesse Caen France, Pôle Traitement et Analyse d'Images de Basse Normandie

Acquisition conditions can affect to a large extent numerical image quality. Their possible effects on image analysis measurements are numerous and more often under-estimated. The aim of the present study is to assess variations of individual morphometric parameters classically used for cell sorting (area, perimeter, compactness, elongation and circularity) as a result of digitising conditions: position of objects under the sensor and resolution.

For this purpose, eight synthetic objects were drawn on a computer and printed (approximately same area) in order to mimic digitised cell nuclei of various shapes.

In the first experiment, the resolution was arbitrary chosen to get 1000 pixels per object. Five acquisitions were successively done using a flat scanner (HP Scanjet 4100c) while changing the object position. The variation of the measures obtained appeared to be highly dependent on the measured parameter. This variation can reach 15 % (for compactness) while ranging from 5 to 10 % for the other parameters.

In the second experiment, the same objects were digitised at various resolutions: from 4 to 93000 pixels (average values). As expected, variations obtained increase when the number of pixels per object decreases but, amazingly, a relative stability of parameters is only reached for approximately 4000 pixels per objects. One must notice that significant individual variations can still be observed for objects of 9300 pixels.

Similar experimentation is in progress in the laboratory for the measurement of parameters on cell nuclei at a microscopical level.

X004**HOW THE GLARE CORRECTION FACTOR CAN CONCRETELY BE ESTIMATED ?**

Hubler M., Oberholzer M.

Department of Pathology of the University, Schoenbeinstrasse 40, CH-4003 Basel, Suisse

Aim: The correction of the Glare-effect belongs to the quality signs of a DNA-cytometric measurement. An adequate surveillance of this correction is requested by the European Society of Analytical Cellular Pathology (ESACP). It is not easy to decide which value is important for the correction factor because exact criteria for this decision are missing.

Design: For an empiric definition of exact criteria, a model was chosen in which the different methodical parameters on the results were kept as constant as possible. Transmission, integrated optical density (IOD), area (A) and different texture parameters of 90-96 carbon particles, 32 2c-hepatocytes, 33 4c hepatocytes and 239 lymphocytes have been measured. In all four groups, the Pearson-correlation coefficients of the relation $IOD = f(A)$ (r) have been calculated. For the calculations, six different factors have been used for the Glare-correction (0%, 2%, 4%, 6% 8% and 10%).

Results: The lowest value for transmission is in the collective lymphocytes 2.78, in the collective hepatocytes 2.70 and in the collective charcoal particles 2.23. The absolute value of r shows in the collective lymphocytes the lowest value at a correction factor of 4%, in the collective 2c-hepatocytes at a correction factor of 8% and in the collective 4c-hepatocytes at 6%.

Conclusion: The correction factor of the Glare effect should be defined per every new collective. For this purpose, r should be empirically estimated in the frame of a pilot calculation with respectively systematically defined correction factors. The correction factor is correct when the smallest value of r results. On the background of the study, the control of the Glare correction by the server EUROQUANT has proven to be very justified.

X005**MOLECULAR PATHOLOGY TECHNIQUES IN CLINICAL VIROLOGY**

Savillo I.T.

Fisheries and Marine Sciences Division, Iloilo State College of Fisheries, Barotac, Nuevo, Iloilo, Philippines

Pathogenic viruses are not given much importance especially on their identification in most of the microbiology laboratories of third world countries. This paper will not only provide means of identifying pathogenic viruses using a series of molecular

protocols but also serve as an eye opener for enthusiasts in this area. The techniques will run from specimen accessioning to sample processing to lymphocyte preparation and subsequent DNA extraction, purification and isolation to standard preparation of PCR reagents and PCR set ups. This will also include discussion on the proper ways of radioactive labeling of the viral DNA probes, dot blot hybridization techniques, membrane washing conditions, autoradiography and result interpretation. Agarose gel electrophoresis and Southern blot methods of PCR products will be discussed as alternative ways. To work out all these procedures there is a need of a standard laboratory plan which will facilitate easy flow in the identification process. This will be undertaken together with the introduction of work sheets for PCR runs and DNA labeling, as well as half –life calculation of the radioactive DNA probes. Having to work with radioactive isotopes, it is a requirement to understand the proper radioactive monitoring and disposal thus there is a need to undergo rigorous training.

Y001

TELEPATHOLOGY EXPERIMENT MANAGEMENT USING DYNAMIC WEB TECHNOLOGY

Tucker J.H. 1, Spatz A.J. 2

1) Dept. of Pathology, University of Edinburgh, medical School, Teviot Place, Edinburgh EH8 9AG. UK, 2) Dept. de Pathologie, Institut Gustave-Roussy, 39 rue Camille-Desmoulins, Villejuif Cedex, France.

One of the major problems in carrying out web-based telepathology experiments such as the Melanocytic Lesion Protocol experiment is that of information distribution, data collection and management. Previous reports described the value of using the www as the major information transfer tool for such purposes. However the tasks of web site maintenance, manual transposition of data prior to analysis, and the analysis of the data, proved unmanageable in all but the smallest of experiments when using conventional static web page generation techniques. The use of dynamic www techniques was therefore investigated as a way of overcoming this problem.

The system consists of three units:

- a web site constructed with the Allaire "Cold Fusion" dynamic web page system,
- an experiment data base (Microsoft Access),

-an image web server.

The system is designed to work in conjunction with (but separately from) a commercial static-image telepathology system (Samba Technology TPS). The Cold Fusion site, apart from a general (static) set of introduction, protocol management, results and indexed link pages, contains dynamic template pages which use SQL queries to the database. These pages are arranged to provide data and service requests for each individual stage of the experiment. Where necessary, images are displayed using filenames generated from information extracted from the data base. The Access data base is therefore automatically updated by the contributors as the experiment progresses. The system has now accumulated over several thousand records over a period of one year, and has proved easy and rapid to use.

Y002

MULTIMEDIA COURSEWARE COMBINED WITH A KNOWLEDGE BASED DIAGNOSTIC SYSTEM: "EFFUSION CYTOLOGY INCLUDING ADJUVANT METHODS" ON CD

Böcking A., Motherby H., Kinzel P.

Institute of Cytopathology, Heinrich-Heine-University, Moorenstr. 5, D-40225 Düsseldorf, Germany

Aims: To develop a new type of didactic tool as a combination of computer based teaching and learning multimedia software with a knowledge based diagnostic system in cytopathology of effusions.

Methods: Using various types of commercially available software packages, the tool was developed to run from CD (on PC or Mac).

Results: The software encyclopedically contains all media for higher education in "Effusion Cytology Including Adjuvant Methods" (images, texts, graphs, histograms, tables, references) in a networked fashion. The teaching material is based on >200 screens of multimedia-(hyper-)text concerning 93 different diagnoses and >1500 high-resolution microscopic color-images at different magnifications and stainings, which are described in an intelligent database. They may also be used to perform diagnostic courses without using a microscope. The database can be searched using various diagnostic aspects of images for virtual online expertise in daily routine to solve problematical cases including full text recherche and multiple hyperlinks. Pairs of images of any diagnosis, magnification and staining

can be compared on the same monitor at two different sizes. The software uses the knowledge-database to create an almost infinite number of open multimedia questions to convey examinations. The software is also designed to be used as a tool to develop further CBT-titles by other IAP-authors. Even non-computer-experts can easily implement their knowledge and images.

Conclusions: First practical experiences comparing conventional slide-based and new type multimedia courses have been made on an IAP-Tutorial on "Cytopathology of Effusions Including Adjuvant Methods", November 2000 in Bonn.

Y003

TELEPATHOLOGY - DESIGN OF A MODULAR SYSTEM

Brauchli K., Christen H., Meyer P., Haroske G., Meyer W., Kunze K.D., Otto R., Oberholzer M.
Department of Pathology of the University of Basel, Schoenbeinstrasse 40, CH-4003 Basel, Switzerland

Telepathology systems are still not a widespread tool for routine diagnostic applications. Lacking interoperability, software that is not satisfying user needs as well as high costs have been identified as reasons. With a clear separation of the tasks required for a telepathology application, telepathology systems can be built in a modular and user friendly way, where many modules can be implemented using standard software components. In 1996 we replaced our first system (#1, 1992) by a new one (#2) based on Microsoft NetMeeting. Data and images are stored in a self designable FileMaker database. Recent developments in internet technology - like the platform independent programming language JAVA - make it possible to use the familiar web environment for telemicroscopy. To evaluate the possibilities of such a web based approach, we have developed an experimental telepathology system (#3) based on a http server and the Common Object Request Broker Architecture (CORBA), an industry standard for the implementation of distributed software. The main design goal in all three systems was to use as many "off the shelf" components as possible. In order to overcome the incompatibilities between different systems, a technical standard for telepathology systems should be created. For this purpose, it is inevitable (i) to clearly specify all the interfaces needed by a telepathological application (ii) and to allocate clearly all functions to distinct technical

components. In the paper, a standardization of some such technical standards is proposed.

Y004

TELEPATHOLOGY SYSTEM BASED ON WEB

Lee. B.I. 1, Nam. S.H. 2, Choi. H.K. 1

1) Department of Computer Science, Inje University, Kim-hae, Kyung-Nam, Korea, 2) Department of Biomedical Engineering, Inje University, Kim-hae, Kyung-Nam, Korea

In this paper, we introduce an implementation and a design for a telepathology system (TPS) based on WEB environment. The current WEB systems of HTML type have limits in their efficiency and security. We attempted to solve this problem using component base application coded by Delphi. The server of TPS is composed of four parts : DB part, chatting part, image transmission part and management part. When a client requests a connection to the TPS server, the TPS manager certifies a permission to each client who downloaded the component for image processing. The TPS manager transfers a topic image which is uploaded by the host client of the conference room to every client at the same conference room. And conference participants can exchange their opinions with other clients through the chatting server. Each participant can send the processed image to the selected or all participants by the image transmission server. The general server application has some load-balancing to response to the client. However, our developed system removed load-balancing of the server because we designed the TPS with the concept of component. In the aspect of maintenance cost, the designed system has a good quality. Moreover, TPS is designed on WEB environment. Every participant can connect to the conference at any time, if a local system is connected on WEB. We implemented TPS at Pentium-III (450MHz) PC and the network is 10MBPS on LAN environment. The test images were microscopic images (640x480). By using the proposed system, it is possible to easily open conferences for pathologists by communicating between hospitals on WEB.

Y005

DEVELOPING PROTOCOLS TO IMPROVE STATIC IMAGE TELEPATHOLOGY RELIABILITY

Spatz A. 1, Cook M.G. 2, McLaren K. 3, Lam King 4, Tucker J. 3

1) Dept. de Pathologie, Institut Gustave-Roussy, 39 rue Camille-Desmoulins, Villejuif Cedex France, 2) Royal County Hospital, Guildford, Surrey, UK, 3) Dept. of Pathology, University Medical School, Teviot Place, Edinburgh, EH8 9AG UK, 4) Rotterdam, Netherlands.

The reliability of a diagnosis test depends on the reproducibility of the results. Most inter-observer variability studies have been based on the specimen diagnosis, rather than studying the variability in labelling morphological features on which this depends. In preparation for the introduction of telepathology into EORTC trials, the EORTC Pathology Study Group has supported a study of the inter-observer variability in histopathological diagnosis of melanocytic lesions at the morphological feature level, in order to develop protocols to assist pathologists in selecting appropriate images for telepathology.

The study was based on a commercial telepathology system working in conjunction with a dynamic www site using Cold Fusion and an Access data-base. From 18 "difficult" melanocytic lesion cases, an independent non-specialist pathologist selected and captured "representative" telepathology images. The images were sent to each of three melanoma expert pathologists, who (independently) examined each, gave a decision on technical suitability, then annotated each by drawing round areas of particular diagnostic significance. Labels were attached to each drawn area with a morphological designation and a decision on its importance (Pathognomonic, Major, minor). The final images were then transmitted to the study site.

Finally, a consensus session between the experts was arranged to discuss all the area description data, to eliminate redundant areas (a.k.a., same or different topographical areas selected by different investigators which carried the same type of information) and to reach a consensus on the terminology used to label the informative areas. From this, a protocol to assist non-expert pathologists with difficult melanocytic lesions in selecting fields for telepathology was drawn up and agreed.

Y006

TELEDIAGNOSIS OF TRANSBRONCHIAL FINE NEEDLE ASPIRATIONS - A FEASIBILITY STUDY

Kayser K. 1, Kayser G. 1, Becker H.D. 2, Herth F. 2
1) Department of Pathology, Thoraxklinik, Heidelberg, 2) Department of Endoscopy, Thoraxklinik, Heidelberg, Germany

Aim: To analyze the diagnostic accuracy of telediagnostic procedures for transbronchial fine needle aspirations.

Material and methods: A double blind study was performed on cytological slides of 54 randomly selected cases with transbronchial fine needle aspirations. The slides were digitized using a Leica digital camera DC100 mounted on a microscope Leica Laborlux S, and analyzed by an experienced pathologist without knowing the definite diagnosis or any additional clinical data. The diagnoses stated by analyzing the digital images were compared to the final conventional diagnoses. In addition, the duration of the digital diagnosis, used magnifications, and difficulties for correct sampling were documented.

Results: The "digital" diagnoses of the 54 cases were all in general agreement with the definite diagnoses. No wrong positive or wrong negative case in respect to malignant/non malignant (31/23) or to small cell/non small cell (9/22) occurred. The performance of a digital diagnosis lasted for 110 s at average (15 - 260 s), and is significantly longer compared to that of conventional fine needle aspiration judgement (20 s). The screening magnification was commonly set to x10, that for definite diagnostic analysis x40. Benign diseases (2 tuberculosis and 3 sarcoidosis cases) were correctly classified.

Conclusions: Telepathology systems can probably be used for fine needle aspiration analysis without major diagnostic errors. Their use can improve the endoscopic sampling and avoid second anesthesia when missing the lesion of request during the first examination.

Y008

WEB SEARCH ENGINES FOR FINDING INFORMATION IN BIOLOGY AND PATHOLOGY

Boudry C.

URFIST/Ecole nationale des chartes. Paris. France, with the Pôle Traitement et Analyse d'Images de Basse Normandie.

Internet takes a more and more important place in the "harvest" of the necessary information in biological research but also in pathological research. Paradoxically, due to the exponential increase of information sources in biology on the internet, collecting pertinent information for researchers in pathology and biology is a more and more difficult task. Indeed, the navigation in this ocean of information requires to get under control navigation tools which functionality is more often unknown from researchers in biology. The recent apparition of specialized searching information tools (biolinks.com, biocrawler.com...) for biological purposes is supposed to facilitate this collect. Is it really the case ? After a fast presentation of these principal tools available on the internet and of their functionality, critical analysis are done and limitations of these tools are exposed. Necessary notions and methodology for an optimized interrogation of these tools are also briefly presented.

Y009
INTEROPERABILITY AND STANDARDS IN TELEPATHOLOGY AND TELEMEDICINE IN GENERAL

Binder B., Schwarzmam P., Klose R.
 University of Stuttgart, Pfaffenwaldring 47, Germany

Telepathology and Telemedicine in general will be able to find its way to daily routine use, if the formation of networks incorporating large user communities, exchanging all types of information, will become possible. If we compare the capabilities of the well-known internet applications like WWW and email with the current telemedicine tools, we find a lack of interoperability, e.g. the ability of working together in systems from different suppliers. Developers of telemedicine equipment need to provide solutions enabling the user to make his daily routine work easier and more effective. Therefore, the interoperability problem between equipment of different manufacturers has to be solved. Also the integration of telemedical applications into already existing in-house systems like HIS or PACS Systems has to be realized.

This contribution provides an overview of different standardisation efforts in medical information technology which are applicable to telemedicine. Standards like DICOM, HL7 and CORBAMed will be discussed. Special focus will be set on telepathology. In this field, several suppliers with equipment for different modes of telepathology, like still image 2nd opinion telepathology on one side, and telemicroscopy for frozen section analysis on the other side, are present and need tools to establish interoperability. The EU project EUROPATH and its descending activities promoted standardisation and interoperability concepts. Results of EUROPATH as well as from ongoing efforts will be reported.

Y010
HOW FAR IS TODAY'S TELEPATHOLOGY EQUIPMENT AWAY FROM A PERFECT COPY OF THE CONVENTIONAL PROCEDURE ?

Schwarzmam P., Binder B., Klose R.
 University of Stuttgart, Pfaffenwaldring 47, Stuttgart, Germany

Telepathology equipment, even for its most challenging application -frozen section diagnosis-, has reached a high level of functionality compared with the conventional procedure. This has been demonstrated in many studies with different aims of the tests. However, two main features of the conventional procedure are still missing: i) the haptic impression from a distance ('telefeeling') and ii) the online transmission of the full microscopic field of view in full resolution.

For the first item, ideal technical solutions are not yet known ; the second item is a matter of the affordability of online broadband telecommunication links. Modern techniques for intelligent data management, coding and automation of procedure steps compensate partly the missing transmission capacity. All other procedures in conventional diagnosis in pathology have perfect counterparts in telepathology.

At the example of HISTKOM, as a representative of online telepathology systems, the achieved degree of telepresence, functionality, utilities and working comfort is demonstrated.

Beyond the original aim - just to replace the conventional process by a diagnosis at a distance -

modern telepathology equipment offers some additional attractive features. One of those is the opportunity for requesters and suppliers of telepathology services to join networks in telepathology and more generally in telemedicine. They may create an open market with improved access to 2nd opinion, full diagnosis and in general to immediate expertise all over the world.

Y011
EXPERIENCES GAINED IN
TELEPATHOLOGY FIELDTESTS WITH
HISTKOM EQUIPMENT

Binder B., Schwarzmann P., Klose R.

University of Stuttgart, Pfaffenwaldring 47, Stuttgart, Germany

In parallel to routine operation, HISTKOM underwent and continuously undergoes fieldtest studies to evaluate the procedure, the components and the working comfort of telepathology.

Studies have been carried out to test all components of the HISTKOM equipment family:

- The active online telepathology system HISTKOM designed for the frozen section scenario,
- The passive offline system HistConsult for 2nd opinion purposes,
- KAMEDIN as the teleradiology component,
- The patient folder for documentation and archiving of telepathology sessions and as a link to other systems in telepathology networks,
- The tools to achieve data security and data confidentiality.

Additionally, studies for different modes of operation have been carried out: for the frozen section scenarios in retrospective and prospective tests, and for embedded material retrospective tests evaluated the suitability for rendering final diagnoses. Besides histopathology, slides of cytology have also been investigated.

In a presently running test a Web-based network for telehematology is investigated for suitability in daily routine to get fast access to expertise from outside.

All studies revealed that telepathology is an excellent tool to bring expertise nearer to the patient and to provide also small and medium hospitals, and especially hospitals in developing countries, with

modern services in pathology.

Y012
THE USE OF TELEPATHOLOGY AND
DIGITAL IMAGING IN CLINICAL
MEETINGS

Gardner T.W. 1, Al-Nafussi A. 1, McLaren K.M. 1, St.J.Thomas J. 2, Harrison D.J. 1

1) Department of Pathology, University of Edinburgh Medical School, Edinburgh, U.K, 2) Lothian Universities NHS Trust, Edinburgh, U.K

Objective: To assess the use of this telepathology in clinical meetings and teaching.

Method: Images are acquired in advance on the telepathology equipment and saved within a session file with annotations. Sessions can then be presented via a freely distributable viewer program on a laptop connected to a digital projector. Data for this study was collected through a combination of questionnaires and interviews.

Results: The multidisciplinary meetings where this technology has been used have included combined gynaecology and oncology; liver and liver transplant pathology, and lymphoma meetings. Subjective assessment: The equipment has proved to be very easy to use, gives excellent image quality and the ability to scan in an overview of the whole specimen for presentation is a valuable feature.

Objective assessment: Pre-preparation of cases takes between 5-15 minutes per case, depending on the number of images selected and the amount of annotation. This investment of time is repaid in the meetings themselves, where many more cases can be presented in a faster and more organised manner with a much better image quality than previously. The ability to annotate the images improves the clarity of the presentation. The clinicians attending have been very appreciative of these improvements and gain more from the meetings as a consequence.

Conclusions: The use of telepathology equipment, coupled with digital projection facilities, for presentation of cases at multidisciplinary clinical meetings has proved to be a very useful advance on the traditional method of live videomicroscopy in the meeting room. We are now extending this application to presenting clinical meetings remotely using the built-in videoconferencing facility in the telepathology software.

Y013
TELEPATHOLOGY FOR REMOTE
CONSULTATION AND TRAINING IN
SCOTLAND

Gardner T.W., McLaren K.M., St.J.Thomas J.,
 Harrison D.J.

Department of Pathology, University of Edinburgh
 Medical School and Lothian Universities NHS Trust,
 Edinburgh, U.K

Objectives: To evaluate the uses that can be made of telepathology between sites for second-opinion consultation, remote diagnosis, and remote teaching sessions of pathology trainees.

Method: We have linked dynamic telepathology systems at the Pathology department at Teviot Place and the Western General Hospital in Edinburgh. Pathologists use the systems to consult on cases that would otherwise have been physically referred, and meetings between sites are held remotely. Data was collected through a combination of questionnaires and interviews.

Results: With familiarity, live dynamic sessions at regularly scheduled times were the most efficient use of time for consultations. Pre-preparation of images followed by an

on-line discussion of the case can be more time effective for the critical on-line period than an unprepared live session, particularly for complex cases involving multiple slides and stains. These sessions have been deemed useful and have resulted in a saved journey and an enhanced mutual learning experience. There has been limited call for remote consultation within a large teaching hospital, due in part to available expertise on-site, and in part to a regular established system for specimen exchange between sites. For training purposes, there is reduction in time lost in travelling to meetings, and more trainees can view cases simultaneously than via a multi-headed microscope.

Conclusions: Telepathology proved to be of most value for discussion of difficult cases in the context of a regular scheduled meeting, but is considered too time consuming by many for routine referral. However, increased usage is likely to come with greater familiarity coupled with integration into standard work practices. It is likely to have an increasingly important role as more sites are linked up in telemedicine programs locally and nationally, both for consultation, but also for teaching and other

meetings between different sites.

Y014
TELEPATHOLOGY: THEORY AND
PRACTICE

Weinstein R.S.

Department of Pathology and The Arizona
 Telemedicine Program, The University of Arizona,
 Tucson, Arizona, USA.

Telepathology is the practice of pathology at a distance, viewing images on a video monitor rather than directly through a light microscope. A current classification lists 7 classes of telepathology systems. Human performance studies and diagnostic efficiency data show that HDSF telepathology (hybrid dynamic store-forward) telepathology may be the system of choice. Options for telecommunications systems include T1 and ISDN linkages. Dynamic-interactive telepathology is carried out using ATM or IP (Internet) telecommunications protocols.

Proven applications of telepathology include: routine surgical pathology; intraoperative frozen section services; teleconsultation; telemicrobiology; telehematology; tele-electron microscopy; and telementoring. Additional applications being evaluated include telecytology, teleimmunohistochemistry, and the use of telepathology for assessing adequacy of FNAs, proficiency testing, "virtual" tumor boards, and others.

The diagnostic accuracy of telepathology is statistically equivalent to the diagnostic accuracy of conventional light microscopy. There are some problem diagnoses for telepathology that are currently being catalogued including some cases of invasive lobular carcinoma of breast and diffuse adenocarcinoma of stomach. Identification of atypical mitoses may be problematic with some low-resolution telepathology systems.

Advanced uses of telepathology include second generation applications such as diagnostics and quality assurance for complex molecular pathology laboratory testing. Use of telepathology within specimen analytical production lines may expedite throughput and reduce costs for complex testing. The technology may prove useful for implementing the laboratory component of tailored therapy strategies for the treatment of cancer patients and others.

Z001**THREE DIMENSIONAL DISTANCE MEASUREMENTS WITH AXIAL PRECISION IN THE NANOMETER RANGE USING SPATIALLY ILLUMINATION MICROSCOPY**

Albrecht B. 1, Schweitzer A. 1, Failla A.V. 1, Jaeger T. 1, Kroll A. 1, Weisel A. 1, Edelmann P. 1,2, Cremer C. 1,2

1) Kirchhoff Institute of Physics, University, D-69120 Heidelberg, Germany, 2) Interdisciplinary Center for Scientific Computing (IWR), University, D-69120 Heidelberg, Germany

The determination of the three dimensional nanostructure of specific chromatin regions is highly relevant for an improved understanding of the functional topology of the genome. The use of different spectral signatures for the labeling and high accuracy nanodistance measurements in the Spectral Precision Distance Microscopy (SPDM) mode allows the investigation of the topology of such targets in three dimensionally conserved nuclei. To obtain the required high-accuracy nanolocalization of small targets, interferometric illumination is a well established and reliable tool.

New approaches use spatially modulated illumination (SMI) in various ways. In our laboratory, a stage controlled optical sectioning through the object was applied. In this case, the SMI point spread function (effective PSF) is the product of the axial illumination modulation (illumination PSF) and of the conventional PSF of the microscope objective (detection PSF). Using this approach and appropriate analysis algorithms, distances in three dimensions between point-like fluorescent objects were determined with an axial precision in the range of a few nanometers.

Z002**PRE-FILTERING APPLIED TO 3-D DECONVOLUTION**

Colicchio B. 1, Xu C. 1, Jung G. 2, Dieterlen A. 1, Haeberlé O. 1

1) Groupe Lab.EL, laboratoire MIPS, IUT GEII, 61 rue Albert Camus 68093 Mulhouse Cedex, France, 2) Laboratoire d'Hématologie, Centre Hospitalier de Mulhouse, 87 avenue d'Altkirch 68051 Mulhouse, France

Optical sectioning microscopy is commonly used for 3-D biological investigations. Images formed in a conventional fluorescence microscope contain light

from throughout the specimen. Then for quantitative measurements of size and intensity, original images cannot be used directly, but need to be restored before any analysis. Numerous deconvolution methods have been described in the literature. Deconvolution being an ill-posed problem, all techniques use regularization strategies. But in most cases the threshold levels of regularization parameters are difficult to determine. We propose to use a Wiener pre-filtering before deconvolution, in order to gain in stability. We have tested our method on CD34 hematopoietic progenitor cells from cord blood samples. Results show that after deconvolution the noise and artifacts were reduced. This improves the repeatability of the restoration process. Restoration of the same data with the EPR process without pre-filtering do enhance the quality of the contrast and the resolution. But noise remains which is presently cut by clipping 10% of the maximum intensity. This threshold is arbitrarily fixed. Using pre-filtering, the restored data exhibit low remaining noise avoiding this arbitrary clipping. More repeatable quantitative analysis are then possible.

Z003**MICROSCOPIC OPTICAL TOMOGRAPHY**

Dlugan A., MacAulay C., Lane P.

Cancer Imaging Department, British Columbia Cancer Research Centre, 601 West 10th Avenue, Vancouver, British Columbia, V5Z 1L3, Canada

An ongoing project in our laboratory is the incorporation of digital micromirror devices (DMD's, from Texas Instruments) into the light path of a microscope for the purposes of investigating existing and novel modes of microscopy. Our goal is high-resolution confocal imaging of "thick" tissue, to supplement other research activities in our lab focussed on early cancer detection.

We have placed DMD's in conjugate planes of the aperture and field diaphragms of a microscope, and thus have achieved flexible and precise control over the angle and spatial location of light illuminating the sample and light being collected from the sample. Previously, we have demonstrated the ability to produce confocal images with such a system through a fiber-optic bundle.

Our presentation will focus on our development system that allows optical tomography on a microscopic scale. Images are gathered while illuminating the specimen from a number of unique

angles; this illumination is achieved by switching of a DMD placed conjugate to the aperture diaphragm of a conventional microscope. Post-processing algorithms that generate 3-dimensional image stacks will be discussed, and images will be presented

Z004

3-DIMENSIONAL IMAGE PROCESSING: APPLICATION TO THE CHARACTERIZATION OF CELL TRANSFORMATION IN THE SYRIAN HAMSTER EMBRYO TEST

Angot F. 1, Elmoataz A. 1, Revenu M. 1, Vasseur P. 2, Sichel F. 3

1) GREYC-ISMRA, 6 Bd du Maréchal Juin, 14050 CAEN Cedex, 2) Centre des Sciences de l'Environnement, 57040 METZ Cedex, 3) GRECAN, Centre F. Baclesse, 14076 CAEN Cedex 05

Syrian Hamster Embryo (SHE) transformation test can predict carcinogenic potential of chemicals. A major difficulty results from the identification of transformed colonies. In order to characterize architecture of transformed and non-transformed cell colonies, we acquired 3-dimensional images of these colonies with a confocal scanning microscope. Automated analysis of such images was performed in order to study the relative position of cells within those colonies.

To achieve this goal, in order to cope with the light attenuation resulting from the acquisition device, we have chosen not to take into account the acquisition process but rather to propose a software correcting method only based on the image contents.

Here are also presented several classes of image processing operators developed within the framework of the PANDORE library, in which a complex segmentation process is obtained by linking "atomic" operators. Our approach to the localization of each cell in a 3D image is based on a combined processing of the 3D image and its 2D projection.

Z005

AUTOMATIC SEGMENTATION OF 3D IMAGES FROM CONFOCAL MICROSCOPY

Elmoataz A. 1, Schüpp S. 1, Sichel F. 2, Bloyet D. 1

1) GREYC Image, Bd Marechal Juin, Caen, France, 2) GRECAN, Université de Caen, Centre François Baclesse, Caen, France

In this study, we address the problem of automatically segmenting 3D images from confocal microscopy. The confocal microscope provides images at different depths of the cells which can be considered as the images slices of the tissue sections. Segmentation of these images to obtain 3D surface is a difficult task. We have developed an approach where the 2D image, representing the projection of all slices, is automatically segmented and the other images slices are segmented in a layered approach.

Author Index (Abstract Numbers)
--

- Adam R.L. R009, R010
Ajchembaum-Cymbalista F. A006
Akerman M. M004
Al Achkar W. A003, I005
Al Nafussi A. Y012
Albertson D. W002
Albrecht B. Z001
Albregtsen F. R028, R029
Allouch P. S002
Alonso Guervos M. T001
Alvarez B. O007, O008
Anatskaya O.V. M001
Anderson N. B002, X001
Angot F. Z004
Angulo J. R023
Ardelean C. B012
Arthur K. H001
Aubele M. W003
Aubery M. H015
Auer G. N001
- Baak J.P.A. A016, B018, B019, H009, K004, K005, T001, W002
Bagwell C.B. B006
Bakker J. E006
Bakowska A. B010
Baldetorp B. B006, G002
Balm A. R016
Banfalvi G. I006
Barbelivien A. P004
Baretton G. B007, G005, I007, R005, R011
Bartels P.H. R002
Bartova E. I002
Becker H.D. Y006
Bedner E. H008, S005
Begg A. R016
Behr J.-P. C003
Beil M. F003
Belhomme P. R032
Belien J.A.M. D001, R012
Bendahl P.-O. B006, M004
Bengtsson E. P001, R003
Benito L. O007, O008
Berke G. L001
Bernheim A. K001
Bertino B. A012
Bester M.J. L006
- Beveridge J. A015
Beyer T.V. M001
Beyser K. U003
Bezborodkina N.N. C002, R008
Bezrookove V. N002
- Binder B. Y009, Y010, Y011
Birembaut P. V001
Bloemena E. H009
Bloyet R033, R034, R036, S004, Z005,
Blyweert E. R016
Bochkareva N. E004
Bocking A. A002, M002, M003, O003, X002, Y002
Boev S.F. R021
Bol M.G.W. B018
Bonnet N. H014, V001
Borba G. H003
Borovecki A. O006
Bos S. B018
Boudry C. X003, Y008
Brakenhoff R.H. R012
Branch J. K008
Brauchli K. Y003
Braut-Boucher F. H015
Breton M.F. D003
Briand M. E007
Bringuier A. H015
Bruel A. F003
Brugal G. J002, R006
Bruneau de la Salle S. L002
Bruvere R. H002
Brydak L. A005
Buhmeida A. A001
Buikis I. H012
Bulten J. A010, E006
Burgemeister R. U001
Burvenich C. F001
- Calin D.L. B015
Canet V. R006
Cardot H. R024
Carreiras F. D003
Castelli C. H006
Ceccarelli C. T002
Chaitchik S. L001
Chasle J. P005
- Chassoux D. P005
Chermant J.-L. R025 R031
Chirana A. B012
Cho N.H. R014
Choi H.J. R019
Choi H.K. R014, R019, Y004
Christen H. Y003
Christen M.-O L003
Ciobanu A. B012, B014
Clement - Sengewald A. U001
- Colicchio B. Z002
Collan Y. A001, A007, B003
Connault E. D002
Cook M.G. Y005
Cornillet-Lefebvre P. K002
Costa F.P.S. O001
Coster M. R025, R031
Coudrey T. R025, R036
Coullin P. K001
Cragg M. B008
Cremer C. J001, K009, Z001
Cremer T. J001
Crisan Dabija R. B015
Cruet-Hennequart S. E005
Cuijpers V. R027
- Dalla Palma P. B005
Danielsen H.E. R028, R029
Danieri M.C. G004
Darbeida H. D003
Darzynkiewicz Z. H008, S005
Dauphin F. P004
Dawe C. J003
De Bruin P.C. A016
De Grandmaison G.L. E002
De Grooth B.G. O009
De Méo M. R038
De Wilde P. A010, E006, K006, K007, R027, S003
De Wind-van de Burg M. N002
Debout C. L007
Delaere P. R016
Dengler R. P006
Denoux Y. E005, P005, R025
Depreux P. C001
Derappe C. H015
Diamond J. R002
Dieterlen A. Z002
Dietmaier W. U003

- Dimmer V. G005, I007, R011
 Divan C. B005
 Djavidan M. N001
 Dlugan A. Z003
 Dobyszyk A. A005
 Doco-Fenzy M. K002
 Dolan G.L. O009
 Dosogne H. F001
 Dowsett M. B017
 Drobchenko E.A. I001
 Duerschmied D. F003
 Dufer J. I003, K002, P002
 Duigou F. P005
 Dumas P. E002
 Dussert C. R004
 Dutoit S. E005
 Dutrillaux B. N004

 Edelmann P. J001, Z001
 Ekhtiar A. I005
 El Ayat G. G009
 Elias Z. G004
 Elie H. R035
 Elie N. R025
 Elkablawy M.A. B002, H001, R002, X001
 Elmoataz A. R024, R033, R034, R036, Z004, Z005
 Elzagheid A. B003
 Engels H. N002
 Erenpreisa J.E. B008
 Erlandsson F. P001, R003

 Failla A.V. Z001
 Falkenberg K. R007
 Farabegoli F. T002
 Fehm T. N001
 Feldmane G. H002
 Feldman G. H015
 Ferno M. B006, M004
 Ferrari C. O005
 Filatov M. V. I001
 Filipenko M. E001
 Flandrin G. R023
 Flezar M. R015, R020
 Foerster J. A005
 Freivalds T. H012, S001
 Friedemann G. U001
 Friedrich K. G005, I007, P003, R005, R011
 Friedrichs N. M002
 Frincu D.L. B012, B014

 Frincu L.L. B012, B014, B015
 Frouin F. K001

 Gabius H.-J. B011
 Gambert Ph. H014
 Ganova A. I002
 Garcia Marco J.A. O007, O008
 Garcia Vela J.A. O007, O008
 Gardner T.W. Y012, Y013
 Garner D. A015
 Gauduchon P. D003, E005, E007, L007
 Gault N. E002
 Gazdar A. A014
 Gemmink J. A010, K006
 Gendron M.C. H015
 Gerbat S. L001
 Gerstner A. P007
 Ghadimi B.M. N001
 Giaretti W. K004, O012
 Giuffre G. U002
 Giroud F. R006, R018, X002
 Godard T. L007
 Gohde W. O005
 Gougeon G. R032
 Goutet M. G004
 Gouwenberg Y. R012
 Grefte J. A010
 Greve J. O009
 Griscelli F. D002
 Groma V. F002
 Gruson N. K002
 Gschwendtner A. A004
 Guervos M.A. K005
 Guillaud M. A014, J003
 Guillot R. H015
 Guilly M.N. N004
 Gulyaeva L. E001
 Güntzschel U. N005

 Haerberle O. Z002
 Hamilton P.W. B002, H001, R002, X001
 Hammou J.C. A012
 Hanselaar A. A010, E006, K006, K007, R027, S003
 Harju L. H012
 Haroske G. G005, I007, P003, R005, R011, X002, Y003
 Harrison D.J. Y012, Y013
 Haugland H.K. Q001

 Hauser C. K003
 Haustermans K. R016
 Hedley D.W. Q001
 Heinmöller E. U002, U003, U004
 Helmrich A. N005
 Hemmer J. K003
 Henßge E. A002
 Herlin P. R025, R031, R032, R033, R034, R036, S004, X003
 Hermsen M.A.J.A. K004, K005, T001, T002
 Herth F. Y006
 Heselmeyer K. K006, K007
 Heselmeyer-Haddad K.M. N001
 Hitzler H. U001
 Hložek P. I002
 Hoebbers F. R016
 Hoffmann K. B007
 Hofland I. R016
 Hofler H. W003
 Homsy C. F004
 Hubler M. X004
 Huseyin G. A011
 Hwang H.G. R014

 Illidge T. B008
 Irinopoulou T. F003
 Ivanchuk I. H004, H005
 Ivanov A. B008
 Ivanova I.A. R021

 Jaeger T. Z001
 Jaksic B. O006
 Jirsova P. I002
 Johansson M.C. G002
 Jongbloed G. D001
 Jordan S. G009
 Jung G. Z002
 Jurka A. S001

 Kaffy C. L002
 Kahn E. K001
 Kaledin V. E001
 Kallioniemi O.-P. W004
 Kanitz W. O004
 Kapp A. M003, R007
 Kardum M.M. O006
 Kardum-Skelin I. O006
 Katzir N. S003
 Kayapinar R. A011
 Kayser G. B011, Y006

- Kayser K. B011, Y006
 Kemp R. R030
 Kerboeuf D. O002
 Kerstens H. S003
 Kibangou Bondza P. P002
 Kiehl P. M003, R007
 Kildal W. M005, R029
 Killander D. B006
 Kinzel P. Y002
 Kisman O. B018
 Klose R. Y009, Y010, Y011
 Knops K. A002
 Knutsson Y. M004
 Kolomijets L. E004
 Kondakova I.V. E004, G006, G007
 Kooy-Smits M. E006
 Korbelic J. J003
 Korobova F.V. R001
 Kotsch M. G005
 Koutna I. I002
 Kozinets G.I. R001, R021, R022
 Kozubek M. I002
 Kozubek S. I002
 Krampe R. B008
 Kreth G. J001, K009
 Kroll A. Z001
 Kruse A-J A016
 Kube M. O003
 Kudryavtsev B.N. C002, R008
 Kudryavtseva M.V. C002, R008
 Kuipers E.J. H009, W002
 Kujari H. A001
 Kunze K.D. B007, G005, I007, P003, R005, R011, Y003
 Kuopio T. A007, B003
 Kurten N. A016
 Kurth-Franke E. P003

 Lachard A. R004
 Lahorte C. H011
 Lam K. Y005
 Lam S. A014, J003, R030
 Lamfarraj H. S002
 Lane P. Z003
 Lavrencak J. R015, R020
 Le Riche J.C. A014, J003
 Lebailly P. E007, E008
 Lebeau C. R031
 Lebrethon E. E007
 Lecluse M. R035

 Lee B.I. R014, R019, Y004
 Leers M.P.G. O011
 Lefaix J.-L. E002
 Leite N.J. R009, R010
 Leonardi E. B005
 Lequeux N. F004
 Leroy-Dudal J. D003
 Lesieur D. C001
 Levasseur R. R033
 Levina T.N. R021
 Levina V.V. I001
 Lezoray O. R024, R035, S004
 Li H. D002
 Liautaud-Roger F. I003
 Liliemark J. B016
 Linares-Cruz G. F004, P005
 Linden T. M004
 Lizard G. H014
 Lobodasch K. P006
 Loehrke B. O004
 Lorand-Metze I.G.H. H003, O001, R009
 Losa G.L. H006
 Loza V. H002
 Lubrano T. K008
 Luciani L.G. B005
 Lukasova E. I002
 Lyakhovich V. E001

 MacAulay C. A014, J003, R030, Z003
 MacLaren K.M. Y012, Y013
 Machala M. A005
 MacKenzie E.T. P004
 MacNamara B. B016
 Macro M. O010
 Macville M. E006, K006, K007, S003
 Mairinger T. A004
 Malahova E.V. G006
 Malet M. O010
 Malfoy B. N004
 Malmstrom P. M004
 Manfait M. S002
 Marcelli C. R033
 Marcelpoil R. J002, J004
 Marchalant Y. P004
 Marchetti Ph. H011
 Marcos C.A. K005
 Martin I. O007, O008
 Martin P.M. R004

 Marx W. B018
 Masson L. K002
 Massuger L. E006
 Matos M. V001
 Matthäi A. N005
 Matula P. I002
 Maubant S. E005
 Maxwell P. B002, H001, R002, X001
 Mazarevica G. S001
 Mazur J. B016
 Mazzini G. O005
 McLaren K. Y005
 Meijer G.A. H009, K004, K005, T001, T002, W002
 Melchers W. E006
 Metze K. R009, R010
 Meuwissen S.G.M. H009, K004, W002
 Meyer E. F001
 Meyer P. Y003
 Meyer W. B007, G005, I007, P003, R005, R011, X002, Y003
 Michel N. K002
 Michels J.J. P005
 Mikhailova O. E001
 Millot C. P002
 Millot J.M. P002
 Mohr S. W001
 Montmasson M.P. R006
 Morel D. J002
 Morrison L. N001
 Moslemi S. C001, L005
 Motherby H. M002, O003, Y002
 Motsokane N.A. L006
 Mravunac M. K007
 Mulhall J.P. K008
 Muller C.D. C003
 Mutter G.L. B019
 Mysliwska J. A005, B010
 Mysliwski A. A005

 Nagy G. I006
 Nam S.H. Y004
 Nap M. O011
 Narozni M. R004
 Nativelle C. C001, L005
 Naumova I.N. R021
 Nazor A. O006
 Neviere R. H011

- Nicklee T. Q001
Nielsen B. R028, R029
Nolte U. F003
- Oberholzer M. X002, X004, Y003
Okovity S.V. C002
Ona F. O007, O008
Oosterhuis J.W.A. O011
Opolon D. D002
Orbo A. B019
Oredsson S.M. G002
Ormerod M.G. B017
Orsière T. R038
Otto R. Y003
- Pachmann K. P006
Pachmann M. P006
Pachmann U. P006
Pahlplatz M. R027, S003
Palcic B. A015
Palmari J. R004
Park C.H. C001
Paschke S. F003
Pereira F.G. H003, O001
Perricaudet M. D002
Petersen I. A013
Petillot P. H011
Picard F. A006
Pichon J. H015
Pina P. S002
Pinkel D. W002
Pjanova D. H002
Plancoulaine B. R025, S004
Planinc - Peraica A. O006
Plantin-Carrenard J. H015
Ploem J.S. A012, S006
Poddighe P. E006
Pogorelov V.M. R021, R022
Poirot O. G004
Polette M. V001
Pomjanski N. A002, M002, O003
Poncy J.-L. E002
Porwit-MacDonald A. B016
Postma C. K004
Potron G. K002
Poulain L. C003
Pouzaud F. H013, L003
Pretorius E. L006
Puchelle E. H014
- Raap A.K. N002
Raby B. V001
Rachon D. B010
Racz P. P007
Radulescu R. B015
Rahmy A. O011
Raleigh J. R016
Rapallo A. K004
Rat P. H013, L002, L003
Reich A. B005
Reith A. J004, M005
Remmerbach T. A002
Renke B. U002, U003, U004
Rep S. B018
Revenu M. Z004
Richter C. U002
Richter N. B011
Ried T. E009, K007, N001
Rigaut J.P. Q002
Rihn B.H. W001
Robben J. E006, K006
Rocchi E. V002
Rosenberg C. N002
Rothert F. R011
Rottman M. D001
Rüschoff J. U002, U003, U004
- Salaun V. A006, O010
Salet-van de Pol M. A010
Salmon J.M. V002
Salms G. F002
Sampedro A. K005
Sangha P. A004
Santini D. T002
Sapoval B. R039
Sarytcheva T.G. R021
Sastre-Garau X. N004
Savatier J. V002
Savillo I. X005
Sazonov V.V. R021, R022
Scardigli A. B005
Scheithauer J. G005, I007
Schiffenbauer Y.S. L001
Schneider F. O004
Schoffelen R.H.M.G. O011
Schröck E. N005, T001
Schupp S. R033, R034, R036, Z005
Schutze K. U001
Schwarzmann P. Y009, Y010, Y011
Schweitzer A. Z001
- Sciot R. R016
Selim A.A. G009
Semetkowska-Jurkiewicz E. B010
Seralini G.-E. C001, L005
Serra J. R023
Shabalina E.V. I001
Shankey T.V. K008
Sharifi-Salamatian V. Q002
Sherman M. N001
Shilov B.V. R026
Sichel F. Z004, Z005
Sidorenko N.V. M001
Siebers A. R027
Siftar Z. O006
Simon M.-J. L005
Sipahutar H. L005
Skagers A. F002
Skalnikova M. I002
Slegers G. H011
Smida J. W003
Smirnova L.P. G007
Smolewski P. H008, S005
Snijders A.M. W002
Sockalingum G.-D. S002
Sommer S. S. U004
Soria C. D002
Soria J. D002
Sourdaine P. C001
Soussaline F. F004, N004
Souza Filho W. R009
Spatz A.J. Y001, Y005
Spitschak M. O004
St.J.Thomas J. Y012, Y013
Staedel C. E005
Stal O. B006
Stolnicu S. B014
Stromberg M. B016
Strusky S. K002
Sudbø J. J004, M005
Sukhareva E.B. I001
Sustercic D. O006
Szepessy E. I006
Szmit E. A005
Szuhai K. N002
- Tan W. O011
Tanke H.J. N002
Tänzer S. N005, T001
Tarnok A. P007
Tenner-Racz K. P007
Terstappen L.W.W.M. O009

- Terzetti F. G004
 Theissig F. B007, G005, I007,
 R005, R011
 Theunissen P.H.M.H. O011
 Thevenin M. L003
 Thiebot B. D003
 Thuillier J. R031, S004
 Tibbe A.C.J. O009
 Timofeeva O. E001
 Todd-Pokropek A. K001
 Todorovic C. A015
 Tourdes F. E002
 Tran T.K.N. R025, R031
 Trentesaux C. I003
 Troussard X. A006, O010
 Trubniykov E. L001
 Trumpfheller C. P007
 Truong K. N004
 Truquet F. O010
 Trzonkowski P. A005
 Tuccari G. U002
 Tucker J.H. Y001, Y005
 Tugusova V. G001
 Tulusan A.H. P006

 Uhr J. N001
 Ulrich E. K002
 Urnov F.D. I008
 Us-Krasovec M. R015, R020

 Valensi F. A006
 Valet G. B016
 Van de Goot F.R.W. A016
 Van der Laak J. R027, S003
 Van Diest P.J. B019, D001,
 K005, Q003, R012, T002
 Van Grieken N.C.T. H009
 Van Merris V. F001
 Varia M. R016
 Vasseur P. Z004
 Vd Bijl H. O011
 Velthuysen L. R016
 Verbeek D. K007
 Verdenskaya N.V. R021
 Vielh P. N004
 Viergutz T. O004
 Vinogradov A.G. R021
 Vogelbruch M. M003, R007
 Volrate A. H002
 Vukovic V. Q001

 Wahlby C. P001, R003
 Warnet J.-M. H013, L002, L003
 Weidenbach H. A002
 Weinstein R.S. Y014, Y015
 Weisel A. Z001
 Weiss M.M. K004, T002, W002
 Wells C.A. G009

 Werner M. W003
 Wichelo C. K007
 Wiegant J. N002
 Wienk S. K006
 Wilber K. N001
 Wild C.P. E008
 Williams R. K004
 Williamson K. B002, H001,
 X001
 Wolf R. K007
 Wolffe A.P. I008

 Xu C. Z002

 Yang Y.I. R019
 Yatouji S. I003
 Yeh P. D002
 Yous S. C001

 Zabaglo L. B017
 Zacharia B. L001
 Zagrebelnaja G.V. G006
 Zahm J.M. H014, V001
 Zalcmane V. F002
 Zetterberg A. P001, R003
 Zganec M. R015, R020
 Zink S. B011
 Zitzelsberger H. W003
 Zorena K. B010

Subject Index (Abstract Numbers)

Main Keyword :

Diagnosis A
 Prognosis B
 Therapy C
 Angiogenesis D
 Carcinogenesis E
 Cell differentiation F
 Cell proliferation G
 Cell death H
 Chromatin I
 Computer simulation and modelling J
 Cytogenetics K
 Cytotoxicity L
 DNA content M
 FISH N
 Flow cytometry O
 Fluorescence imaging P
 Heterogeneity Q
 Image analysis R
 New microscopy techniques S
 Karyotyping T
 Laser microdissection U
 Live cell imaging V
 Microarrays W
 Quality control and standardisation X
 Telemedicine Y
 3D imaging Z

Other Indexing Keywords

20Q13 W002
 3-D deconvolution Z002
 3D imaging P001, F003, R003
 Acridine orange uptake H012
 Actin F002
 Active Caspase-3 H009
 Adenomyosis G001
 Adherence receptors D003
 Adherent cells L003
 Aging I005
 AgNORs M002, R006
 Aneuploidy E009
 Angiogenesis D003, Q001, R031
 Animal pathology O002
 Annexin V H003, H011, O007
 Antioxidant enzymes G007

Antiradical activity E004
 Apocrine metaplasia of the breast G009
 Apoptosis B016, G001, H004, H005, H013, H014, L007, O007, O008
 Aromatase C001, L005, O004
 Atopic dermatitis R007
 Autofluorescence P002, S002
 Automated cell sorting R024
 Automated rare event detection system R012
 B-cell non-Hodgkin's lymphoma U003
 B-CLL O007, O008
 Back-propagation neural networks R014
 Bacteria classification S002
 BCL-2 O008
 Benzene E008
 Biomarkers A014
 Biomonitoring E007
 Bladder cancer B018
 Blood flow P004
 Blood platelet R001
 Blood smears R021
 Bone R033
 Bovine bone marrow F001
 Brain P004
 Breast cancer B003, B006, B007, B017, C001, G005 H005, I007, M004, N004, O011, P003, P006, Q002 R011, R014, T002, W003
 Bright field microscopy S003
 Bromodeoxyuridine G002
 Bronchial Dysplasia J003
 Bronchial epithelial cells V001
 Buccal mucosa R015
 Calponin F002
 Cancer B011
 Cancer markers W001
 Carcinogenesis R004, U004
 Cardiomyocytes H011, R010
 Caspases H008
 CD20 A006
 CD38 O010
 Cell adhesion D003
 Cell classification R035
 Cell culture L006
 Cell cycle O005, O010, V002
 Cell death B002, L002, O005, R002
 Cell imprints P005
 Cell morphology R021
 Cell proliferation A010, B002, B005, B012, B014, F004, P003, P005, R011
 Cell transformation assay E002, Z004
 Cellular sociology V001
 Centromer F003
 Cervical intraepithelial neoplasia A016
 Cervix E006, K006, K007, R027
 Chemiluminescence E004
 Chemoprevention A014
 Chromatin H006, F003, R028, R029
 Chromatin-folding I006
 Chromatin conformation I005
 Chromatin features R010
 Chromatin structure I008, P003
 Chromosomal aberrations E009, N005
 Chromosomal instability K008
 Chromosome aberrations H004
 Chromosome aneusomy E006
 Chromosome territories J001, K009
 Chronic lymphocytic leukemia H003
 Chronic lymphoproliferative disorders A006
 Chronic myeloid leukemia A003
 Circulating tumor cells P006
 Cirrhosis C002
 Clinical cytometry X002
 Clinical meetings Y012
 COBRA-FISH N002
 Cold light cytofluorometry L003
 Colon cancer T001
 Color image R014, R032

- Colorectal Cancer B002, K004, O012, X001
 Comet assay E007, L007, R038
 Comparative genomic hybridization G005, I007, K002, R006, W002, W003
 Component tree R009
 Condoms L006
 Confocal laser microspectrofluorometry S002
 Confocal microscopy Z004, Z005
 Corba Y003
 Courseware Y002
 Cryptosporidiosis M001
 Cutaneous follicular tumors M003
 Cyclin D1 G009
 Cyclin expression B007
 Cytochrome P450 E001
 Cytofluorometry A006, H013, O010
 Cytogenetics N001, W003
 Cytokeratin H009, O011
 Cytokines B010
 Cytology K006, K007, R027
- Data pattern analysis B016
 Diabetes Mellitus B010
 Diabetic patients S001
 Diagnosis M003, N001, O001, R022, Y005
 Digital imaging Y012, Y013
 Diploid reference cells R027
 DNA-fragmentation H005
 DNA analysis B007, O001, R027
 DNA aneuploidy K003
 DNA content H001, I002, R026
 DNA cytometry P005, X004
 DNA damage E008
 DNA image cytometry A002, M002, M003, O003, X002
 DNA ploidy A012, M004
 Double-stranded RNA H002
 Double minute chromosomes J001
 Doubling time R006
 Drug-resistance I003, K002
 Drug response L001
- Dynamic internet protocols Y001
 Dysplasia M005
- E-Cadherin B003
 Education Y013
 EF5 Q001
 Effector-target conjugate L007
 Effusion cytology M002, Y002
 Endocrine disruptor L005
 Endometrial hyperplasia B019
 Endometrium G001
 Endothelial cells D003
 Endotoxin H011
 Eosinophilia R007
 Epidermoid carcinoma B015
 Epigenome I008
 Epithelial cells E002
 Epstein-Barr virus H004
 Erythrocytes S001
 Erythroleukemia cancer cells P002
 Essential thrombocythemia R001
 Extracellular matrix E005
- FCM DNA ploidy B006
 FCM S-phase B006
 Feasibility study Y006
 Fibronectin D003
 Fieldtest Y011
 Fine needle aspiration biopsies A001, Y006
 FISH A013, E009, I002, K001, K002, K003, T002
 Flow cytometry B005, B008, C003, G002, G004, H001, H015, I001, I005, K003, O005
 Fluorescence O005
 Fluorescence imaging H001, K001, N001, O009, V002
 Fluorescent microscopy I006
 Fourier analysis R010
 Fractal morphometry H006
 Fractals R039
 Free radicals P002
 Frozen section diagnosis Y003
 Fuzzy classification R033, R034, R036
- G2 arrest B008
 Gamma-rays radiation E002
- Gastric cancer W002
 Gastric mucosa H009
 Gene regulation E001
 Gene transfer C003, D002
 Genetic alterations K005
 Genetic toxicology R038
 Genome function I008
 Genotoxicity E008, G004
 Geostatistics Q002
 Giant cell tumour B012
 Glare correction X004
 Glare effect X004
 Glucose-6-Phosphatase R008
 Glycogen C002
 Grading and staging Q002, R020
 Graph theory J004
- Hair loss F004
 Head and neck cancers J004, K003
 Healthy elderly A005
 Hepatitis C002
 Heterogeneity B005, R008, R031, T002
 High-density filter array W001
 High definition microscopy S006
 High resolution microscopy Z001
 Histological grading R004
 Histone acetylation I003
 HNPC associated adenomas U002
 Homeostasis J002
 Hormesis L002
 HPV A012, A016, E006
 HSD analysis S003
 Human bone marrow culture A003
 Human lymphocyte I005
 Human scalp biopsies F004
 Hypoxia Q001, R016
- Image analysis D002, H006, I006, J004, K001, M005, P001, R022, V001
 Image cytometry I003, N004
 Image processing R035, X003, Z004
 Image segmentation R014, R030, R032, R033, R034, R036, Z005

- Immunohistochemistry D002, M002, P004, R003
 Immunomagnetic beads L007
 Immunophenotype O006, P007
 In situ hybridization K006, K007
 Infectious mononucleosis R026
 Infrared spectrometry E002
 Integrins E005
 Interferometric illumination Z001
 Interferon H002
 Internet Y004, Y008
 Interoperability Y009
 Interphase cytogenetics N004
 Invasive front J004

 Johnsen score A004

 Ki-67 A016

 Laboratory diagnosis O002
 Larynx carcinoma K005
 Laser microdissection U001
 Laser pressure catapulting U001
 Laser scanning cytometry B017, H008, P006, P007, S005
 Latex L006
 Leukemia A011
 Leukoplakia M005
 Ligand histochemistry B011
 Liver M001, R008
 Lung A014
 Lung biopsy R030
 Lung cancer A015, H005
 Lung cytology A010
 Lutein cells O004
 Lymph node aspiration O001
 Lymphatic P007
 Lymphocytes H004, H005
 Lymphoma A011, B016, O001
 Lymphoproliferative disorders R023

 Male infertility A004
 Malignancy Associated Changes R005
 Mathematical morphology R023
 Mathematics simulation D001
 Medical devices L002
 Melanoma Y005
 Mesothelioma W001
 Metastasis R011

 Mib1 G005
 Micro-densitometry R018
 Microarrays A013, O009
 Microcell markers H012
 Microcopy Z003
 Micromirrors Z003
 Micronucleus test R038
 Microsatellite instability U002
 Microspectrofluorometry H015
 Mitochondria H008, H014
 Mitotic activity B012
 Molecular genetic analyses U004
 Morphological features R019
 Morphometry A001, R001, X003
 Morphometry microscopy S006
 Mosaic image S004
 Multi drug resistance I001
 Multifactorial analysis V002
 Multiple Myeloma O010
 Multiple staining P001, R003
 Multiresolution S004
 Multivariate analysis R004, R005
 Myeloid maturation F001
 Myoepithelium F002

 Necrosis H013
 Network model J002
 Nitric oxide G006
 Nuclear architecture J001
 Nuclear image analysis I007
 Nuclear morphology R011
 Nucleolus A001

 Oral cancer A002, B015, M005
 Ovarian cancer C003, D003, E005, R020, R028, R035
 Oxidative stress H015, L003, P002

 P21 G009
 P27 A006
 P53 K008
 Paired analysis R005
 Patient monitoring R022
 PCR analyses U003, U004
 Peroxides G006
 Pesticides E007
 Peyronie's disease K008
 Phenols G004

 Philadelphia chromosome A003
 Polyploidy M001
 Pre-filtering Z002
 Prognosis A013, B015, H003, J004, M004, M005, R002, R028, R029, X001
 Proliferation D001
 Prostate cancer A001
 Protein kinase PKR H002

 Quality control R018, R031, X003
 Quantitative cytology A012, A015, R023, R024
 Quantitative diagnosis B014
 Quantitative immunohistochemistry B003, B018, R007, R016, R034, X001

 Radioresistant tumours B008
 Recurrence B015, B018
 Reference slides R018
 Reflection contrast microscopy S006
 Refractive index S001
 Resolution X003

 S-phase G005, O001
 Salivary glands F002
 Sampling Q003, U002, U003
 Screening R024
 Search engine Y008
 Serous effusions O003
 Sex-dependent differences R015
 Simulations J003
 Single cell preparation U001
 Slide scanner R025, R031, S004
 Smoking R015
 Spectral analysis T001
 Spectral imaging S003
 Spectral karyotyping N005
 Spectral precision distance microscopy Z001
 Sporosis H012
 Sputum A015
 Standardisation R031, Y009
 Steroidogenesis O004
 Stroma R035
 Structural entropy B011

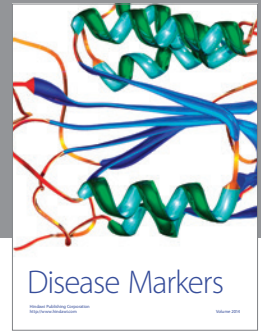
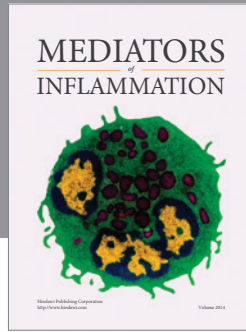
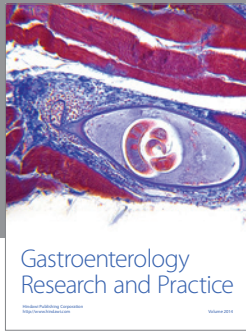
T-Lymphocytes O006
T-Lymphoproliferative disease
O006
Technical standardization Y003
Telecytology Y011
Teleeducation Y010
Telelearning Y002, Y008, Y015
Telemedicine networks Y009
Telemicroscopy Y010
Telepathology R021, X002,
Y003, Y004, Y010, Y011,
Y012,
Y013, Y014, Y015
Testis biopsies A004
Texture analysis R009, R029
Texture features A004, R002,
R014, R019, R020, R028, R035
Therapy F004
Tissue architecture J003
Tissue cartography F004
Tissue imaging I002
Tissue microarray W004
Tomography Z003
Topology R009
TPOT G002
Translocation T001
Tuberculosis U003
Tumor cells G006
Tumor chemotherapy L001
Tumor progression K004, K005
Tumour cell lines I001

Ultrastructure A011
Uveal malignant melanoma
B014

Vaccination A005
Veterinary pathology O002,
X005
Videomicroscopy H014
Virtual microscopy K009
Virus identification X005
Voronoi graph J002

Wavelet transform R019
Whole genome amplification
U004

Xenobiotic E001, L005



Hindawi
Submit your manuscripts at
<http://www.hindawi.com>

